UNIVERSITY OF CALGARY

Measurement and Modeling of the Phase Behavior of Solvent Diluted Bitumens

by

PAWAN AGRAWAL

A THESIS

SUBMITTED TO THE FACULTY OF GRADUATE STUDIES

IN PARTIAL FULFILMENT OF THE REQUIREMENTS FOR THE

DEGREE OF MASTER OF SCIENCE

DEPARTMENT OF CHEMICAL AND PETROLEUM ENGINEERING

CALGARY, ALBERTA

March, 2012

UNIVERSITY OF CALGARY

FACULTY OF GRADUATE STUDIES

The undersigned certify that they have read, and recommend to the Faculty of Graduate Studies for acceptance, a thesis entitled " Measurement and Modeling of the Phase Behavior of Solvent Diluted Bitumens " submitted by PAWAN AGRAWAL in partial fulfilment of the requirements of the degree of MASTER OF SCIENCE IN ENGINEERING.

_____

Supervisor, Dr. HARVEY W.YARRANTON

_____

Dr. MINGZHE DONG

_____

Dr. ZHANGXING CHEN

_____

Dr. EDWARD D. GHENT

_____

Date

Abstract

The design of solvent-based and solvent assisted heavy oil recovery processes requires accurate predictions of phase behaviour as straightforward as saturation pressures and as potentially complex as vapour-liquid-liquid equilibria and asphaltene precipitation. Among the various methods of predicting the phase behaviour of crude oils, the equation of state (EoS) is the most commonly used. To use an EoS, the amounts, critical properties, acentric factor, molecular weight and binary interaction parameters of the constituent components are required to characterize the fluid. For conventional oils, techniques such as distillation are used to obtain a normal boiling point curve which can be divided into pseudo-components. The boiling point curve is extrapolated over the relatively small heavy residue fraction and then correlations are used to determine the properties of each pseudo-component. However, for heavy oils, only about 30 to 50% of the oil can be distilled even with vacuum distillation. Hence, there is a need for a methodology to characterize the large residue fraction of heavy oils for EoS models.

The objective of this thesis is to adapt a heavy oil characterization method for an equation of state model for not only conventional vapour-liquid and liquid-liquid equilibria but also asphaltene precipitation for mixtures of heavy oil and solvents. Literature data on saturation pressures and liquid-liquid phase boundaries were collected for pseudo-binaries of bitumen and carbon dioxide, methane, ethane, and propane. Saturation pressures and the onset of asphaltene precipitation were measured for a pseudo-binary of bitumen and *n*-pentane. Saturation pressures were measured in a Jefri PVT cell at temperatures from 20 to 180°C. The onset of precipitation was determined at 20 and 180°C by titrating the bitumen with *n*-pentane and periodically circulating the mixture past a high pressure microscope. Saturation pressures were also measured for a live bitumen diluted with a multi-component solvent also at temperatures from 20 to 180°C.

The data were modeled with the Advanced Peng-Robinson equation of state. The maltene fraction of the bitumen was characterized into pseudo-components based on extrapolated distillation data. The asphaltenes were characterized based on a Gamma distribution of

the molecular weights of self-associated asphaltenes. The APR EoS was tuned to fit the saturation pressure and asphaltene onset data of the pseudo-binaries by adjusting the binary interaction parameter between the solvent and the bitumen pseudo-components. A temperature dependent binary interaction parameter correlation was developed for the interaction parameters. The model with temperature dependent binary interaction parameters fit the saturation pressures, liquid-liquid boundaries, asphaltene onset over a wide range of temperatures. The model predicted saturation pressures of live oil and live oil diluted with condensate solvent generally within experimental error. The model also predicted the asphaltene onset in propane diluted bitumen although the asphaltene yield at higher dilution was underestimated. The model extends the capability for modeling the phase behaviour of solvent based heavy oil processes to a broad range of operating conditions.

Acknowledgements

First and foremost, I am deeply indebted to my supervisor, Dr. H.W. Yarranton for his constant guidance, support and encouragement during my Master's degree program. It was my privilege and pleasure to be a member of his research group.

I also wish to thank our PVT Lab manager Florian Schoeggl for his training and technical help to use PVT cell and High Pressure Microscope.

I appreciate and thank Dr. M. Satyro for his help to provide and use the simulation software and his invaluable technical support and assistance. He was very kind to allow me to use Virtual Materials group (VMG) software packages for the modeling work.

I am also thankful to Elaine Baydak, Kim Johnston, Orlando Castellanos, Diana Ortiz, Diana Barrera, Hamed Reza Motahhari for their assistance and the great help during my Master's thesis.

I am thankful to the Department of Chemical and Petroleum Engineering, Asphaltene Research Group, Faculty of Graduate Studies at the University of Calgary for their assistant, NSERC, Shell Energy Ltd., Schlumberger-DBR, Petrobras for their financial support throughout my Masters program.

Finally, from the deepest of my heart, I would like to thank my family for their constant support and encouragement. I am really grateful for their caring and understanding.

Dedication

I dedicated this Dissertation to:

My Parents and Brother

Table of Contents

List of Tables

List of Figures and Illustrations

List of Symbols, Abbreviations and Nomenclature

Abbreviations

ABVB	Athabasca Vacuum Bottoms
BIP	Binary Interaction Parameters
CEoS	Cubic Equation-of-State
CO_2	Carbon dioxide
CPA	Cubic-Plus-Association Equation-of-State
EoS	Equation-of-State
FBP	Final Boiling Point
GC	Gas chromatography
MW	Molecular Weight
NBP	Normal Boiling Point
PC-SAFT	Perturbed Chain Statistical Associating Fluid Theory
PR	Peng Robinson
SAFT	Statistical Associating Fluid Theory
SG	Specific Gravity
SimDist	Simulated Distillation
SRK	Soave-Redlich –Kwong
TBP	True Boiling Point
VLE	Vapour-Liquid-Equilibrium
VLLE	Vapour-Liquid-Liquid-Equilibrium
W	Cumulative Weight
Wt%	Weight Percent

List of Symbols

a	Attractive constant in Equation of State
b	Repulsive constant in Equation of State
c	Volume translation
k_{ij}	Binary interaction parameter between two component i and j
M	Molar Mass
P	Pressure
R	Universal Gas Constant
T	Temperature
V	Volume
x	Mole fraction
Z	Compressibility factor

Greek Symbols

ω	Acentric factor
γ	Specific Gravity
β	Shape factor in the Gamma distribution function
Γ	Gamma function

ε^{AiBj}	Cross-association energy between molecules i and j
β^{AiBj}	Cross-association volume between molecules i and j

Subscripts

Avg	Average
b	Boiling Point
c	Critical
m	Asphaltene monomer
r	Reduced

CHAPTER ONE: INTRODUCTION

In Western Canada, thermal recovery methods such as cyclic steam stimulation and steam assisted gravity drainage are the methods of choice to recover heavy oil and bitumen with viscosities exceeding 10,000 mPa.s. These methods require significant volumes of natural gas and water to generate steam: approximately 34 m^3 of natural gas and 0.2 m^3 of groundwater (assuming 90 to 95% recycle) are required to produce one barrel of bitumen (Canada's Oil Sands Report, 2007). Solvent based and solvent assisted recovery methods are a potential alternative to reduce or replace steam usage. However, potential solvents such as light *n*-alkanes (Jiang, 1997) are expensive relative to the value of heavy oil, and the success of the process depends on how much solvent can be recovered. Predicting the performance of solvent-based and solvent-assisted processes (including both oil and solvent recovery) is challenging because the introduction of a solvent can lead to complex phase behaviour. For any given heavy oil and solvent mixture, liquid-liquid (LL), vapour-liquid (VL), vapour-liquid-liquid (VLL) and asphaltene precipitation regions may occur. It is necessary to predict the phase boundaries and amounts and compositions of these phases at all operating conditions.

Cubic equations-of-state (CEoS) are widely used for modeling the phase behaviour of crude oil (Whitson *et al.* 2000, Pedersen *et al.* 2007). To use CEoS, the composition, critical properties, molecular weight and density of each component or pseudo-component of the fluid are required. However, a complete compositional analysis of heavy oils and bitumens is not available. Even with high temperature vacuum distillation, only 20 to 40 wt% of the heavy oil is distillable. Simulated distillation assays can extend the characterization to approximately 50 wt% of the heavy oil, but the boiling point calculations are based on extrapolations that cannot be validated against measured data. Hence, for heavy oils, a methodology is required to extrapolate the true boiling point curve to obtain accurate phase behaviour predictions.

Castellanos Díaz *et al.* (2011) developed such a methodology to characterize Athabasca bitumen and predict the phase behaviour of mixtures of solvent and bitumen using the Advanced Peng Robinson Equation-of-state (VMGSim 2010). They assessed several extrapolations of the true boiling curve including Gaussian and Gamma distribution-based extrapolations. They then divided the extrapolated curve into number of pseudo-components and assigned the critical properties and acentric factors for the pseudo-components using well known property correlations. Interaction parameters between solvent and bitumen pseudo-components were optimized to fit the experimental saturation pressures of pseudo-binary mixtures of bitumen and propane or carbon dioxide. The model correctly predicted saturation pressures and the boundaries of the vapour-liquid-liquid region for pseudo-ternaries of these components. However, asphaltene precipitation data were not available for these mixtures and therefore model predictions for asphaltene precipitation could not be tested.

1.1 Objectives

The purpose of this thesis is to test the capability of the characterization methodology proposed by Castellanos Diaz *et al.* (2011) for modeling both saturation pressure and asphaltene precipitation data. The goal is to find a single oil characterization for an equation-of-state model that describes the full range of phase behaviour observed in heavy oil and solvent mixtures. A bitumen from Northern Alberta was used for this case study. The solvents considered are a solution gas (a mixture of methane and carbon dioxide), a condensate, and *n*-pentane.

The model selected for this study is the modified Peng-Robinson equation-of-state (PR EoS), which includes volume translation, and is well suited to petroleum fluids. Note that, while the exact tuning may vary for different equation-of-state models, the same general trends are expected for any of these models. The PR EoS was implemented using VMGSim^{TM} (Version 6.0, 2010).

Specific objectives are to:

1. measure characterization data including density, distillation, gas chromotagraphy, SARA analysis, and asphaltene density and molecular weight distributions
2. construct fluid characterizations of the condensate and the bitumen based on the assays
3. measure saturation pressures of the live oils, mixtures of bitumen and condensate, and mixtures of bitumen and pentane
4. measure yield of precipitated asphaltenes and the compositions at which asphaltenes first precipitate (onset) for *n*-pentane diluted bitumen
5. test the proposed characterization and equation-of-state model on the measured saturation pressures and asphaltene precipitation data
6. modify the characterization method as required and test model sensitivities

For *n*-pentane, the composition at the onset of asphaltene precipitation and the amount of asphaltene precipitated from the dead oil at different solvent contents were measured at room temperature. Also onset of asphaltene precipitation was measured at 180ºC. The saturation pressures of the dead oil and *n*-pentane mixture at solvent contents up to 30 wt% and temperatures ranging from 90 to 180ºC were also measured. *n*-Pentane was selected because it is a pure component and, therefore, there is less ambiguity in its contribution to the saturation pressure and asphaltene onset. Also, *n*-pentane is a liquid at ambient conditions and asphaltene yield data can be readily collected to provide more data. Hence, the *n*-pentane dataset is ideally suited for model tuning.

For the condensate, saturation pressures were measured with the live oil at solvent contents up to 10 wt% and temperatures from 20 to 200°C. The multi-component condensate was first selected for practical reasons; it is a cheaper alternative to pure solvents in commercial applications. From a modeling point of view, since it is a multi-component mixture and is combined with live oil over a broad temperature range, it provides a more challenging test of the characterization and modeling methodology.

1.2 Organization of Thesis

This thesis is organized into six chapters as outlined below.

Chapter 2 presents a brief review of petroleum chemistry, crude oil phase behaviour, oil characterization, and phase behaviour modeling with equations-of-state. Published phase behaviour data of heavy oil/solvent systems are reviewed along with the application of equations-of-state to these systems.

Chapter 3 presents the chemicals and materials used in the experiments; the assays and property measurements of the bitumen and condensate samples; the experimental techniques for live oil preparation, saturation pressure measurement and asphaltene precipitation onset and yield measurements.

Chapter 4 presents the characterization and modeling approaches. First, an overview of the crude oil characterization and modeling is provided. Then, the extrapolation of vacuum distillation and chromatographic (SimDist) data to characterize dead bitumen is presented. The method used to define pseudo-components is discussed, including the correlations used for estimation of critical properties and acentric factor. The characterization of the condensate is also presented. Finally a method to adjust binary interaction parameters is provided.

Chapter 5 presents the experimental data collected for bitumen/solvent and bitumen/*n*-pentane mixtures. Related datasets from literature for bitumen/carbon dioxide and bitumen/methane, bitumen/ethane, bitumen/propane are also provided. Adjustments of binary interaction parameters to fit the saturation pressure and asphaltene onset data are discussed. Live oil modeling and model predictions for saturation pressure, asphaltene onset, asphaltene yield are presented. The effect of different NBP extrapolation, asphaltene average molecular weight, and model sensitivity to a number of pseudo-components is examined.

Chapter 6 summarizes the major findings of this thesis and provides recommendations for future work.

CHAPTER TWO: LITERATURE REVIEW

This chapter presents a brief review of petroleum chemistry, crude oil phase behaviour, oil characterization, and phase behaviour modeling with equations-of-state. Phase behaviour data of heavy oil/solvent systems are reviewed along with the application of equations-of-state to these systems.

2.1 Crude Oil Chemistry

UNITAR defines conventional oil as a petroleum fluid with a viscosity less than 100 mPa.s. and a density less than 934 kg/m³. Heavy oil is defined as a petroleum fluid with density in the range of 934 to 1000 kg/m³ and viscosity in the range of 100 to 100000 mPa.s. and it usually, but not always, contains higher than 2% by weight sulphur. UNITAR defines bitumen as a petroleum fluid with a density greater than 1000 kg/m^3 and a viscosity greater than 100000 mPa.s. Bitumen, also called as natural asphalt, consists of a variety of reddish brown to black materials which are semi-solid, ranging from viscous to brittle behaviour depending on the temperature and composition (Speight, 1991).

2.1.1 Oil Constituents

Petroleum fluids primarily consist of hydrocarbons with small amount of inorganic compounds such as nitrogen, carbon dioxide, hydrogen, and sulphur. Due to the limited solubility of water in hydrocarbons, water is mostly found as a separate phase. Although oils contain few atomic species, they consist of literally millions of different molecular species. The simplest and most common species is methane, the lightest of all hydrocarbons. Since methane contains one carbon atom, it is often referred as C1. Similarly, the term C2 is used for ethane (C_2H_6), C3 for propane (C_3H_8) and so on. Hydrocarbons with seven and more carbon atoms are called C7+ components and the sum of all C7+ components is called the C7+ fraction.

The heavier carbon number fractions consist of a variety of structures, not just *n*-alkanes, and the complexity of the molecules increases as the components become heavier, Figure 2.1. Therefore, the heavier fractions are typically characterized into classes of components. A particular C7+ component will belong to one of the following component classes:

Paraffins: In paraffins, the carbon atoms are connected by single bonds. Paraffins are divided into normal paraffins and *iso*-paraffins. In normal paraffins, carbon atoms are connected to form straight chains, whereas in *iso*-paraffins there is at least one side chain. Paraffins are also referred to as alkanes.

Naphthenes: These hydrocarbons contain one or more cyclic structures. Segments in the ring structure are connected by the single bond. Most naphthenic ring structures contains six carbon atoms, but naphthenic compounds with five or seven carbon atoms connected in the ring structure are also common in petroleum fluids.

Aromatics: Aromatics contain one or more cyclic structures but the carbon atoms in the aromatic compound are connected by aromatic double bonds. Benzene is the simplest aromatic component.

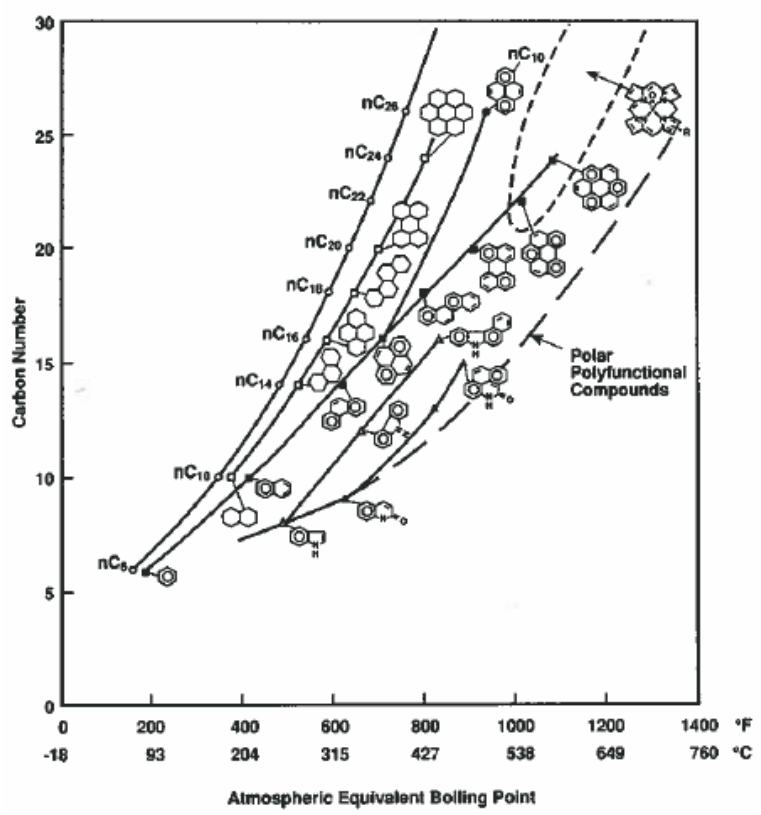

Figure 2.1: Composition and analysis of heavy petroleum fractions (Altgelt K., 1993)

The heavy fractions (C7+ fraction) of crude oils can also be characterized in terms of the relative amount of the different hydrocarbon classes present in the oil. The percentage contents of paraffinic (P), naphthenic (N), aromatic (A) components is referred to as a PNA distribution (Pederson and Christensen, 2007). A similar method to classify crude oil is based on solubility and absorption classes: that is saturates (paraffins and naphthenes), aromatics, resins, and asphaltenes (SARA fractions). Asphaltene are precipitated from crude oil by addition of excess of *n*-pentane. Saturates, aromatics, resins are separated using liquid chromatography. The chemistry of each fraction is described below.

Saturates: Saturates consist of paraffin and cycloparaffins (naphthenes) (Speight, 1991). The single-ring naphthenes, or cycloparaffins, present in the petroleum are primarily alkyl substituted cyclopentane and cyclohexane. The alkyl groups are usually quite short, with

methyl, ethyl, or isopropyl groups as the predominant substituent. As the molar mass of the naphthenes increases, the relative proportion of condensed rings also increases. Saturates are the least polar of the SARA fractions. The molar mass of saturates ranges from 300 g/mol to 600 g/mol (Wiehe and Liang, 1996) and their density is found to vary in range of 853 to 900 kg/m³ (Akbarzadeh *et al*., 2005) .

Aromatics: Aromatics consist of those compounds containing an aromatic ring and vary from mono-aromatics (containing one benzene ring in a molecule) to di-aromatics (substituted naphthalene) to tri-aromatics (substituted phenanthrene). Higher condensed ring systems (tetra-aromatics, penta-aroamitcs) are also known, but are somewhat less prevalent than the lower ring systems. Aromatics have a higher polarity than saturates. The molar mass of aromatics ranges from 450 to 550 g/mol and densities are reported to vary from 960 to 1003 kg/m³ (Akbarzadeh *et al.*, 2005).

Resins: Resins are larger more complex aromatics which are soluble in *n*-pentane but cannot be extracted from an absorbent by *n*-pentane. Another definition is that resins are soluble in n-pentane but insoluble in propane. The molar mass of resins varies from 859 to 1240 g/mol and densities are reported in the range of 1007 to 1066 kg/m³ (Akbarzadeh *et al*., 2005).

Asphaltenes: Asphaltenes are defined as the constituents of an oil mixture that are insoluble in *n*-pentane or *n*-heptane, but soluble in benzene or toluene. Asphaltenes include hundreds of thousands of chemical species and their structure is not readily defined. They have the highest molar mass, aromaticity and heteroatom content of all the crude oil components (Wiehe *et al.* 1996). Speight *et al*. (1991) concluded that vapour pressure osmometry (VPO) gives the most representative value of the molar mass of the asphaltenes. The molar masses of asphaltene monomers from VPO measurements range from 800 to 2,000 g/mol (Moschopedis *et al.*; 1976; Chung *et al*.; 1979; Wiehe, 1992).

Asphaltene Self Association

An interesting feature of asphaltenes is that they self-associate into larger structures. VPO measurements show that the average asphaltene molar mass increases dramatically with asphaltene concentration until a plateau is reached at concentrations above approximately 10 kg/m³ (Agrawala *et al.*, 2001), Figure 2.2. The asphaltenes associate into aggregates of 2-6 monomers on average, depending on the temperature and composition (Rogel, 1995; Yarranton *et al*. 1996). The limiting molar mass was found to decrease with temperature, solvent power and resin content (Moschopedis *et al.*, 1976; Yarranton, 2005).

There are two different models proposed for asphaltene self-association: the colloidal model (Yen *et al.*, 1974) and the oligomer model (Agrawala *et al.*, 2001). In the colloidal model it is assumed that asphaltenes are colloidal particles surrounded by adsorbed resins. In the oligomer model, asphaltenes are assumed to aggregate with each other in a manner analogous to polymerization but via van der Waals forces rather than chemical bonding. The aggregates are treated as macromolecules in solution rather than colloidal particles.

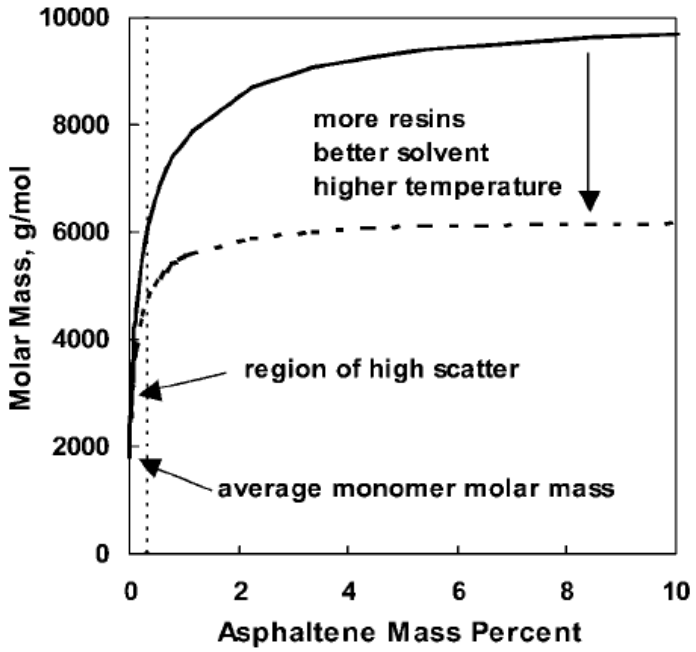

Figure 2.2: Trends in asphaltene molar mass observed from VPO measurements (Yarranton, 2005)

2.1.2 Crude Oil Assays

The distribution of components or classes of components in a crude oil is determined from assays including gas chromatography, distillation, and SARA fractionation.

2.1.2.1 Gas Chromatography

Gas chromatography (GC) analysis was originally developed for determining the composition of gas samples. This technique is now also being used for oil analysis (Danesh, 2007). In this analysis a small amount of the sample is injected in heated zone, vaporized and transported by the carrier gas usually helium into the column packed or internally coated with a stationary non-polar liquid or solid phase, resulting in partitioning of the injected sample. A stream of the carrier gas sweeps these eluted compounds to the detector where the component concentration is related to area under the response time curve.

The mass fraction of the light pure components (typically up to *n*- and *i*-pentane) is determined directly from their peaks in the GC chromatogram. For the C6+ fraction, as a good approximation for a paraffinic sample, the GC response for carbon number C*i* starts at the bottom response equivalent to paraffinic *n*-C_{i-1} and extends to the bottom response equivalent to paraffinic *n*-C*i*. The mass fraction of carbon number C*i* is calculated as the area under the curve from the baseline to the GC response in the *n*-C*i-1* to *n*-C*i* interval. Some empirical adjustments are applied to account for the typical non-paraffin components in the fluid. Each component shows a peak in the GC chromatogram. The mass fraction of each peak is determined by integrating the area of the chromatogram. The boiling point range of each increment is correlated from the known boiling points of the easily recognizable *n*-paraffins. With mass fractions and boiling points, a simulated distillation curve is constructed from the gas chromatographic data.

Another type of GC analysis is a simulated distillation or SimDist. SimDist is based on the observation that non-polar adsorbents elute hydrocarbons nearly in order of their

boiling point. A defined temperature program is used and the boiling point of the eluted material is correlated with elution time or with column temperature at the time of the emergence.

One of the limitations of gas chromatography is that the number of the possible components in any given molecular weight range increases markedly with the molecular weight, and there is significant drop in the differences in physical properties among similar structural entities. This limits the ability of gas chromatography to discriminate heavier components (Speight, 1991).

2.1.2.2 TBP Distillation

A TBP analysis separates the components of the oil into boiling cuts. The standard ASTM boiling analysis consists of two tests, the D86 and D1160 (Erwin, 2002). The D86 is performed at atmospheric pressure, wherein the sample is simply boiled out of a container flask and totally condensed in the receiving flask. As the D86 involves cracking or molecular breakdown of the crude sample at temperatures above 260 ºC, this test method is extremely inaccurate at temperatures of 232 ºC and above. Therefore, the D1160,which uses vacuum, is used to distill the residue from the D86 at atmospheric pressure equivalent temperatures at 232 ºC and above. The D1160 uses the same setup as the D86, only with an overhead vacuum, usually 40 mmHg absolute pressures.

In the 1930s, the D86 ASTM-type test was discovered to be inaccurate as every boiling cut has boiling components from its adjacent cuts. The ASTM commission then adopted a method called D2892. This method employs a fractionating column having an efficiency of 14 to 18 theoretical plates operated at a reflux ratio of 5:1 (ASTM D2892-10). This test method can be used to distil a crude oil to a final cut temperature of 400ºC Atmospheric Equivalent Temperature.

Normal boiling point means that the boiling point is measured at normal or atmospheric pressure. In practice, to avoid thermal decomposition, distillation (ASTM D2892-10)

starts at atmospheric pressure and is changed to sub-atmospheric distillation after reaching a limiting temperature. Sub-atmospheric boiling-points are converted to normal boiling-point temperatures using of a vapour-pressure correlation that corrects for the amount of vacuum and the fraction's chemical composition (Whitson and Brule, 2000). The boiling-point range for the fractions is not specified in the ASTM standard. Katz and Firoozabadi recommend use of paraffin normal boiling points (plus 0.5ºC) as boundaries, a practice that is widely accepted.

2.1.2.3 SARA Fractionation

SARA fractionation is the method of separating saturates aromatics, resins and asphaltenes from the crude oil. The first step in SARA fractionation is the separation of the asphaltenes by precipitation in an excess of *n*-pentane. After removal of the asphaltenes, the maltenes (the mixture of saturates, aromatics and resins) are recovered by evaporating the solvent from solvent/maltene mixture using a rotary evaporator. The maltenes are then fractionated using the ASTM D2007M procedure. First maltenes are dissolved in *n*-pentane (5 g maltene in 25 cm^3 *n*-pentane) and fractionated by liquid chromatography using two columns: an upper column containing Attapulgus clay and a lower column containing silica gel. Resins adsorb on the pre-activated clay and aromatics adsorb on the pre-activated gel and saturates pass through. The column is separated and resins and aromatics are desorbed using different mixtures of solvents.

2.2 Phase Behaviour of Crude Oil

2.2.1 Conventional Crude Oil

Crude oil exhibits multiphase equilibria as a function of pressure, temperature, and overall composition. The most common phase transition is liquid-vapour equilibrium. Gas reservoirs and undersaturated oil reservoirs are initially in the single phase region. Saturated oil reservoirs usually have a gas cap; that is, they are in the two phase region. In either case, oil splits into a gas and a liquid phase as pressure is reduced during

production. Similarly, rich gas will drop out liquids as it is produced. The pressure at which second phase (oil or gas) forms is generally called the saturation pressure.

For enhanced oil recovery processes, various gas such CO_2, nitrogen, or lighter hydrocarbon gases are injected into the reservoir. Addition of these gases to reservoir fluids can lead to complex phase behaviour over a range of the pressures and temperatures. For example, Shelton and Yarborough (1976) found that the addition of carbon dioxide or an approximately equimolar mixture of methane, ethane, and propane at low temperature (35 to 40 ºC) to a condensate-rich reservoir fluid yielded three phases (vapour-liquid-liquid).

Asphaltenes are also known to precipitate from crude oils due to changes in temperature, pressure, or composition (Hirschberg *et al*. 1984, Speight *et al.* 1984, Tharanivasan *et al.*, 2011, Kokal *et al.*, 1995). Typical examples are precipitation from relatively light oils with the drop in pressure (Burke *et al.,* 1990) and precipitation from heavy oils diluted with light components (Akbarzadeh *et al*., 2005). Shelton and Yarborough (1976) have noted that on addition of carbon dioxide to condensate-rich mixture, a third asphaltene-rich dense phase appeared to exist in the multiple liquid phase regions. Jamaluddin *et al.* (2000, 2002) and Tharanivasan *et al.* (2009) have collected asphaltene precipitation data from different crude oils by depressurizing oil at various temperature conditions. They have seen that the asphaltene precipitation onset pressure decreased with an increase in temperature.

2.2.2 Heavy Oil and Solvents

From a phase behaviour perspective, heavy oil and solvent mixtures are highly asymmetric and are expected to exhibit complex phase behaviour including liquid-liquid-vapour equilibria. The simplest and most common phase behaviour of interest is the solubility of light components in heavy oils. Mehrotra and Svrcek (1985) have measured solubility of gases such as nitrogen, methane, ethane, carbon dioxide, and carbon monoxide in different Alberta bitumens (Athabasca, Peace River and Wabasca). They

found that the solubility of the gases in the bitumen increased in the following order: N_2<CO<CH_4<CO_2<C_2H_6. As expected, the solubility of all the gases increased with pressure and decreased with temperature. Frauenfeld *et al*. (2002) measured solubility of ethane and propane in Cold Lake blended oil at 15ºC and pressure below the vapour pressure of the solvent. Consistent with the above trend, they found that solubility of propane in oil was much higher than the solubility of ethane.

Mehrotra and Svrcek (1985) have noted that binary mixtures of carbon dioxide and Peace River bitumen form a second carbon dioxide-rich liquid phase at carbon dioxide contents above approximately 10 wt% at 23 ºC. Badamchi-Zadeh *et al*. (2009) obtained a similar result for Athabasca Bitumen and carbon dioxide, observing a second carbon dioxide-rich liquid phase at carbon dioxide contents above approximately 11 wt% at 25 ºC. They also observed multiple liquid phases in a ternary mixture of 13.1 wt% propane, 19.2 wt% carbon dioxide and bitumen. Zou *et al*. (2007) studied the phase behaviour of Athabasca vacuum bottoms (ABVB), a 525+ºC boiling fraction, and *n*-pentane mixtures using x-ray transmission tomography. They found that these mixtures exhibit three and four phase equilibria depending on the overall composition.

Addition of solvent to heavy oil can also cause asphaltene precipitation. Speight and Mitchell demonstrated that the amount of asphaltene precipitation increased as the carbon number of the *n*-alkane solvent decreased. Speight *et al*. (1984) noted that the solubility of asphaltene increased with increasing temperature. Akbarzadeh and Alboudwarej *et al*. (2005) collected asphaltene yield data for heavy oils and bitumen (from different parts of the world) diluted with *n*-alkane for different *n*-alkane content at different temperature conditions. Their data showed the same trends as observed by Speight and Mitchell. Luo *et al*. (2010) measured asphaltene precipitation from *n*-alkane (propane, *n*-pentane, *n*-heptane) diluted Lloydminster oil. They observed that the heavy phase separated by propane from the heavy oil was a highly viscous liquid and different from the asphaltene precipitated by addition of *n*-pentane to the oil. Jossy *et al*. (2008) also studied the phase behaviour of a propane/UTF bitumen system at 10 to 40 ºC and observed partitioning of

mixture into a solvent-rich oil phase and a heavy-ends-rich (mostly asphaltene) oil phase at a propane/bitumen volume ratio greater than unity.

There are few datasets that include both VLE and asphaltene precipitation data, particularly for live oils. This combination of data is required to ensure that the fluid characterization and model is self-consistent (Chapman *et al*. 2007)

2.3 Equations-of-State Models of Phase Behaviour

Before introducing equations-of-state, note that there are two different types of model proposed for asphaltene precipitation: colloidal models (Leontaritis *et al*., 1987) and thermodynamic models (Hirschberg *et al*., 1984). In the colloidal model, resins are assumed to partition between the asphaltene particles and the medium. If sufficient resins desorbs from the asphaltene, asphaltenes aggregate to the micron scale and physically separate from the oil. In the thermodynamic model, it is assumed that asphaltenes are macromolecules that are part of a non-ideal mixture and that their behaviour is governed by thermodynamics; that is, they a undergo phase transition into a second liquid phase. According to thermodynamic models, asphaltene precipitation is reversible while it is irreversible according to the colloidal model. Hirschberg *et al*. (1984) demonstrated asphaltene precipitation is reversible. Permanu *et al*. (2001) have also observed that asphaltene precipitation is reversible although they observed some hysteresis. Thermodynamic models have been used extensively to model asphaltene precipitation (Burke *et al.* 1990, Chapman *et al*. 2003). A thermodynamic phase behaviour model is used in this thesis.

Phase behaviour models predict the number of phases and composition of the phases as a function of pressure, temperature and overall composition. Phase behaviour models have many applications in chemical and petroleum engineering. There are varieties of phase behaviour models but equations-of-state models are the most commonly used in commercial simulators. Only equations-of-state models are reviewed here.

2.3.1 Van der Waals Equation-of-State

Van der Waals improved the ideal gas equation by introducing the non-zero size of the molecules and considering the intermolecular attractive and repulsive forces (van der Waals, 1873). His well known cubic equation-of-state (CEoS) was the first equation capable of representing vapour-liquid coexistence and is given by:

$$P = \frac{RT}{V - b} - \frac{a}{V^2} \qquad \textbf{2-1}$$

where P is the pressure of the fluid, V is the volume of the container and R is molar universal gas constant. The parameter a is a measure of the attractive forces between the molecules, and the parameter b is the covolume occupied by the molecules. The term $RT/(V-b)$ represents the repulsive force between the molecules.

The constants a and b are found by evaluating the pressure-volume curve for the critical temperature. This curve also called as critical isotherm has inflexion point at the critical point, implying,

$$V\left(\frac{\partial P}{\partial V}\right)_{TatT=Tc,P=Pc} = \left(\frac{\partial^2 P}{\partial V^2}\right)_{TatT=Tc,P=Pc} = 0 \qquad \textbf{2-2}$$

At the critical point, V equals the molar critical volume Vc, which is related to Tc and Pc through Eqs. 2-1. On solving Eqs. 2-1 and 2-2, the following expressions for a and b are obtained:

$$a = \frac{27R^2T_c^2}{64P_c} \qquad \textbf{2-3}$$

$$b = \frac{RT_c}{8P_c} \qquad \textbf{2-4}$$

The Van der Waals equation gives a qualitative description of the vapour and liquid phases, but it is rarely sufficiently accurate for phase equilibria calculations. The Van der Waals equation has been superseded by a large number of other more accurate equations-of-state.

2.3.2 Redlich-Kwong Equation

The equation of Redlich and Kwong is, by many, considered the first modern equation-of-state (Pederson and Christensen, 2007) and takes the form:

$$P = \frac{RT}{V-b} - \frac{a}{\sqrt{T}V\ (V\ +b)} \qquad \textbf{2-5}$$

This equation has a more complicated temperature dependent attractive term compared with the van der Waals equation. This term serves to improve vapour pressure predictions. To improve the predictions of the liquid-phase molar volumes, the term V^2 in the denominator of the attractive term was replaced by $V(V+b)$. The parameter a and b are given by following expressions:

$$a = \frac{0.42748R^2T_c^{2.5}}{P_c} \qquad \textbf{2-6}$$

$$b = \frac{0.08664RT_c}{P_c} \qquad \textbf{2-7}$$

2.3.3 Soave-Redlich -Kwong (SRK) Equation

Soave found that the pure component vapour pressure calculated by the Redlich-Kwong equation to be somewhat inaccurate. He suggested replacing the $a/T^{0.5}$ in the RK equation by a more general temperature dependent term, $a(T)$, giving an equation-of-state of the form:

$$P = \frac{RT}{V\ -b} - \frac{a(T)}{V\ (V\ +b)} \qquad \textbf{2-8}$$

The equation is usually referred as Soave-Redlich-Kwong equation-of-state.

Soave found that the term $(a(T)/a)^{0.5}$, evaluated by fitting vapour pressure data, plotted linearly against the square root of the reduced temperature for a number of pure hydrocarbons (Soave, 1972). He proposed the following temperature dependence:

$$a(T) = a\alpha(T_r,\omega) \qquad \textbf{2-9}$$

where

$$a = \frac{0.42748 R^2 T_c^2}{P_c} \quad \textbf{2-10}$$

$$b = \frac{0.08664 R T_c}{P_c} \quad \textbf{2-11}$$

$$\alpha(T_r, \omega) = \left(1 + m\left(1 - \sqrt{T_r}\right)\right)^2 \quad \textbf{2-12}$$

$$m = 0.480 + 1.574\omega - 0.176\omega^2 \quad \textbf{2-13}$$

In Eq. 2-13, ω is the acentric factor defined by Eq. 2-17. Eq. 2-9 and 2-13 can be combined to give:

$$\sqrt{\frac{a(T)}{a}} = (1 + m) - m\sqrt{\frac{T}{T_c}} \quad \textbf{2-14}$$

Eq. 2-14 is in accordance with Soave's observations of a linear relationship between the square root of the *a* parameter ratio and the square root of the reduced temperature.

2.3.4 Peng Robinson Equation-of-State

After Soave's proposal, many modifications were presented in the literature for improving predictions of one or more property. These modifications were not limited to proposing new temperature models for α(Tr, ω), but also included the volume dependence of the attractive pressure term. The most popular of all these modifications is the one proposed by Peng and Robinson (1976).

Peng and Robinson improved upon Soave's equation by recalculating $\alpha(T_r, \omega)$ function and by modifying the temperature dependency of the attractive term. These changes gave better results for liquid volumes and better representations of vapour-liquid equilibrium (VLE) for many mixtures. The general form of the PR EoS is given by:

$$P = \frac{RT}{V - b} - \frac{a\alpha(T_r, \omega)}{V(V + b) + b(V - b)} \quad \textbf{2-15}$$

where

$$\alpha = \left[1 + m\left(1 - \sqrt{T_r}\right)\right]^2 \qquad \textbf{2-16}$$

$$m = 0.37464 + 1.54226\omega - 0.26992\omega^2 \qquad \textbf{2-17}$$

and T_r is the reduced temperature (T/T_c), T_c is the critical temperature,

Two years later, Peng and Robinson (1978) presented the following modification of Eq. 2-18 to be used for $\omega > 0.49$:

$$m = 0.3796 + 1.4850\omega - 0.1644w\omega^2 + 0.01666w\omega^3 \qquad \textbf{2-18}$$

This equation provides a more accurate vapour pressure prediction for pure heavy hydrocarbons over wide range of temperature.

Peneloux Volume Translation

Due to poor liquid-phase density predictions, the SRK equation was essentially limited to phase equilibrium and gas-phase density predictions until 1982. The SRK equation was often applied with external liquid phase density correlations. This caused problem, for example, near critical systems for which it is difficult to distinguish between the gas and liquid phases. Peneloux *et al*. (1982) modified the SRK with a volume translation parameter. The SRK-Peneloux takes the form:

$$P = \frac{RT}{V - b} - \frac{a\alpha(T_r, \omega)}{(V + c)\ (V\ + b + 2c)} \qquad \textbf{2-19}$$

The parameter *c* is called volume translation. Volume translation corrects molar volumes and phase densities without influencing phase equilibrium calculations. The Peneloux volume translation concept is not limited to the SRK equation, but has been applied to the PR equation by Jhaveri and Youngren (1988). With the Peneloux volume correction, the PR equation becomes:

$$P = \frac{RT}{V\ - b} - \frac{a\alpha(T_r, \omega)}{(V + c)(V + b + 2c) + (b + c)(V - b)} \qquad \textbf{2-20}$$

Mixing Rules

Equations-of-state are applied to multi-component systems by employing mixing rules to determine the *a* and *b* parameters of the mixture. Quadratic mixing rules, originally

proposed by Van der Waals, are used extensively in mixture calculations involving equations-of-state. The attractive force between molecules *i* and *j* is represented by the parameter, a_{ij}, and, as is typical for energy terms, is expressed as a geometric average of the component parameters:

$$a_{ij} = \sqrt{a_i a_j} \qquad \textbf{2-21}$$

The parameter b_{ij}, a volume term, is determined by the arithmetic average:

$$b_{ij} = (b_i + b_j)/2 \qquad \textbf{2-22}$$

By applying the quadratic mixing rule, the following equations are obtained for the parameters of the mixture:

$$a = \sum_i \sum_j x_i x_j a_{ij} \qquad \textbf{2-23}$$

$$b = \sum_i \sum_j x_i x_j b_{ij} \qquad \textbf{2-24}$$

where x_i is mole fraction of the component *i*. It is common practice to incorporate an additional parameter to account for non-ideal interactions between pairs of non-similar molecules:

$$a = \sum_i \sum_j x_i x_j a_{ij} (1 - k_{ij}) \qquad \textbf{2-25}$$

where, k_{ij} is binary interaction parameter (BIP).

Binary interaction parameters are generally determined by minimizing the difference between the predicted and experimental data (mainly the saturation pressures) of the binary systems. The k_{ij} is therefore treated as a fitting parameter and not a rigorous physical term. Several authors have attempted to obtain binary interaction parameters from binary mixture of pure components. Chueh and Prausnitz (Chueh *et al.* 1968) developed a correlation based on critical volume to estimate the binary interaction parameter:

$$k_{ij} = \upsilon i \left(1 - \left(\frac{2(V_{ci} V_{cj})^{1/6}}{V_{ci}^{1/3} + V_{cj}^{1/3}} \right)^{\theta} \right) \qquad \textbf{2-26}$$

where the constant θ and υi, are determined for each EoS using the available binary data. Arai and Nishiumi (Arai *et al.*, 1988) developed a semi empirical correlation for the interaction parameter in Peng Robinson equation in terms of the critical volumes and acentric factors of the pure components. Gao *et al.* (1992) correlated the interaction parameters in the PR equation as functions of the critical temperatures and critical compressibility factor of the pure components. Kordas *et al*. (1994) have investigated interaction parameter in PR EoS for CO_2-hydrocarbon binary mixture and have found that k_{ij} decreases with increasing carbon number and with increasing temperature, Figure 2.3.

Kordas *et al.* (1995) modeled saturation pressures of methane/hydrocarbon (*n*-alkanes up to C44 plus isomers and cycloalkanes) binary systems using the PR EoS, Figure 2.5. They found that the Gao *et al*. correlation gives good results up to *n*-C16 but fails for higher carbon numbers. For higher carbon numbers, they calculated negative k_{ij} value between methane and the hydrocarbon. They correlated the k_{ij}'s with the acentric factor of the heavier component, Figure 2.4.

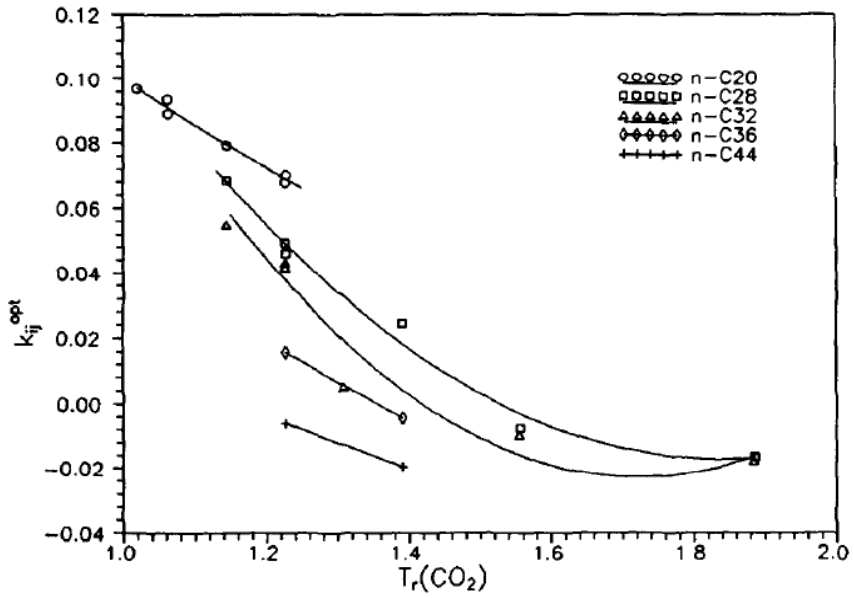

Figure 2.3: Variation of k_{ij} value with $T_r(CO_2)$ for heavy *n*-alkanes (Kordas *et al*. 1994)

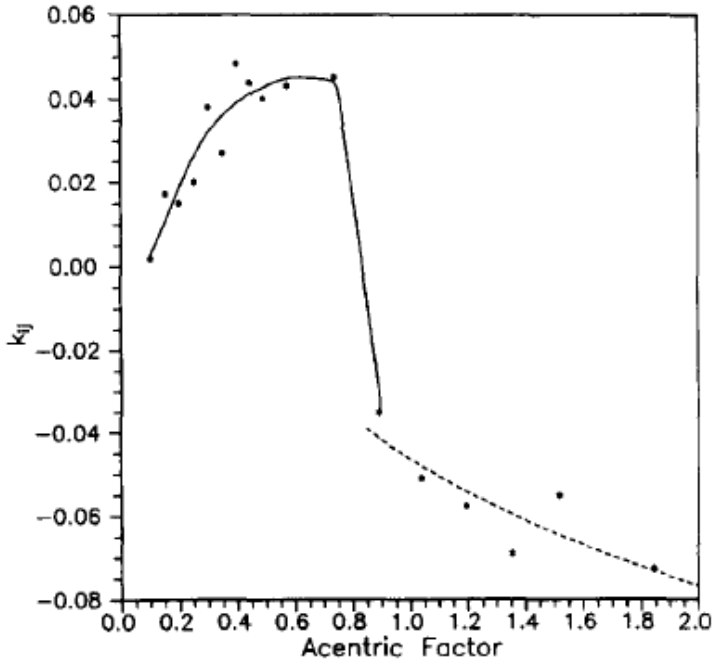

Figure 2.4: k_{ij} value vs. acentric factor for methane/*n*-alkane system (Kordas *et al*. 1995)

Pseudo-Components

Critical properties such as critical temperature (Tc), critical pressure (Pc), acentric factor (ω) for each component in a mixture must be known in order to perform phase equilibrium calculations using an equation-of-state. Generally, critical properties have been measured experimentally for pure components. However, crude oil contains thousands of different components. It is impractical to perform flash calculation using such high number of components. Therefore some components are lumped together and represented as pseudo-components. Critical properties of the pseudo components are estimated using several established correlations such as the Lee-Kesler (1980), Twu (1984), and Nji *et al*. (2008) correlations.

The PR EoS is the most commonly used method for modeling the phase behaviour of hydrocarbons and was chosen for the modeling presented in this thesis. Details of the oil characterization and modeling are provided in Chapter 4.

2.3.5 Cubic-Plus-Association Equation-of-State

Mixtures containing associating compounds, such as alcohols with hydrocarbons and water with hydrocarbons, exhibit extremely non-ideal phase behaviour due to strong hydrogen bonding interactions. Kontogeorgis *et al*. (1996) successfully coupled Wertheim's association theory (1984, 1986) with a cubic equation-of-state in the so-called Cubic-Plus-Association (CPA) EoS to model associating fluids. Application of these models to mixtures containing hydrogen bonding molecules is straightforward once the decision is made on how many association sites (electron donor and acceptor) exist on a self-associating molecule. CPA requires three component parameters for non-associating compounds, namely Tc, Pc, ω, while for self-associating compounds two additional parameters are needed: the association energy, ε^{AB}, and the association volume, β^{AB}. To apply the CPA EoS to mixtures containing two or more associating compounds, combining rules for the association energy and association volume parameters are also required.

Perakis *et al*. (2006) used the geometric mean to determine cross-association energy, ε^{AiBj}, and the cross-association volume, β^{AiBj}, between molecules *i* and *j* :

$$\varepsilon^{AiBj} = \sqrt{\varepsilon^{AiBi}\varepsilon^{AjBj}} \qquad \textbf{2-27a}$$

$$\beta^{AiBj} = \sqrt{\beta^{AiBi}\beta^{AjBj}} \qquad \textbf{2-27b}$$

2.3.6 Statistical Associating Fluid Theory

Statistical Associating Fluid Theory (SAFT) is a versatile molecular model capable of predicting the effects the molecular shape, van der Waals forces, polar interactions, and association on the thermodynamic properties and phase behaviour of the fluids. SAFT was developed by Chapman *et al*. (1988, 1990) based on the Wertheim's theory (1984, 1986) for associating fluids. In SAFT, molecules are modeled as chains of bonded spherical segments. As shown in Figure 2.5, SAFT determines the free energy of a fluid as the sum of the free energy for a collection of spherical "segments" (from which molecules are constructed) plus the change in free energy on "bonding" these spherical

"segments" in a prescribed manner to form the molecules of interest. This change in free energy can be calculated from Wertheim's theory. Finally, if the molecules have association sites, the change in free energy due to these directional interactions are explicitly accounted by using Wertheim's theory. The perturbed chain modification to SAFT (PC-SAFT) was proposed by Gross and Sadowski (2001) to account for the effects of chain length on the segment dispersion energy. For each non-associating species in PC-SAFT, the equation-of-state requires the specification of three physical parameters: σ, the diameter of each molecular segment, *m*, the number of segments in the molecule, and ε/k, the interaction energy (van der Waals attraction) between each molecular segment. There are different correlations for estimating these three parameters for different components and pseudo-components (Chapman *et al*. 2003).

With crude oils, it is assumed that that asphaltenes have self-associated in the crude oil to form pre-aggregates and that, during the precipitation, no further association occurs. Hence, the phase behaviour of the asphaltenes can be qualitatively described in the term of London dispersion interactions and contribution of the polar interactions is assumed to be insignificant. Based on the assumption asphaltene precipitation can be modeled by determining the parameter σ, m, ε/k for each components and pseudo-component.

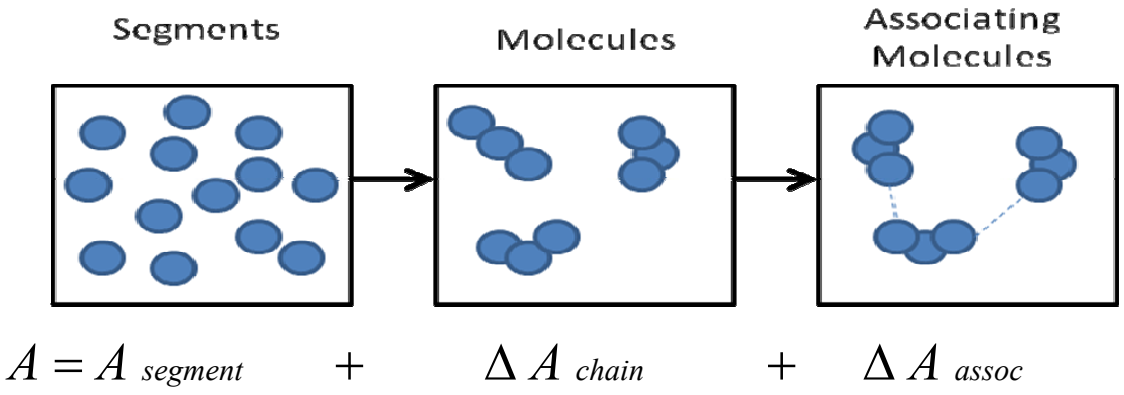

Figure 2.5: Contributions to the SAFT equation-of-state for an associating polyatomic fluid (Chapman *et al*. 2003)

2.4 Application of EoS to Heavy Oil and Bitumen

Many investigators have used equations-of-state to model gas solubility in heavy oils. Mehrotra *et al.* (1985) have characterized Athabasca and Peace River bitumen and predict gas solubility data of mixtures of bitumen and solvent using the PR EoS. They used five and four pseudo-components to characterize the Athabasca and Peace River bitumen, respectively. In both cases, the first three components correspond to the distillable fraction based on SimDist data. For Peace River bitumen, the fourth component corresponds to the non-distillable maltene plus asphaltene fraction. For Athabasca bitumen, the fourth component corresponded to the heavier distillable maltene and the fifth corresponded to the asphaltenes. They adjusted the binary interaction parameter between the solvent and the pseudo-components in order to match the experimental data. Thee binary interaction parameter between the pseudo-components were set to zero. They predicted a second, solvent-rich, liquid phase for CO_2/Athabasca bitumen which was observed in the experimental data. They also tested different critical property correlations such as the Lee-Kesler, Huang-Daubert, and Whitson correlations and found that the Lee-Kesler correlations gave the best results.

Fu *et al*. (1986) predicted gas solubility data of various bitumen and solvent mixtures using the PR EoS. They modified Twu's correlation for estimating critical properties for bitumen. They adjusted binary interaction between solvent and bitumen pseudo components in order to match experimental data.

Kokal and Sayegh (1993) predicted the phase behaviour for mixtures of carbon dioxide and Lone Rock heavy oil using the PR EoS. They collected solubility data for temperatures of 21 and 140ºC at pressures up to 12.4 MPa. They characterized the heavy oil with three pseudo-components: 1) distillable maltenes; 2) non-distillable maltenes; 3) asphaltenes. Critical properties and acentric factor were calculated from the Twu and Kesler-Lee correlations, respectively. Binary interaction parameter between CO_2 and each of Pseudo 1 and Pseudo 2 were regressed to fit the experimental data.

Yazdani *et al.* (2010) modeled the solubility of butane in Frog Lake oil. They divided bitumen into two pseudo components and were able to fit vapour-liquid equilibrium data at 22 ºC using Peng-Robinson EoS.

Jia *et al.* (2011) modeled the phase behaviour of a heavy oil/solvent/steam system with the Peng Robinson EoS. They used five pseudo components to characterize the C7+ fraction of the bitumen. They tested eighteen different characterization combinations (three molecular weight distribution functions and six property correlations). They found that an exponential distribution function for molecular weight and the Lee-Kesler property correlations provided the best fit for the phase envelope and density.

There are fewer investigations of multiple phase behaviour. Pedersen *et al*. (2006) modeled phase behaviour data (involving VLLE regions) of various heavy oil and gas mixtures using the SRK equation-of-state. They adjusted critical properties of pseudo component of heavy oil and noted that phase behaviour involving VLLE regions could be achieved by characterizing the fluid such that the *a* parameter increases more steeply with increasing carbon number.

Castellanos Díaz *et al*. (2011) characterized Athabasca bitumen to model the phase behaviour of mixtures of bitumen, propane, carbon dioxide, and heptane using the Advanced Peng Robinson Equation-of-state. The dataset included saturation pressures, liquid-liquid equilibrium, and asphaltene precipitation. They assessed several extrapolations of the true boiling curve including Gaussian and Gamma distribution based extrapolations. They then divided the extrapolated curve into number of pseudo-components and assigned the critical properties and acentric factors for the pseudo-components using well known property correlations. Interaction parameters between solvent and bitumen pseudo-components were optimized to fit the experimental saturation pressures of pseudo-binary mixtures of bitumen and propane or carbon dioxide. The model correctly predicted saturation pressures and the boundaries of the vapour-liquid-liquid region for pseudo-ternaries of these components. However, the

model under-predicted asphaltene yields at high solvent contents. Also, asphaltene precipitation and saturation pressure data were not available for the same mixtures preventing a more rigorous test of the model.

Chapman *et al*. (2003) applied the SAFT EoS to model asphaltene phase-behaviour in a model live-oil and a recombined oil sample at reservoir conditions. They assumed three pseudo-components for the stock-tank oil and three pseudo-components for the separator gas. SAFT parameters for all pseudo-components except asphaltenes were estimated from correlations based on molecular weight. For asphaltenes, these parameters were determined from the composition and refractive index of the mixture at the onset of asphaltene aggregation with an *n*-alkane titration. To reduce the fitting parameters, binary interaction parameters between asphaltenes and other components were set to zero. They reported very good agreement between the predicted and experimental bubble point pressure and asphaltene onset.

CHAPTER THREE: EXPERIMENTAL METHODS

In this chapter, the experimental methods used in this thesis are presented including: the chemicals and materials used in the experiments; the assays and property measurements performed on the bitumen and condensate samples; the experimental techniques for live oil preparation, saturation pressure measurement, and asphaltene onset and yield measurement.

3.1 Materials and Bitumen Characterization

Bitumen from the Peace River area was supplied by Shell Canada and was distilled and centrifuged by the Alberta Research Council to remove water and solids. The residual water content was less than 1 wt%. This sample will be referred to as Bitumen A.

The synthetic solution gas used to make live oil samples was purchased from Praxair Canada Inc. and had the following composition: 37.80 mol% methane, 61.11 mol% carbon dioxide, and 1.09 mol% nitrogen. For asphaltene extraction and SARA fractionation, commercial grade *n*-pentane (99.7% purity) and *n*-heptane (96% purity) were obtained from ConocoPhillips Co. and ACS grade toluene was purchased from BDH. The condensate used as a solvent in this study was a multi-component mixture obtained from Shell Canada Inc.

3.1.1 Asphaltene Extraction

Asphaltenes were precipitated from the bitumen using a standard procedure (Alboudwarej, 2002). *n*-Pentane was added to the crude oil at a 40:1 (cm^3/g) ratio, the mixture was sonicated for 45 minutes in an ultrasonic bath and left to equilibrate for a total contact time of 24 hours. After equilibration, the supernatant was filtered without disturbing the whole solution. At this point, approximately 20% of the original mixture remained unfiltered. Additional *n*-pentane was added to the mixture at a 4:1 ratio of *n*-pentane to original bitumen mass. The mixture was sonicated again for 45 minutes, left to

settle for 16 hours, and then filtered through the same filter paper. The filter cake (asphaltenes and solids) was washed with approximately 30 ml of *n*-pentane for 5 days (three times per day) after which effluent color was almost colorless. The filter cake was then dried for three days in a fume hood and for an additional day under vacuum conditions to remove the remaining *n*-pentane.

3.1.2 Asphaltene Fractionation

The asphaltenes were fractionated into solubility cuts by dissolving whole asphaltenes in toluene and then adding *n*-heptane to precipitate a desired fraction of the asphaltenes. A given mass of asphaltenes was dissolved in a specified amount of toluene at 23°C and sonicated for 60 to 90 minutes to ensure complete dissolution. A specified amount of *n*-heptane was added and the solution was left to equilibrate for 24 hrs. Then the solutions were centrifuged at 3500 rpm for 5 min. The supernatant was decanted and the solvent was evaporated to obtain a "light" asphaltene cut. The precipitate was dried to obtain a "heavy" asphaltene cut. A series of fractionations were performed at different heptane-to-toluene ratios to obtain different cuts. The asphaltene fractionation was carried out by Diana Barrera at the University of Calgary.

3.2 Assays and Property Measurements

A C30+ compositional analysis was performed on the condensate by Core Laboratories Canada Ltd. (Calgary). The following assays were performed on the bitumen: an ASTM D5307 simulated distillation (SimDist) by Core Laboratories Canada Ltd. (Calgary); a spinning band vacuum distillation by Diana Ortiz at University of Calgary; a modified ASTM D2007 Clay-Gel Adsorption Chromatography method (SARA analysis) at the University of Calgary. The SARA analysis was performed by Diana Ortiz and details of the procedure are provided elsewhere (Alboudwarej, 2003).

Densities of the dead bitumen were measured at temperatures from 19 to 175°C and pressures up to 10 MPa on an Anton Paar DMA HPM density meter. The apparatus for measuring density consists of two transfer vessels in a temperature controlled oven,

connected with an in-line Anton Paar DMA HPM density meter with an external Anton Paar mPDS 2000V3 evaluation unit. Hydraulic oil was used as the displacement fluid which transfers the controlled flow rate from the pump to the sample contained in the transfer vessels. Pressure in the apparatus was controlled using a back pressure regulator on the return line of the hydraulic oil. The densities were repeatable to within 0.5% (Motahhari *et al*., 2011). These measurements were taken by Hamed Motahhari and Fatemeh Saryazdi at the University of Calgary.

The densities of the SARA fractions and asphaltene cuts were measured in another Anton Paar density meter ambient conditions. The resin and asphaltene densities could not be measured directly. Instead, the density of solutions of different concentrations of asphaltenes (or resins) in toluene were measured. The asphaltene (or resin) density was determined by extrapolation the molar volume versus mass fraction (assuming no excess volume of mixing). These measurements were taken by Diana Ortiz at the University of Calgary.

Molecular weights were measured in toluene at 50°C using a Jupiter Instrument Model 833 Vapour Pressure Osmometer and were repeatable within 15%. These measurements were taken by Diana Barrera at the University of Calgary and details of the procedure are provided elsewhere (Yarranton *et al*., 2000).

3.3 Preparation of Live Oil and Solvent Mixtures

All of the live oil and asphaltene onset experiments described below were conducted by the author.

Live Oil:

Live oil samples were prepared using a contactor which consisted of a 600 cm^3 horizontal 5 cm diameter stainless steel cylinder equipped with a piston at each end and a perforated plate placed in the middle of the cylinder to enhance mixing of the bitumen and synthetic solution gas, Figure 3.1. Dead oil and solution gas were injected through two injection

ports mounted in the middle of the cylinder. Heating tape was used to increase the temperature in order to enhance mixing. Two live oil samples were prepared.

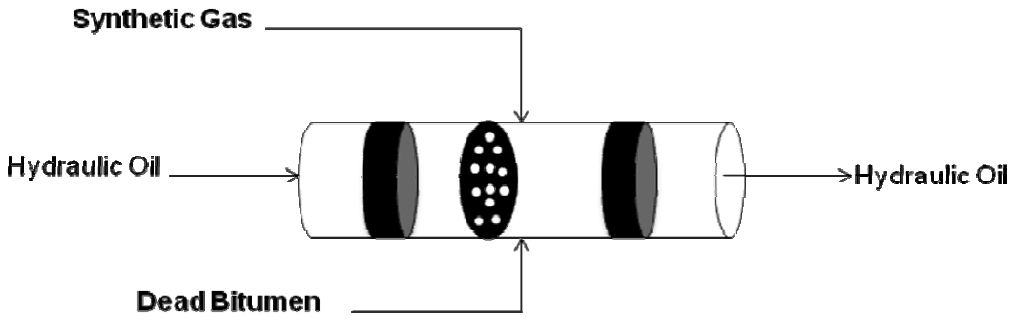

Figure 3.1: Schematic view of the apparatus designed to make Live Oil

To prepare Live Oil 1, 430 g of dead bitumen and 600 cm³ of synthetic gas (37.80 mol% methane, 61.11 mol% carbon dioxide, 1.09 mol% nitrogen) at 17 ºC and 4000 kPaa were injected into the mixing cylinder. The temperature of the cylinder was maintained at 50ºC with a heating tape wrapped around the outside. The dead bitumen and gas mixture was moved back and forth through the mixing plate for 2-3 days and then the pressure was reduced to 2100 ±50 kPaa and the system was equilibrated at 18 ±1ºC for 10 days. After equilibration, any excess gas was displaced slowly at constant pressure. After removing the excess gas, the live oil sample was transferred to a sample cylinder. A small amount of the live oil was taken up in a pycnometer and a single stage flash at 17 ºC and 101 kPaa was carried out in a Jefri Gasometer to determine its gas-oil ratio (GOR).

To prepare Live Oil 2, the same procedure used as for Live Oil 1, except that the system was equilibrated at 18 ±1ºC and 2600 ±50 kPaa. Note that Live Oil 1 was erroneously equilibrated at a lower pressure, but the data are still suitable for modeling purposes

Since the live oils were prepared with an excess of solution gas and the solubility of methane and carbon dioxide in the bitumen are different, the composition of the dissolved solution gas was not the same as the original synthetic gas composition. Therefore, a GC

analysis was performed by Core Laboratories Canada Ltd (Calgary) on the Live Oil 2 solution gas recovered from the Gasometer. The sample for Live Oil 1 was contaminated when sent for testing and could not be analyzed. However, since both live oils were recombined at the same temperature and similar pressures, the solution gas compositions are expected to be the same.

Live Oil Diluted with Condensate:

Condensate-diluted bitumen samples were prepared by mixing known masses of condensate with live bitumen. A known mass of the condensate was placed inside a transfer vessel. Then, a known volume of the live bitumen was pumped into the vessel at a pressure well above the saturation pressure. The volume of the displaced live bitumen was determined from two independent measurements: 1) from the pump displacements and 2) from the displaced hydraulic oil out of the transfer vessel. The mixing of the bitumen and condensate was completed by flowing the mixture back and forth between two transfer vessels.

3.4 Saturation Pressure Measurement

Saturation pressures data were collected for live oil at solvent contents up to 10 wt% and temperatures from 20 to 180°C. Saturation pressures of the *n*-pentane diluted dead bitumen with *n*-pentane content up to 30 wt% were also measured at temperatures ranging from 90 to 180 ºC. Details are provided below.

3.4.1 Apparatus

Saturation pressures measurements were carried out in a DB Robinson Jefri PVT cell, Figure 3.2. The PVT cell was placed in an air-bath which controls the PVT cell temperature to within ±0.1ºC. The PVT cell consists of a transparent Pyrex cylinder inside a steel shell. The PVT cell is equipped with a magnetic stirrer which mixes the fluid to accelerate equilibration. A floating piston furnished with an o-ring separates the sample fluid in the Pyrex cylinder from the hydraulic fluid. A cell window provides a view along the length of the cell.

The volume of the sample fluid in the cell is determined by the calibrated cathetometer. The cathetometer is precise to $\pm 10^{-7}$ m^3. The maximum capacity of the PVT cell is 100 cm^3. The maximum pressure rating is 69 MPa and it can operate at temperature from -15 ºC to 200 ºC. The volume of cell, and hence the pressure of the sample fluid under investigation, were controlled by a variable volume computer-controlled positive displacement pump which allowed for the injection or the removal of the transparent displacing fluid (hydraulic oil). The same hydraulic oil is connected to the outer steel shell to maintain a balanced (minimal) differential pressure on the sapphire cylinder. Equilibration of the fluid under investigation was achieved by means of a magnetically coupled impeller mixer mounted on the bottom end cap.

3.4.2 Dead Volume Measurement

The volume between the magnetic stirrer and Valve 1 in Figure 3.2 is a dead volume since the magnetic mixer could not mix the fluid present in this space. In order to measure the dead volume, the floating piston was placed in its bottommost position and a constant pressure (about 3500 kPaa) was applied. The dead volume was placed under vacuum, toluene was injected into this space at a pressure lower than piston top pressure, and the volume of injection was measured using pump displacement. The dead volume was determined to be 1.9 cm^3.

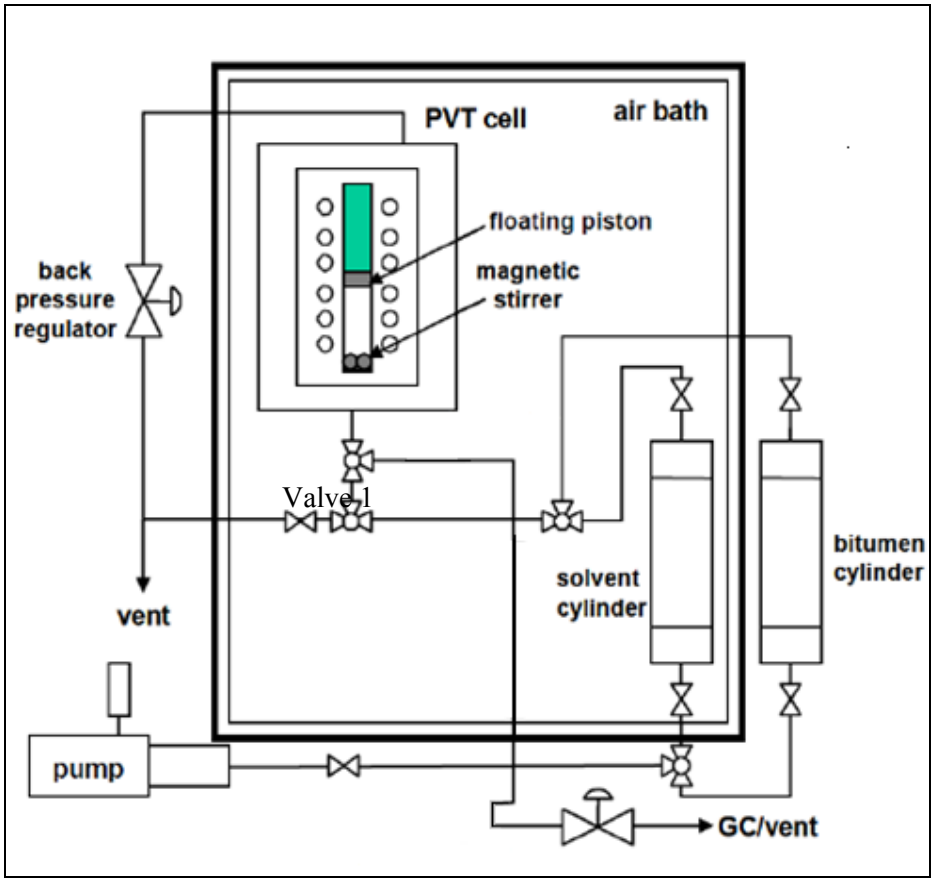

Figure 3.2: Schematic of the PVT Cell (Badamchi-Zadeh, 2009)

3.4.3 Sample Injection Procedure

Before each sample injection, the PVT cell was cleaned and placed under vacuum. Fluid to be injected in the PVT cell was always a single phase and the injection pressure was controlled with a back pressure assembly.

For live oil and solvent mixtures, samples were prepared outside the PVT cell using a contactor cylinder-piston as described in Section 3.3. Then the sample was displaced into the PVT cell using the positive displacement pump. The initial cathetometer and pump volume readings (using a vernier scale on the top and side of the pump) and the injection temperature were recorded. The pump pressures at the start and end of injection were set

equal to avoid accumulation of any fluid in the injection line. After injection of the sample, the cathetometer and final pump volume readings were recorded.

The final cathetometer reading was subtracted from the initial reading and the dead volume was added to determine the volume of fluid injected into the PVT cell. Similarly, the difference between initial and final pump readings also gave the volume of fluid injected. Hence, the injection volume was determined from the two independent measurements, first from the pump displacements and the second from the cathetometer readings. In all cases, the injection volumes measured from the above two methods were equal within error of the measurements (±1.5%).

For the *n*-pentane and dead bitumen mixture, the sample was prepared directly in the PVT cell. First, a known amount of dead bitumen was injected into the cell just above the saturation pressure using the procedure described above. The bitumen mass was determined from volume measurement and its density at the injection pressure and temperature (from interpolation of measured densities – Section 3.2). Then a known volume of *n*-pentane was added to cell while pressure was maintained so that all the system remained in the liquid phase. Mixing the fluid in the liquid phase region accelerated equilibration. The mixture was stirred using a magnetic mixer for about two hours and then it was left to equilibrate until the PVT cell pressure became constant for about four hours.

3.4.4 Saturation Pressure Determination

For the measurement of saturation pressures, the PVT cell was maintained at a constant temperature. The sample fluid was compressed and equilibrated at a pressure well above the bubble point. Then the pressure was decreased by expanding the cell volume using the pump with a step-wise volume expansion. After each step, sufficient time was given for the fluid to equilibrate until the pressure was stable for 2 to 3 hours. In general, the equilibration time required in the single liquid phase region and two-phase region were

approximately 8 and 24 hours, respectively at room temperature condition while at higher temperature it is 2 and 6 hours, respectively.

The volume inside the cell was also measured at each step using the cathetometer. The specific volume was determined from the volume measurements and the known mass of the fluid in the cell. Then, pressure was plotted against the specific volume. Due to the high compressibility of gas, pressure decreases significantly in the liquid phase region, but once vapour appears there is relatively little change in pressure. Hence the bubble point was identified from the change in slope in the pressure-volume plot, Figure 3.3.

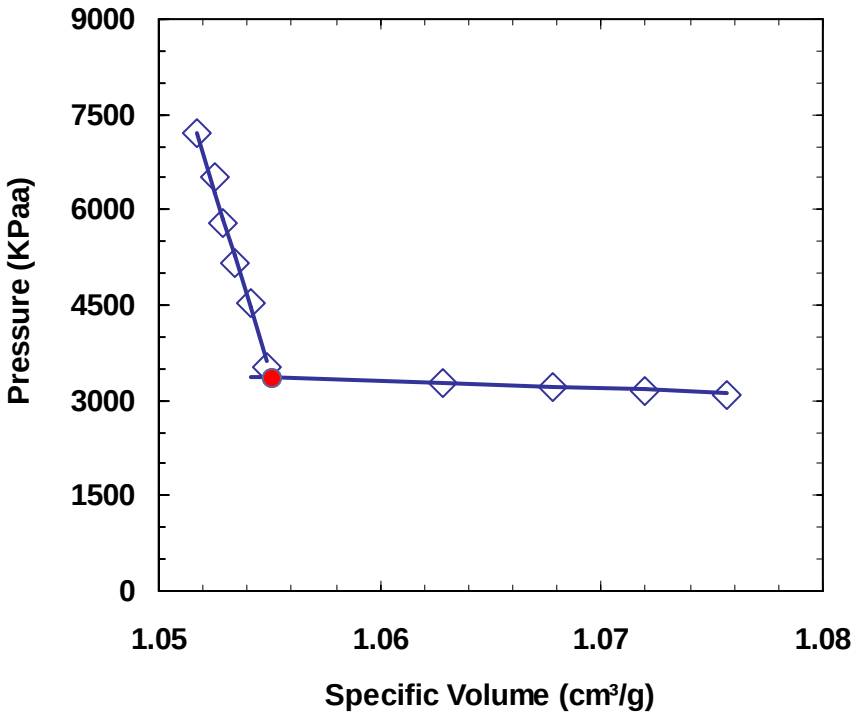

Figure 3.3: Pressure-volume isotherm of Live Oil 1 at 120 ºC

3.5 Asphaltene Precipitation Onset Measurements

In this study, the onset of precipitation is defined as the minimum amount of solvent required to cause asphaltene precipitation at a given temperature and pressure. The onset

of asphaltene precipitation was measured visually using a High Pressure Microscope. The procedure is described below.

3.5.1 Sample Preparation

Bitumen contains approximately 0.2 wt% solid particles (silica, clay, inorganic solids) and 1wt% water. The solids and water droplets act as background noise in the micrograph and have to be removed in order to clearly see the asphaltene precipitation onset. They were removed using a multistage filtration process. Filtration was carried out at 50ºC in order to increase the mobility of the bitumen. Bitumen in a transfer vessel was displaced through a silver membrane filter held in a stainless steel casing. The bitumen was fed through the filter very slowly (about 0.05-0.1 cm^3/min) in order to avoid passage of solid particle through the filter. The filtering was done in three stages: first through a 5 micron filter to remove the larger particles; second through a 1.2 micron filter; and third through a 0.2 micron filter. Figure 3.4 show that the filtration process removed most of the solid particles and water droplets. A small number of water droplets remained in the bitumen (grey dots in the right micrograph) but not enough to obscure the asphaltene precipitation onset measurement.

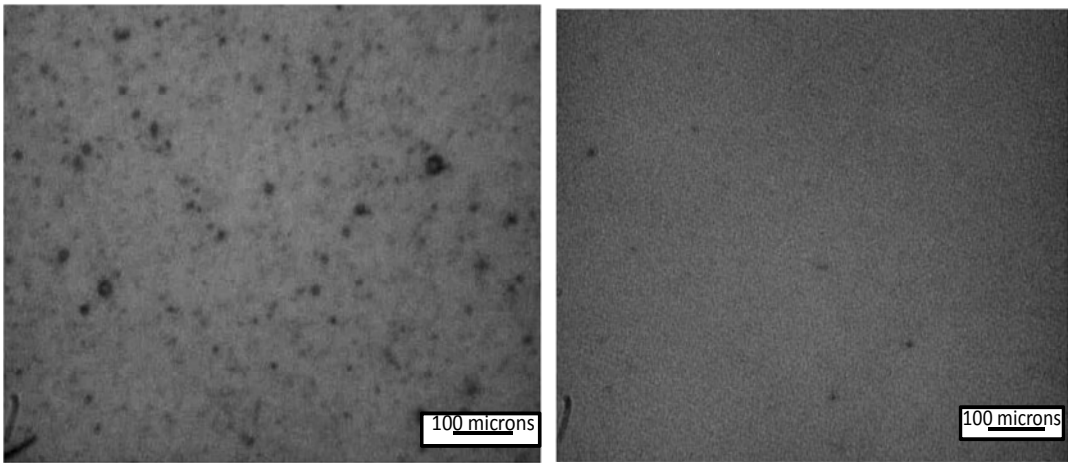

Figure 3.4: Unfiltered (left) and filtered (right) bitumen observed through the HPM cell.

3.5.2 Apparatus

The High Pressure Microscope consists of two mixing cylinders, each having a magnetic stirrer. Both mixing cylinders have floating pistons separating hydraulic oil from the sample fluid. These cylinders are connected to the High Pressure Microscope Cell (HPM Cell). The HPM cell basically consists of two Pyrex windows with the gap between the windows adjusted to 100-400 microns. A small gap between the windows helps to visualize very dark fluids. The samples considered in this thesis are dark and a 100 micron gap was selected. A light source is located on one side of the HPM cell and a high focal length camera on the other side is connected to a computer to capture digital images and video, Figure 3.5.

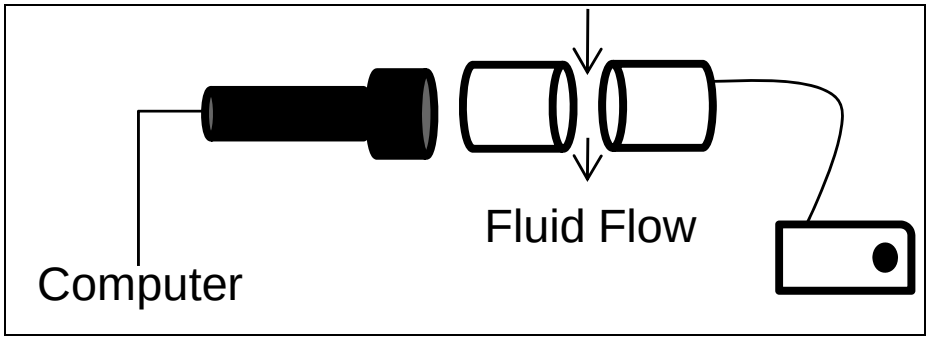

Figure 3.5: Schematic of High Pressure Microscope Cell

Mixing cylinders can be connected to the pump or back pressure assembly which allows moving the sample back and forth between the two cylinders. The High pressure Microscope apparatus is placed in the same air-bath in which the PVT cell was placed. The HPM is rated for temperatures up to 200°C and pressures up to 20,000 psi (138 MPa). Figure 3.6 shows schematic of the High Pressure Microscope.

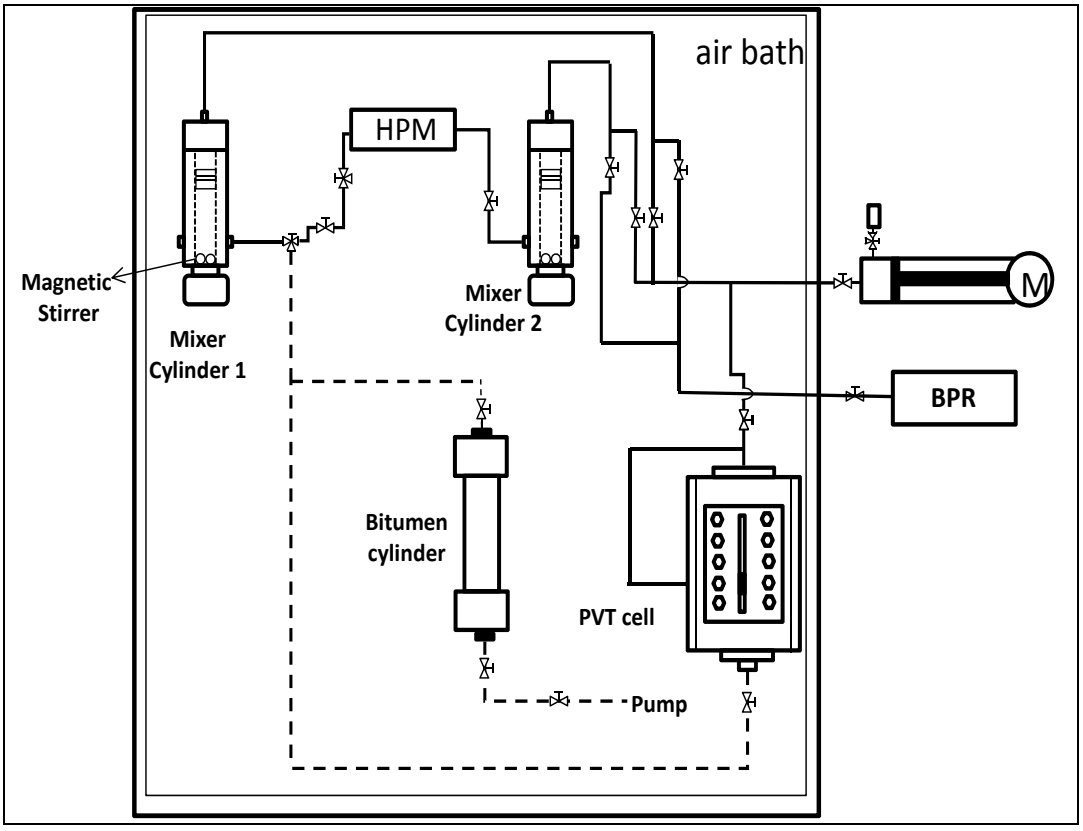

Figure 3.6: Schematic of High Pressure Microscope

3.5.2.1 Dead Volume Measurement

Dead volume here refers to minimum volume of sample required to move pistons of both mixing cylinders. In order to measure the dead volume, the floating pistons of both pistons cylinders were placed in its bottommost position and a constant pressure (about 3500 kPaa) was applied by connecting both cylinders to back pressure regulator. The dead volume was placed under vacuum, toluene was injected into this space at a pressure lower than pistons top pressure, and the volume of injection was measured using pump displacement. The dead volume was determined to be 7.77 cm^3.

3.5.3 Asphaltene Precipitation Onset Measurement Procedure

3.5.3.1 Bitumen Injection

First, the High Pressure Microscope was cleaned and placed under vacuum. The floating pistons of both mixing cylinders were placed in their bottommost positions and both were connected to a back pressure assembly. Initial pump readings, the weight of the hydraulic oil container (a component of the back pressure assembly), and the injection temperature were recorded. Then the bitumen sample was displaced into the HPM. The pump pressures at the start and end of the injection were set equal in order to avoid accumulation of any fluid in the injection line.

After injection of the bitumen, a final pump volume reading was recorded. Also the weight of hydraulic oil which came out from back pressure assembly was measured. The difference between the initial and final pump readings gave the volume of the bitumen injection. The volume of hydraulic oil displaced through the back pressure assembly plus dead volume were measured to verify the volume of bitumen injection. In all cases, the injection volume measurements from the both methods were equal to within error of measurement (± 2%).

3.5.3.2 Solvent Injection

Solvent used for titration was first injected into the cleaned and vacuumed PVT cell. The PVT cell was then connected to the HPM, Figure 3.6. Solvent was injected at a rate of 1-2 cm^3/hr from the PVT cell into the mixing cylinder containing the bitumen in a stepwise process. The volume of injection was determined from the cathetometer and pump displacement readings. During the injection of solvent, a magnetic stirrer was used to ensure mixing between the solvent and bitumen. After injection of the solvent, the contents of the mixing cylinder were displaced slowly to the other mixing cylinder in order to displace the solvent remaining in the transfer line. Then, the fluid was moved back and forth between the two cylinders until a uniform mixture was formed as indicated by constant pump pressure readings at constant flow rate. During this process,

the fluid was also continuously monitored using the HPM cell for indications of asphaltene precipitation. If asphaltene precipitation did not occur, solvent was again injected from the PVT cell and whole process was repeated.

3.5.4 Mixing Methodology

In a preliminary run, the bitumen was titrated with *n*-pentane. During this run, it was found that asphaltene precipitation occurred at a much lower *n*-pentane percentage than expected, Figure 3.7. A local high concentration of the *n*-pentane (sufficient to induce precipitation) occurred because the injection rate was too high (approximately 100 cm^3/h). Once asphaltenes precipitate, it is very difficult to redissolve them and therefore the precipitate persisted throughout the experiment. Therefore, it is necessary to inject solvent at a slow rate in order to avoid premature asphaltene precipitation and an erroneously low estimate of the onset condition.

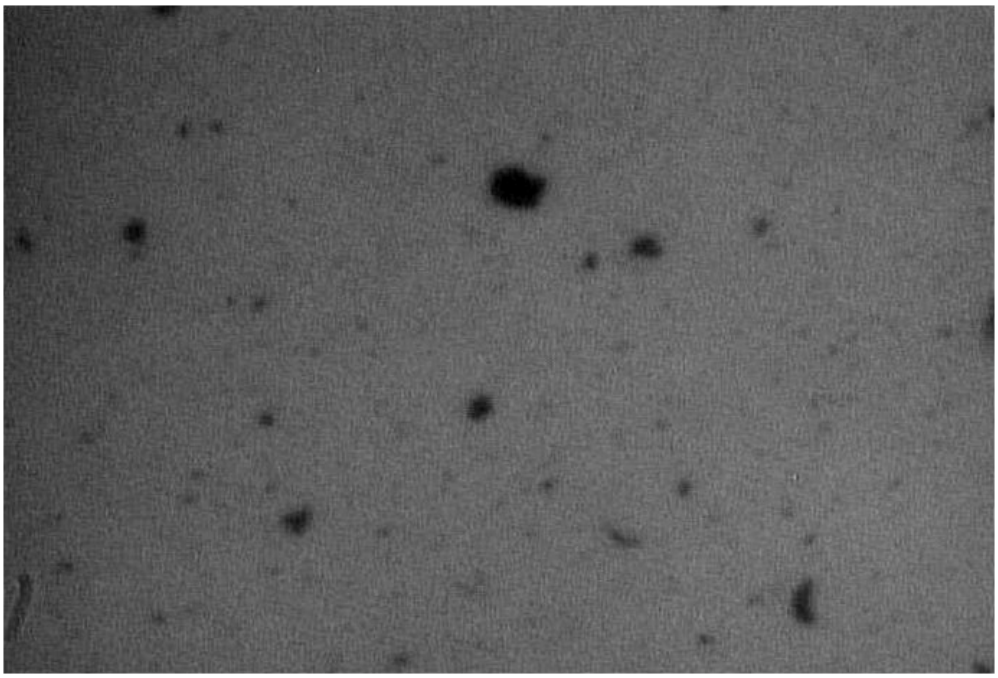

Figure 3.7: Bitumen diluted with 20 wt% of *n*-pentane, precipitation of asphaltenes caused by high local concentration of solvent

3.6 Asphaltene Yield Measurements

Asphaltene yield is the mass fraction of the bitumen that precipitates and is not redissolved after washing the precipitant. Asphaltene yields from diluted bitumen were measured at ambient conditions. Solutions of different proportions of *n*-pentane and bitumen were prepared in centrifuge tubes from specified masses of bitumen and solvent. The solutions were sonicated for one hour in an ultrasonic bath and left to settle for a day to ensure complete precipitation. The mixture was then centrifuged at 3500 rpm for 6 minutes. The supernatant was decanted and the residual asphaltenes were washed with the same solvent and dried. The mass of dry asphaltenes was measured to determine the yield of precipitate (mass of precipitate divided by mass of bitumen) for each solution. The asphaltene yield condition was determined by extrapolating the yield curve to zero yield.

CHAPTER FOUR: FLUID CHARACTERIZATION FOR EOS MODELING

As was discussed in Chapter 2, the Peng-Robinson equation-of-state is well suited to model the phase behaviour of petroleum fluids. The Advanced Peng Robinson EoS (VMGSim^{TM}, 2010), which includes volume translation, was used to predict the phase behaviour of the bitumen/solvent systems considered in this study. To implement the equation-of-state model, a fluid characterization is required; that is, a representative set of pseudo-components each with a defined mass fraction, density, boiling point, critical properties and acentric factors. The characterized fluid and an initial guess of binary interaction parameters are input into the EoS model to determine the number of phases formed plus the amount and composition of the different phases. This chapter presents the bitumen and condensate characterizations.

4.1 Crude Oil Characterization

One approach for crude oil characterization is to divide the boiling point curve of the fluid into cuts (pseudo-components) representing different boiling fractions. The molecular weight and specific gravity are then assigned to each cut using correlations constrained by any additional data available such as the average specific gravity and molecular weight of the oil. The critical properties and acentric factor are then determined using another set of correlations. Once the pseudo-components are characterized and their compositions defined they are input into the EoS. The saturation pressure of mixtures of heavy oil and a given solvent are calculated using a flash calculation (Rachford and Rice, 1952) with a phase stability test (Michelsen, 1982). The binary interaction parameters are iteratively optimized to best fit the measured saturation pressures. Figure 4.1 shows the algorithm for the characterization of crude oil.

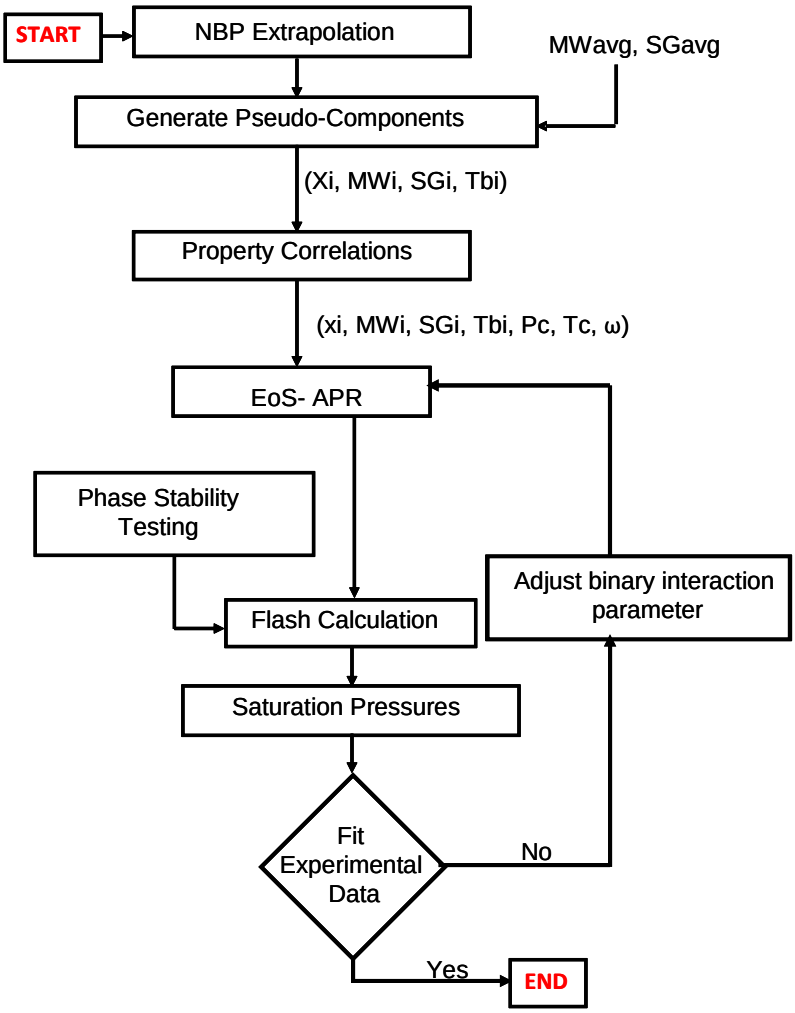

Figure 4.1: Flow diagram algorithm for crude oil characterization.

4.2 Dead Bitumen Characterization

The challenge with heavy oil or bitumen characterization is that a complete compositional analysis of heavy oils and bitumens is not available. Even when high temperature vacuum distillation is used, only 20 to 40 wt% of the heavy oil is distillable. Simulated distillation assays can extend the characterization to approximately 50 wt% of the heavy oil, but the boiling point calculations are based on extrapolations that cannot be validated against measured data. Hence, for heavy oils, a methodology is required to

extrapolate the normal boiling point (NBP) curve to obtain accurate phase behaviour predictions.

There are several approaches to extrapolate the normal boiling point curve; in this study, the method recommended by Castellanos *et al.* (2011) is followed. They characterized the maltenes and asphaltenes separately because the asphaltenes are self-associated components and therefore are not expected to follow the same property trends as the non-associated maltene components. This approach also makes use of the additional molecular weight and density data available for the asphaltenes.

The first step was to define 80.4 wt% of the bitumen as maltenes and the remainder asphaltenes based on the SARA analysis of the bitumen, Table 4.1. Then a characterization was constructed as follows:

1. determine the maltene boiling point, molecular weight, and density distributions; divide into pseudo-components
2. determine the asphaltene boiling point, molecular weight, and density distributions; divide into pseudo-components
3. recombine the distributions into a set of pseudo-components representing the whole dead bitumen; calculate critical properties and acentric factors for each pseudo-component

Each step is discussed below.

Table 4.1: SARA fractions and properties for bitumen

Fraction	**Weight Fraction**	**Density (kg/m^3)**	**MW (g/mol)**
Saturates	0.17	877	350
Aromatics	0.469	1001	490
Resins	0.167	1075	950
C_5-Asphaltenes*	0.194	1177	-

* C_5-Asphaltenes precipitated with a 40:1 volume ratio of *n*-pentane to bitumen

4.2.1 Maltene Partial Characterization

The maltene characterization was constructed from a spinning band vacuum distillation assay performed on the bitumen, Table 4.2. The vacuum distillation data for the bitumen was converted to normal boiling point (NBP) data by converting measured vapour temperature to atmospheric equivalent temperature (AET) using the equations derived by Maxwell and Bonnell (1957). The vacuum distillation was measured on a volume basis and was converted to mass basis using liquid densities calculated with the Katz-Firoozabadi method (1978). The calculated liquid density of each cut was adjusted by a constant multiplier to fit the average values of the bitumen distilled (996.84 kg/m^3). Table 4.3 also shows the converted distillation data.

A SimDist assay (ASTM D5307) is also provided in Table 4.3. The SimDist assay is similar to distillation data for the first 10 wt% of the sample, but deviates for heavier cuts. Therefore, only the vacuum distillation data were used for the maltene characterization. A SimDist characterization is also presented but only for comparison.

The normal boiling point curve of the bitumen was extrapolated using a Gaussian distribution from 26 wt% distilled to 80.4 wt% distilled. The final boiling point for maltenes from the extrapolation was 584ºC, Figure 4.2. As a comparison, the SimDist data were extrapolated in the same way. For SimDist data, the final boiling point for maltenes from the extrapolation was 770ºC, Figure 4.2. This is a significant difference and will result in very different phase behaviour predictions for liquid-liquid equilibria. Distillation data are a more direct measurement of boiling points and are more likely to be accurate than SimDist data which are based on property correlations to retention times. Therefore, Simdist data should be used with caution beyond approximately 20 wt% distilled.

Table 4.2: Vacuum distillation data for the bitumen sample

Volume % Distilled	Measured Vapor Temperature [ºC]	Atmospheric Equivalent Temperature [ºC]
1.68	75.4	218.0
3.36	93.5	237.4
5.04	105.5	252.4
6.72	118.0	267.9
8.40	126.4	278.6
10.08	135.5	289.4
11.76	145.3	301.7
13.44	154.8	313.5
15.13	163.5	324.0
18.49	176.5	339.8
20.17	184.6	349.6
21.85	191.6	358.0
23.53	199.2	367.3
25.21	205.8	375.2
26.89	210.0	380.0
28.57	211.9	382.5
30.25	213.1	384.0
31.93	214.3	385.0

Table 4.3: Simulated distillation and distillation data for the bitumen sample

ASTM D5307		Distillation Data	
Cumulative Mass%	**Boiling Point [ºC]**	**Cumulative Mass%**	**Boiling Point [ºC]**
0.01	185	0.6	202.7
5	262	1.2	210.8
10	304.5	1.8	218.9
15	340.5	2.5	227
20	372.5	3.1	235.2
25	407	3.9	243.3
30	440	4.7	251.3
35	472	5.5	259.4
40	504	6.4	267.8
44	531.5	7.6	275.7
		8.8	283.7
		9.9	291.8
		10.9	300
		11.9	308.1
		13.1	316.2
		14.5	324.4
		16.2	332.4
		17.6	340.3
		19	348.7
		20.5	356.6
		22	364.8
		23.8	373.3
		26	380.5

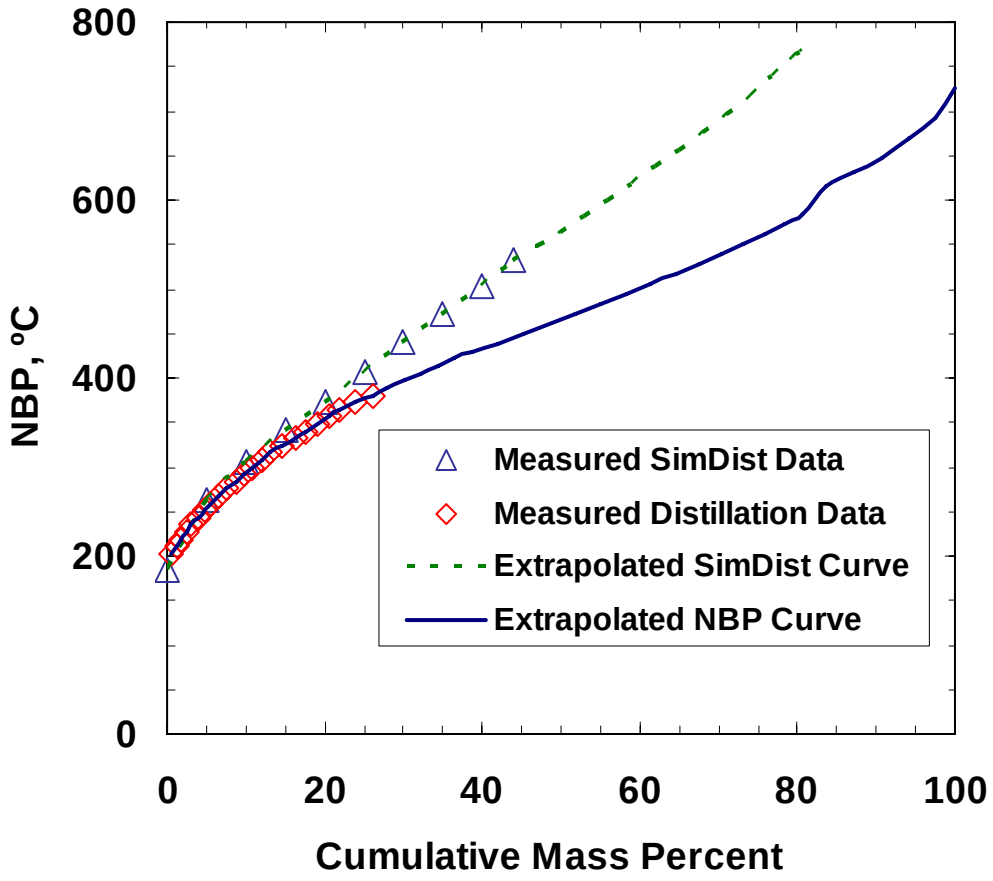

Figure 4.2: Extrapolation of the distillation and SimDist data of bitumen for the maltene fraction

To assign pseudo-components, the NBP curve of the maltenes was divided into three sections: a light oil section (from 200 to 427ºC), a medium oil section (from 427 to 580ºC), and a heavy oil section (580 to 600ºC). This approach allowed the number of pseudo-components to be optimized for the steep and shallow sections of the NBP curve. Preliminary simulations were then performed using VMGSim^{TM} (Version 6.0) to determine the minimum number of pseudo-components required to recreate the NBP curve. The NBP curve of the maltenes could be recreated by dividing it into ten pseudo-components: six for the light oil section, three for the medium oil section, and one for the heavy oil section, Figure 4.3. The molecular weight and specific gravity of each pseudo-component were calculated using the Lee-Kesler (1976) and Katz Firoozabadi (1978)

correlations, respectively. The calculated molecular weight and specific gravity of each pseudo-component were adjusted by a multiplier to fit the average values of the maltene (495 g/mol and 982 kg/m³).

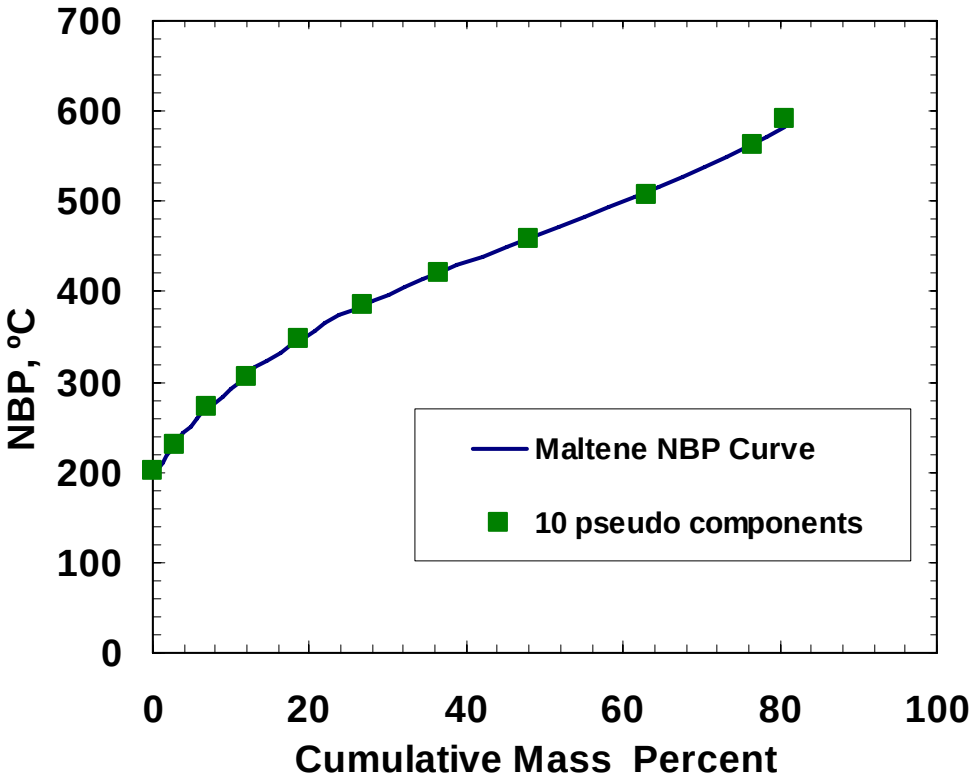

Figure 4.3: Comparison between the maltene distillation curve and NBP curve recreated using ten pseudo-components

4.2.2 Asphaltene Partial Characterization

For asphaltene characterization, asphaltene self association had to be taken into account (discussed in Section 2.1.1). Alboudwarej *et al.* (2003), considered asphaltenes to be macromolecule aggregates formed from the monodispersed asphaltene monomers. Therefore, they divided asphaltenes into pseudo-component fractions of different molar mass based on the Gamma distribution function. The Gamma distribution function is given by,

$$f(MW) = \frac{(MW - MW_m)^{\beta-1}}{\Gamma(\beta)} \left[\frac{\beta}{MW_{Avg} - MW_m} \right]^{\beta} \exp\left[\beta \frac{MW - MW_m}{MW_{Avg} - MW_m} \right] \quad \textbf{4-1}$$

where MW_m, and MW_{avg} are the monomer molar mass and average 'associated' molar mass of asphaltenes, and β a parameter which determines the shape of the distribution.

As discussed in Section 3.1.2, asphaltenes were fractionated into solubility cuts and the density of different cuts was measured, Table 4.4. The lightest cut from the asphaltene fractionation did not appear to self-associate and its molecular weight was taken as the average monomer molar mass. Its measured molecular weight was 840±50 g/mol. Once the monomer properties were fixed, β was set to 2.5 and MW_{Avg} was set to 2000 g/mol based on the previous modeling (Castellanos-Diaz *et al.,* 2011). Then the gamma molar distribution was into 6 pseudo-components of equal weight fraction.

Table 4.4: Asphaltene cut mass fraction and densities

Fraction*	Weight %	Density, kg/m^3
Whole	1	1172
H60L	0.815	1162
H77L	0.462	1138
H92L	0.209	1108
H60H	0.185	1193
H77H	0.538	1186
H92H	0.791	1184

* HXX: XX indicates the wt% heptane in toluene used for fractionation; L = light, H = heavy.

The specific gravity of the asphaltene components was determined from the density data, Table 4.4. The following distribution was found to fit the data:

for $W \leq 0.4$: $\gamma = 1.09 + 0.25W$ **4-2**

for $W > 0.4$, $\gamma = 1.19$ **4-3**

where W is cumulative weight fraction of the asphaltenes and γ is the specific gravity. The distribution was integrated to determine the density of each asphaltene component.

As recommended by Whitson and Brule (2000), the Søreide correlation was used to estimate the NBP of asphaltene components from their molecular weight and density:

$$T_b = 1928.3 - (1.695*10^5)MW^{-0.03522}\gamma^{3.266} * \exp[-(4.922*10^{-3})MW - 4.7685\gamma + (3.462*10^{-3})MW\gamma] \quad \textbf{4-4}$$

where the unit of T_b is ºR and MW is g/mol. The monomer molecular weight was set to 820 g/mol (within experimental error of the measured molecular weight of the lightest asphaltene cut) and the density to 1090 kg/m³ (lightest asphaltene cut density) to give an NBP of 585ºC. This NBP is consistent with the end point of the extrapolated maltene NBP of 584°C. Note that the SimDist characterization had an end point of 770°C which is not consistent with the asphaltene characterization.

4.2.3 Bitumen Characterization

The mass fraction of the bitumen pseudo-components were calculated from the maltene and asphaltene partial characterizations multiplied by the mass fraction of maltene and asphaltene in the bitumen, respectively. The density and molecular weight of each pseudo-component were not altered. Figure 4.4 shows the combined NBP curve for the whole dead bitumen. The mass fraction, density, and molecular weight of each pseudo-component are provided in Table 4.5.

The critical properties were determined from the generalized correlations in terms of specific gravity, γ, normal boiling point, *Tb*, or the molecular weight, *MW*. Although there are many correlations for critical properties estimation (Whitson and Brule, 2000), properties of the pseudo components were estimated using Lee-Kesler correlation.

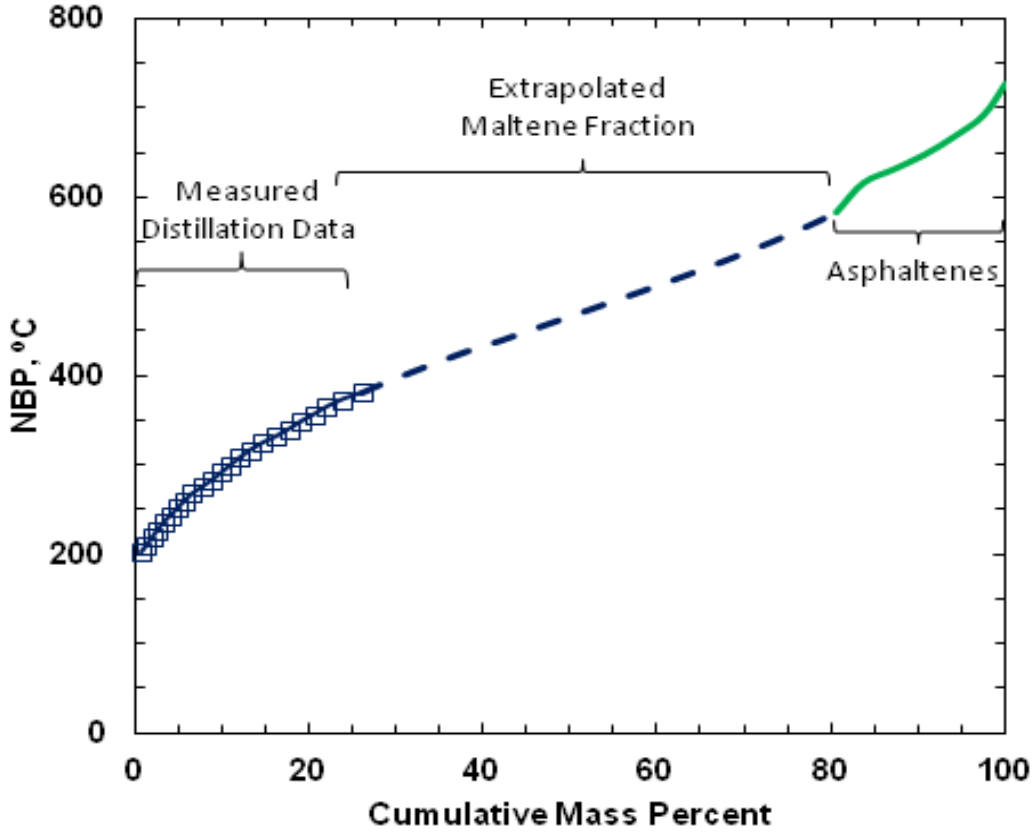

Figure 4.4: Extrapolated curve for the bitumen

Table 4.5: Pseudo-components of bitumen

Names	Mass Fraction	Molecular Weight	Mole Fraction	NBP [ºC]	Density at 15.55°C [kg/m³]
Maltene[214]C	0.029	248	0.067	214	881
Maltene[252]C	0.039	291	0.078	252	902
Maltene[288]C	0.051	334	0.089	288	919
Maltene[328]C	0.066	388	0.099	328	937
Maltene[367]C	0.082	447	0.107	367	956
Maltene[403]C	0.098	501	0.113	403	972
Maltene[440]C	0.113	561	0.117	440	989
Maltene[485]C	0.148	637	0.135	485	1006
Maltene[535]C	0.131	730	0.104	535	1020
Maltene[572]C	0.048	802	0.035	572	1028
Asphaltene 1	0.024	1191	0.012	651	1121
Asphaltene 2	0.031	1549	0.012	682	1161
Asphaltene 3	0.033	1867	0.010	700	1190
Asphaltene 4	0.036	2223	0.009	725	1190
Asphaltene 5	0.038	2718	0.008	749	1190
Asphaltene 6	0.031	3690	0.005	776	1190

4.2.3.1 Lee-Kesler Correlation

In the Lee-Kesler (1976) correlation, specific gravity, γ, and normal boiling point, T_b are used as input to estimate critical pressure, Pc, critical temperature, Tc , and acentric factor, ω. The correlation is presented in its standard form based on Field Units,

$$\ln P_c = 8.3634 - \frac{0.0566}{\gamma} - \left[\left(0.24244 + \frac{2.2898}{\gamma} + \frac{0.11857}{\gamma^2}\right)*10^{-3}\right]T_b + \left[\left(1.4685 + \frac{3.648}{\gamma} + \frac{0.47227}{\gamma^2}\right)*10^{-7}\right]T_b^{\,2} - \left[\left(0.42019 + \frac{1.6977}{\gamma^2}\right)*10^{-10}\right]T_b^{\,3} \quad \textbf{4-5}$$

$$T_c = 341.7 + 811\gamma + (0.4244 + 0.1174\gamma)T_b + (0.4669 - 3.2623\gamma)*10^5 T_b^{\,-1} \quad \textbf{4-6}$$

$$\omega = \frac{\ln(\frac{14.7}{P_c}) - 5.92714 + \frac{6.09648}{T_{br}} + 1.28862\ln(T_{br}) - 0.169347T_{br}^6}{15.2518 - \frac{15.6875}{T_{br}} - 13.4721\ln(T_{br}) + 0.43577T_{br}^6} \quad T_{br}<0.8 \qquad \textbf{4-7a}$$

$$\omega = -7.904 + 0.1352Kw - 0.007465Kw^2 + 8.359T_{br} + \frac{(1.408 - 0.01063Kw)}{T_{br}} \quad T_{br}\geq 0.8 \qquad \textbf{4-7b}$$

$$Kw = \frac{1.8T_b^{1/3}}{SG} \qquad \textbf{4-8}$$

where T_{br}= $T_b/T_{c,}$.and P, T, and V are in psia, ºR, ft³/lbmol, respectively.

Table 4.6: Critical properties and acentric factor of Bitumen pseudo-components using Lee-Kesler correlation

Names	Lee-Kesler correlation		
	Pc [kPaa]	Tc [ºC]	ω
Maltene[214]C	2782	420	0.45
Maltene[252]C	2483	459	0.52
Maltene[288]C	2231	493	0.59
Maltene[328]C	1997	530	0.67
Maltene[367]C	1795	566	0.75
Maltene[403]C	1624	598	0.83
Maltene[440]C	1470	631	0.91
Maltene[485]C	1299	669	1.02
Maltene[535]C	1110	710	1.15
Maltene[572]C	983	739	1.25
Asphaltene 1	978	829	1.24
Asphaltene 2	994	869	1.24
Asphaltene 3	1025	894	1.23
Asphaltene 4	935	911	1.29
Asphaltene 5	854	927	1.34
Asphaltene 6	771	945	1.40

4.3 Condensate Characterization

Figure 4.5 is an NBP curve generated based on the boiling point range from the C30+ analysis of condensate solvent, Table 4.7. Normal and *iso*- butanes and pentanes were treated as pure components. The NBP curve of the C6+ fraction was divided into three sections: a light oil section (from 37 to 90 ºC), a medium oil section (from 90 to 200 ºC), and a heavy oil section (200 to 450 ºC). Preliminary simulations were then performed using VMGSim^{TM} (Version 6.0) to determine the minimum number of pseudo-components required to recreate the NBP curve. The NBP curve of the C6+ fraction could be recreated by dividing it into eight pseudo-components: four for the light oil section, two for the medium oil section, and two for the heavy oil section, Figure 4.5.

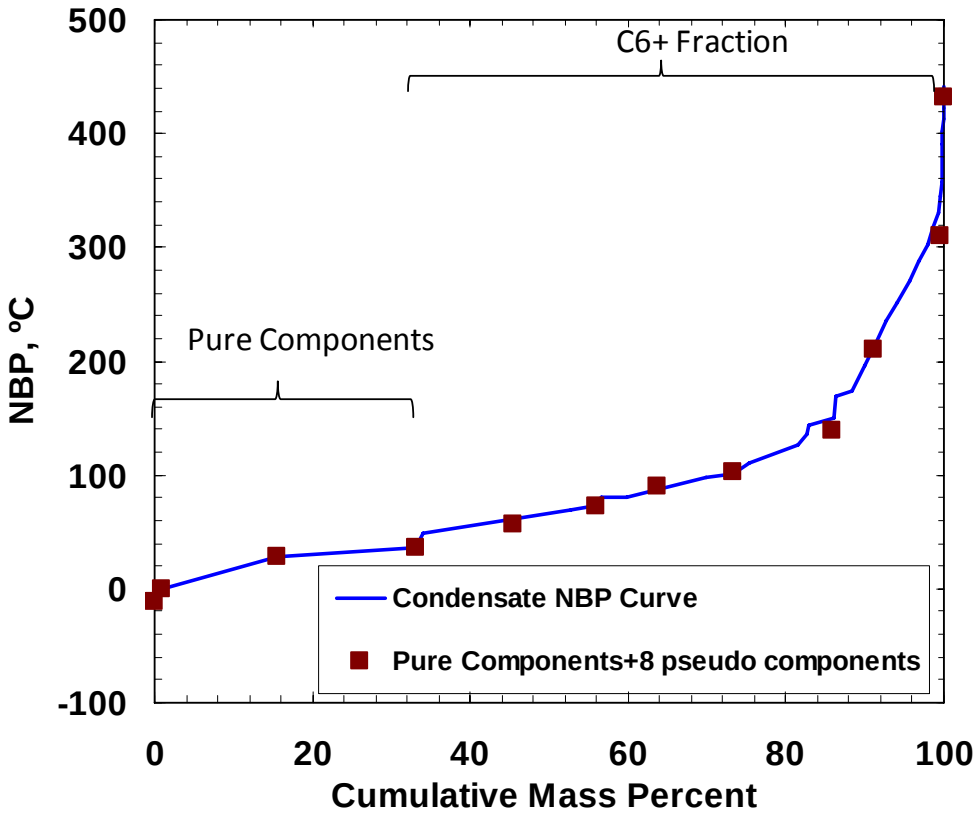

Figure 4.5: NBP curve for condensate solvent and NBP curve recreated using eight pseudo-components

The molecular weight and specific gravity of the pseudo-components were calculated using the Lee-Kesler and Katz Firoozabadi correlations, respectively, and then adjusted by a multiplier to fit the average values of the C6+ fraction (111g/mol, 744 kg/m^3). The critical properties and acentric factor of the each pseudo component were calculated using Lee-Kesler correlations. The properties of pseudo and pure components of the condensate are summarized in Table 4.8.

Table 4.7: C30+ analysis of condensate solvent

Boiling Point Range, ºC	Component	Mole Fraction	Mass Fraction
	*i*C4	0.0005	0.0003
	C4	0.0157	0.0097
	*i*C5	0.1898	0.1458
	C5	0.2268	0.1743
36.1-68.9	Hexanes	0.1921	0.1879
68.9-98.3	Heptanes	0.0889	0.1009
98.3-125.6	Octanes	0.047	0.0607
125.6-150.6	Nonanes	0.0207	0.0301
150.6-173.9	Decanes	0.0133	0.0215
173.9-196.1	Undecanes	0.0095	0.0157
196.1-215.0	Dodecanes	0.0072	0.0131
215.0-235.0	Tridecanes	0.0073	0.0145
235.0-252.2	Tetradecanes	0.0064	0.0138
252.2-270.6	Pentadecanes	0.0063	0.0147
270.6-287.8	Hexadecanes	0.0049	0.0123
287.8-302.8	Heptadecanes	0.0039	0.0104
302.8-317.2	Octadecanes	0.0029	0.0082
317.2-330.0	Nonadecanes	0.002	0.0061
330.0-344.4	Eicosanes	0.0009	0.0027
344.4-357.2	Heneicosanes	0.0004	0.0013
357.2-369.4	Docosanes	0.0002	0.0008
369.4-380.0	Tricosanes	0.0002	0.0005
380.0-391.1	Tetracosanes	0.0001	0.0003
391.1-401.7	Pentacosanes	0.0001	0.0001
401.7-412.2	Hexacosanes	0.0002	0.0006
412.2-422.2	Heptacosanes	0.0001	0.0002
422.2-431.7	Octacosanes	0.0001	0.0002
431.7-441.1	Nonacosanes	0.0001	0.0002

441.1 PLUS	Triacontanes Plus	Trace	Trace
80	Benzene	0.0138	0.0123
110.6	Toluene	0.0195	0.0203
136.1-138.9	Ethylbenzene, p+m-Xylene	0.0103	0.0123
144.4	o-Xylene	0.0024	0.0029
168.9	1,2,4 Trimethylbenzene	0.0023	0.0031
48.9	Cyclopentane	0.0123	0.0097
72.2	Methylcyclopentane	0.0285	0.0271
81.1	Cyclohexane	0.0318	0.0303
101.1	Methylcyclohexane	0.0315	0.035

Table 4.8: Pure and pseudo-components of condensate solvent

Components Name	**Mass Fraction**	**MW [g/mol]**	**NBP [ºC]**	**Pc [kPa]**	**Tc [ºC]**	**Ω**
n-butane	0.01	58.1	-0.5	3797	152	0.2
Isopentane	0.146	72.1	27.8	3381	187.3	0.23
n-pentane	0.174	72.1	36.1	3369	196.5	0.25
Cond[54]C	0.125	85	54.5	3484.4	225.3	0.25
Cond[67]C	0.104	91.5	66.6	3412.2	240.5	0.27
Cond[82]C	0.079	99.5	82.1	3296.9	259.2	0.29
Cond[95]C	0.096	107.9	95.4	3219.4	275.4	0.31
Cond[124]C	0.126	121.6	124.0	2957.6	307.2	0.36
Cond[181]C	0.051	155.3	181.0	2496.6	367.3	0.46
Cond[267]C	0.085	226.5	267.2	1915.2	450.6	0.63
Cond[377]C	0.005	316.2	377.0	1316.7	544.8	0.91

CHAPTER FIVE: RESULTS AND DISCUSSION

In this chapter, experimental data collected for bitumen/solvent and bitumen/*n*-pentane mixtures are presented. Related datasets from literature for bitumen/carbon dioxide and bitumen/methane, bitumen/ethane, bitumen/propane are also provided. An equation-of-state model for Alberta bitumen is developed based on the pseudo-binary data. In particular, adjustments of binary interaction parameters to fit the saturation pressure and asphaltene onset data are discussed. Live oil modeling and model predictions for saturation pressure, asphaltene onset, asphaltene yield are then presented. The sensitivity of the model to different NBP extrapolation, asphaltene average molecular weight, and number of pseudo-components is examined.

5.1 Dataset

The bitumen sample for which data were collected in this thesis is denoted as Bitumen A. The bitumen sample for which Schlumberger provided data is denoted as Bitumen B. Data from the literature are labelled as originally reported. For convenience, mixtures of bitumen and a single solvent are described as pseudo-binary mixtures. In fact they are mixtures of millions of components. The dataset includes saturation pressure data for five pseudo-binary mixtures:

- carbon dioxide and dead Peace River bitumen;
- methane and dead Peace River bitumen;
- ethane and dead Peace River bitumen;
- propane and dead Athabasca bitumen;
- *n*-pentane and dead Bitumen A.

The dataset also includes the following:

- saturation pressures for live Bitumen A and condensate mixtures;
- asphaltene onset data for propane diluted Bitumen B;
- asphaltene onset and yield data for *n*-pentane diluted Bitumen A;

The data and their source for each pseudo-binary are presented below.

5.1.1 Carbon Dioxide and Dead Bitumen

Table 5.1 provides the saturation pressures for pseudo-binary mixtures of carbon dioxide (CO_2) and Peace River bitumen with carbon dioxide contents ranging from 1 to 11 wt% at temperatures of 22 to 107ºC (Mehrotra and Svrcek, 1985).

Table 5.1: Saturation pressures of carbon dioxide/Peace River bitumen mixtures (Mehrotra and Svrcek, 1985)

Temperature (ºC)	Pressure (kPaa)	Weight Percent
23.8	3000	4.68
23.4	4500	7.37
22.2	6100	10.57
22.5	6120	11.77
37.7	1800	2.18
39.4	2800	3.39
40	4500	5.86
40.3	6200	8
55.5	1570	1.64
56.2	3000	2.93
55.8	4560	4.51
57.2	6210	6.17
79.4	1540	1.38
79.0	3100	2.73
78.1	4480	4.11
77.7	6170	5.68
105.5	1500	1.3
104.5	3210	2.55
104.0	4480	3.18
107.0	6180	4.15

5.1.2 Methane and Dead Bitumen

Table 5.2 provides the saturation pressures for pseudo-binary mixtures of methane and Peace River bitumen with methane contents ranging from 0.5 to 1.23 wt% at temperatures of 22 to 114 ºC (Mehrotra and Svrcek, 1985).

Table 5.2: Saturation pressures of methane/Peace River bitumen mixtures (Mehrotra and Svrcek, 1985)

Temperature (ºC)	Pressure (kPaa)	Weight Percent
22	2540	0.5
22.8	5190	0.87
22.9	7200	1.23
53.8	2400	0.44
53.5	5050	0.84
54.8	7670	1.08
78.4	2500	0.41
80	5300	0.77
80	7620	1.07
114.3	2680	0.42
114.3	5080	0.69
114	7650	1

5.1.3 Ethane and Dead Bitumen

Table 5.3 provides the saturation pressures for pseudo-binary mixtures of ethane and Peace River bitumen with ethane contents ranging from 1 to 13 wt% at temperatures of 23 to 107ºC (Mehrotra and Svrcek, 1985).

Table 5.3: Saturation pressures of ethane/Peace River bitumen mixtures (Mehrotra and Svrcek, 1985)

Temperature (ºC)	Pressure (kPaa)	Weight Percent
23	1390	2.81
25	4100	7.14
23	4080	9.63
23	4020	12.75
43.6	1380	2.04
42.8	2580	3.97
47.3	4170	6.62
69.1	1440	1.54
80	2770	2.66
78.7	4300	4.23
103.5	1420	1.08
106.6	2670	2.04
106	4250	3.25

5.1.4 Propane and Dead Bitumen

Table 5.4 provides the saturation pressures for binary mixtures of propane and Athabasca bitumen with propane contents ranging from 5.2 to 25.4 wt% at temperatures of 20 to 60ºC (Badamchi-Zadeh *et al*., 2009).

Table 5.4: Saturation pressures of propane/Athabasca bitumen mixtures (Badamchi-Zadeh *et al*., 2009)

Weight Percent	Temperature (ºC)	Pressure (kPaa)
5.2	20.2	530
	40	789
	60.4	1082
10.9	10	478
	20.1	624
	29.9	741
	40	892
	50	1171
15.6	10	600
	19.9	718
	29.9	941
	39.7	1130
	50.1	1344
	10.1	589
	50.1	1365
25.4	10.1	632
	20.1	831
	20.1	829
	30	1016
	39.9	1290
	50	1537

Schlumberger-DBR have collected asphaltene onset data for propane diluted Bitumen B using a high pressure microscope and a procedure similar to that described in Section 3.5.

The SimDist for Bitumen B is similar to that of Bitumen A, Figure 5.1. The onset of asphaltene precipitation was 17.5 wt% propane at 50ºC and 2070 kPaa.

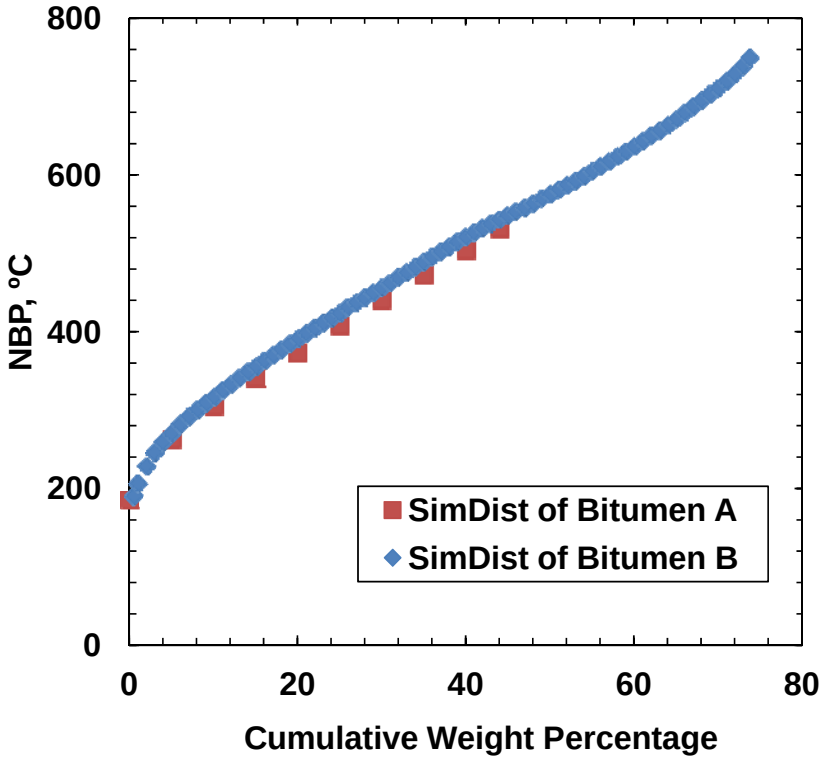

Figure 5.1: Comparison of SimDists of Bitumen A and Bitumen B

5.1.5 *n*-Pentane and Dead Bitumen

Saturation pressures were collected in this study for *n*-pentane diluted Bitumen A with *n*-pentane contents up to 30 wt% and temperature ranging from 90 to 180ºC, Table 5.5.

Table 5.5: Saturation pressures for mixture of *n*-pentane and dead Bitumen A

***n*-Pentane wt %**	**Temperature (ºC)**	**Pressure (kPaa)**
11	90	390±70
	120	605±70
	150	704±70
	180.1	1030±70
30	90	465±70
	120	840±70
	150	1325±70
	180.1	1825±70

The onset of asphaltene precipitation was also measured for *n*-pentane diluted Bitumen A at 23ºC and 180ºC using the High Pressure Microscope. Figure 5.2 shows that the onset of asphaltene precipitation at 23°C and atmospheric pressure occurred between 46 to 48 wt% of *n*-pentane. Asphaltene yield data was also collected for *n*-pentane diluted Bitumen A at 23ºC and atmospheric pressure, Table 5.6. The asphaltene yield curve was extrapolated to zero yield to determine the asphaltene precipitation onset of 45±5 wt% *n*-pentane, Figure 5.5. The onsets determined from the extrapolated yield and the HPM are consistent within experimental error.

Figure 5.3 shows that, at 180°C and 4830 kPaa, the onset of asphaltene precipitation occurred between 48 and 52 wt% of *n*-pentane. The onset shifted by only 3 wt% as the temperature increased from 23 to 180°C. Interestingly, the asphaltene-rich phase at 180°C was a liquid while the asphaltene-rich phase at 23°C resembles a dispersed solid. At 23°C, the asphaltene-rich phase particles are irregular and while they flocculate they do not coalesce, Figure 5.2. At 180°C, the asphaltene-rich phase forms spherical droplets, Figure 5.3, which coalesce into a single phase, Figure 5.4 These observations are

consistent with a glass transition at an intermediate temperature. Lastovka *et al.* (2008) reported a glass transition temperature for dry asphaltenes at approximately 140°C.

Table 5.6: Asphaltene yield for mixtures of *n*-pentane and dead bitumen

***n*-Pentane wt%**	**Asphaltene Yield**
0.428	0.010
0.500	0.037
0.700	0.171
0.636	0.142
0.891	0.175
0.970	0.194

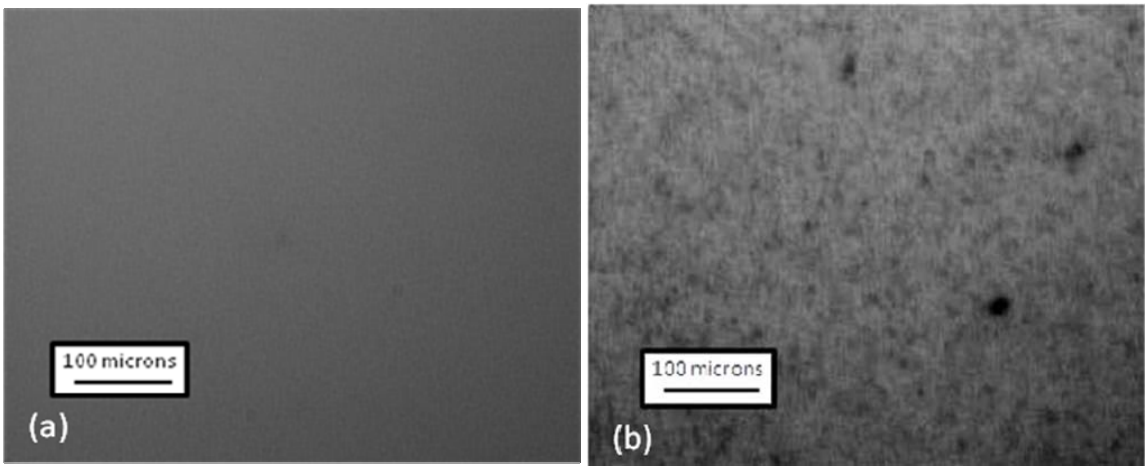

Figure 5.2: Micrographs of *n*-pentane diluted bitumen at 23ºC and atmospheric pressure: a) 46 wt% *n*-pentane; b) 48 wt % *n*-pentane. The dark dots are precipitated asphaltene-rich phase particles.

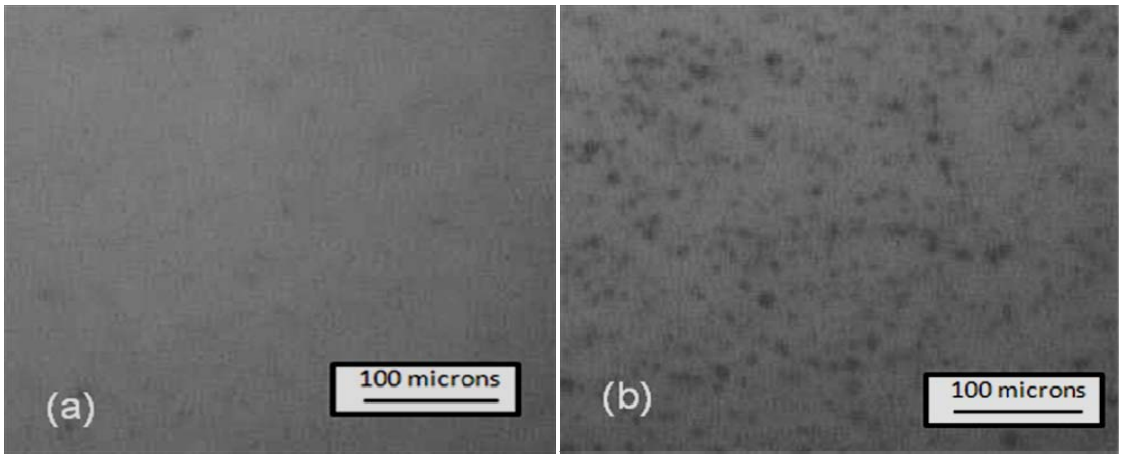

Figure 5.3: Micrographs of *n*-pentane diluted bitumen at 180ºC and 4830 kPaa: a) 48 wt% *n*-pentane; b) 52 wt % *n*-pentane. The dark dots are precipitated asphaltene-rich phase droplets.

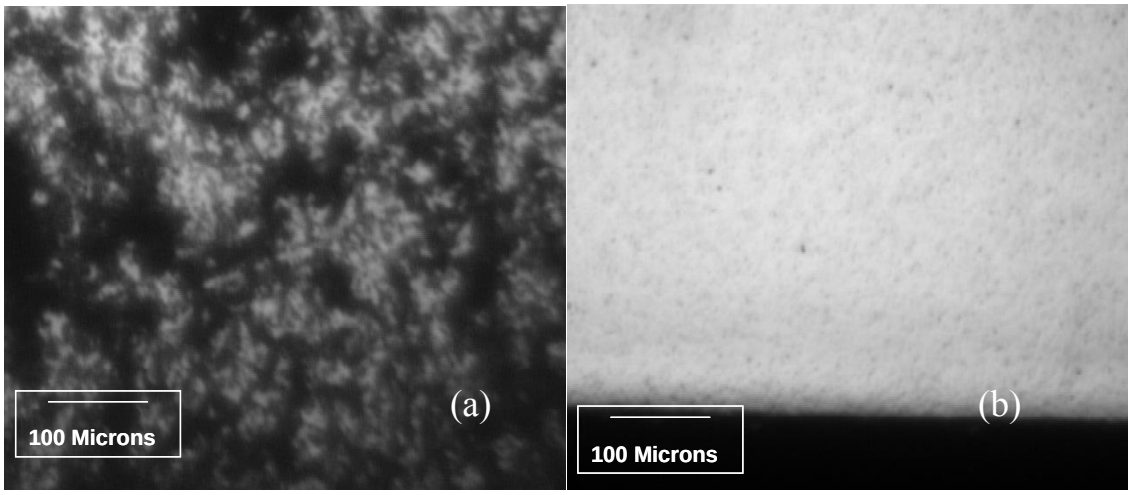

Figure 5.4: Micrograph of 52 wt% *n*-pentane diluted bitumen at 180ºC and 4830 kPaa: a) coalescing asphaltene-rich phase droplets before settling; b) settled asphaltene-rich liquid phase (dark area).

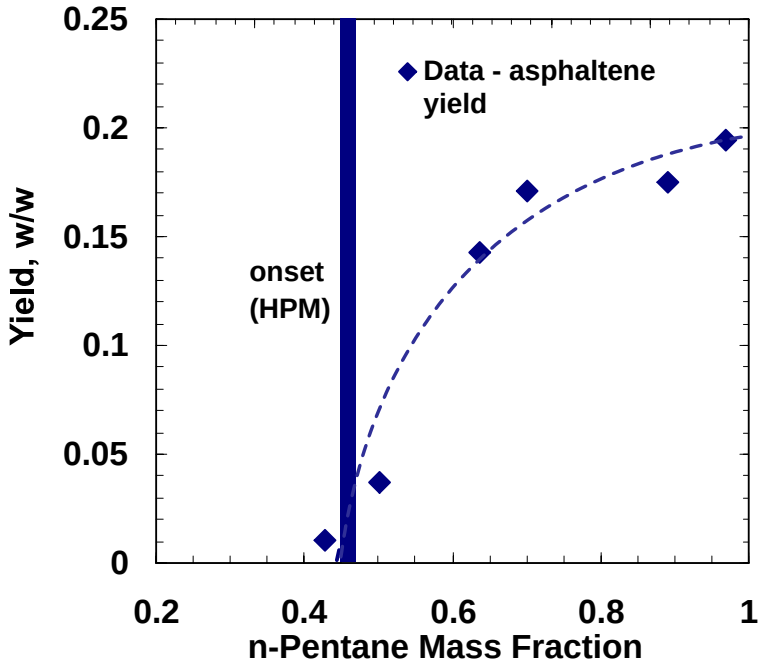

Figure 5.5: Points are the measured asphaltene yields at 23 ºC and ambient pressure; dotted line is the extrapolated asphaltene yield curve.

5.1.6 Live Oil and Condensate

Two live oils were prepared as was discussed in Section 3.3. The solution gas composition and GOR of the live oils are reported in Table 5.7. The saturation pressure for Live Oil 1 was measured at temperatures from 23 to 180ºC, Table 5.8. Saturation pressures were also measured for Live Oil 2 plus 6 and 10 wt% of condensate at temperatures ranging from 23 to 180ºC, Table 5.8.

The saturation pressure of the live oil decreases upon addition of condensate because the concentration of methane, carbon dioxide, and nitrogen is reduced and these components have a significantly higher vapour pressure than the condensate. Also, the solubility of these components is higher in condensate than in bitumen. Hence, an increase in condensate concentration increases the solubility of methane, carbon dioxide, nitrogen in the overall mixture and decreases its saturation pressure.

Table 5.7: GOR and solution gas composition of the live oils

	Mole Fraction			GOR (Sm3/Sm3)
	Methane	**CO2**	**Nitrogen**	
Live Oil 1	-	-	-	11±1
Live Oil 2	0.276	0.717	0.007	13±1

Table 5.8: Saturation pressure for live bitumen at different concentrations of a condensate at temperatures from 20 to 180°C

System	Temperature (ºC)	Saturation Pressure (kPaa)
Live Oil 1	22.4	2276±70
	80	3151±70
	120	3351±70
	180	3565±70
Live Oil 2+ 5.8 wt% Condensate	22.4	2179±70
	80	3222±70
	120	3740±70
	180	4174±70
Live Oil 2+ 10 wt% Condensate	22.4	1890±70
	80	2763±70
	120	3275±70
	180	3497±70

5.2 Equation-of-State Model

The initial fluid characterization was presented in Chapter 4. The distillation curve for the bitumen was extrapolated using a Gaussian distribution for maltenes and a gamma distribution for the asphaltenes. Then the distillation curve was divided into a number of the pseudo-components. Critical properties and the acentric factor of the pseudo components were estimated using the Lee-Kesler correlations. The pseudo-component properties are summarized in Table 4.5, Chapter 4.

The Advanced Peng Robinson Equation of State was used to model the measured data. Flash calculations were performed using VMGSim™ (Version 6.0, 2010). VMGSim™ combines the solution of material balance equations from the Rachford-Rice algorithm (Rachford and Rice, 1952) with a stability test similar to one suggested by the Michelsen algorithm (Michelsen, 1982). The stability test is designed to determine the minimum Gibbs free energy solution of the material and thermodynamic equilibrium equations. The asphaltene precipitation was modeled as a liquid-liquid equilibrium. The tuning of the model to the data was accomplished by adjusting the binary interaction parameters as described below.

5.2.1 Temperature Independent Binary Interaction Parameters

The binary interaction parameters between solvent and bitumen pseudo-components were adjusted using the Gao *et al.* (1992) correlation given by:

$$k_{ij} = 1 - \left[\frac{2\sqrt{T_{Ci} T_{Cj}}}{T_{Ci} + T_{Cj}} \right]^n \qquad \textbf{5-1}$$

where *i* and *j* are a pair of components, *Tc* is the critical temperature in K, and *n* is an adjustable exponent with a default value of 0.27.

The first step was to fit the saturation pressures of the pseudo-binary datasets at lower temperatures. As a starting point, the exponent for pairs of pseudo-components was set to the default value. A single exponent was used for the given solvent with all of the bitumen pseudo-components. This single exponent was adjusted to match the saturation pressures of each pseudo-binary. For the *n*-pentane/dead bitumen system, both saturation pressure and asphaltene precipitation onset data were matched. The exponents which best fit the data for each pseudo-binary are:

CO2	0.65
methane	-0.2
ethane	0.3
n-pentane	0.62

Figures 5.6, 5.7, 5.8 and 5.9 show the measured (symbols) and fitted (lines) saturation pressures for mixtures of carbon dioxide/bitumen, methane/bitumen, ethane/bitumen, *n*-pentane/bitumen, respectively. The model is qualitatively correct and captures all of the significant phase behavior observed experimentally.

First consider the CO_2/bitumen pseudo-binary, Figure 5.6. The saturation pressures at low temperature were well matched but the increase of saturation pressure with temperature was over-predicted. Note how the saturation pressure curve at 23ºC plateaus at CO_2 contents above 10 wt%. The plateau corresponds to the appearance of second liquid phase, a light CO_2-rich phase. The model *predicted* the appearance of light CO_2-rich phase at 11 wt% carbon dioxide.

The methane-bitumen pseudo-binary, Figure 5.7, exhibited only vapour-liquid equilibrium and the saturation pressures at higher temperatures were also over-predicted. The ethane/bitumen pseudo-binary resembled the CO_2/bitumen binary, Figure 5.8. At 23°C, the appearance of a second liquid phase (a light ethane-rich phase) was observed at 7.2 wt% ethane. The model predicted the appearance of a second light ethane-rich liquid phase at 9 wt% ethane. The increase in saturation pressure with temperature was again over-predicted.

For the *n*-pentane/bitumen pseudo-binary, the saturation pressures were also over-predicted at higher temperatures, Figure 5.9. For this system, the model was simultaneously fit to asphaltene onset at 22.4ºC, Figure 5.10. The model was able to fit both the saturation pressure and onset of asphaltene precipitation at 23°C. However, contrary to the experimental data, the model predicted that no asphaltene precipitation occurs at 180ºC for any *n*-pentane concentration. Also the model under-predicted asphaltene yields at 23ºC at high *n*-pentane content, Figure 5.10. The measured asphaltene yields increased monotonically while the model predicted that the asphaltenes become soluble at high dilution. The predicted increase in solubility at high dilution occurs because the model over-predicts the amount of non-asphaltene components that

partition to the asphaltene-rich phase. At high dilutions, too much solvent is predicted to partition to the incipient asphaltene-rich phase and phase separation does not occur. For example, at 23ºC and 60 wt% *n*-pentane, the model predicts that the *n*-pentane content of the asphaltene-rich phase is 17 wt%. Recent data (George *et al*., 2009) show that the *n*-pentane content of the asphaltene-rich phase is less than 8 wt%. These results suggest that the interaction between the asphaltenes and the solvent depends on the concentration; that is, they form asymmetric mixtures.

In summary, the model fit the saturation pressures and liquid-liquid boundaries within the accuracy of the data at lower temperatures but there was significant deviation at higher temperatures. The deviation with temperature in all cases indicates that temperature dependent binary interaction parameters are required.

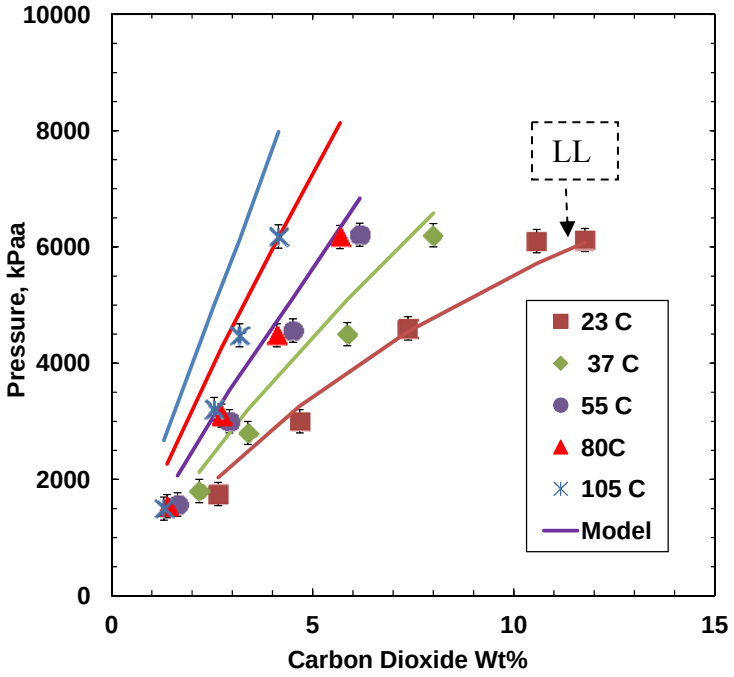

Figure 5.6: Saturation pressure of CO_2/bitumen pseudo-binary. Symbols are experimental data and solid lines are model fit with temperature independent k_{ij}

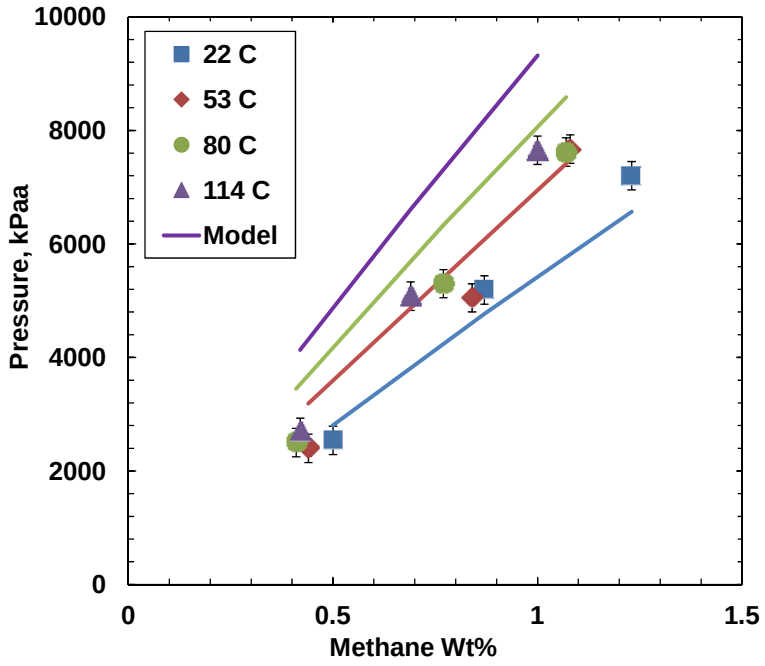

Figure 5.7: Saturation pressure of methane/bitumen pseudo-binary. Symbols are experimental data and solid lines are model fit with temperature independent k_{ij}.

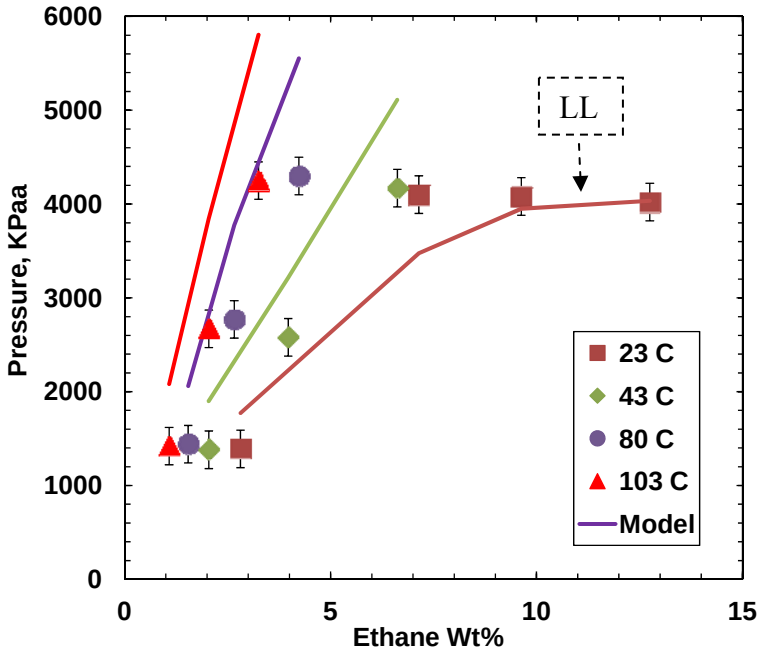

Figure 5.8: Saturation pressure of ethane/bitumen pseudo-binary. Symbols are experimental data and solid lines are model fit with temperature independent k_{ij}

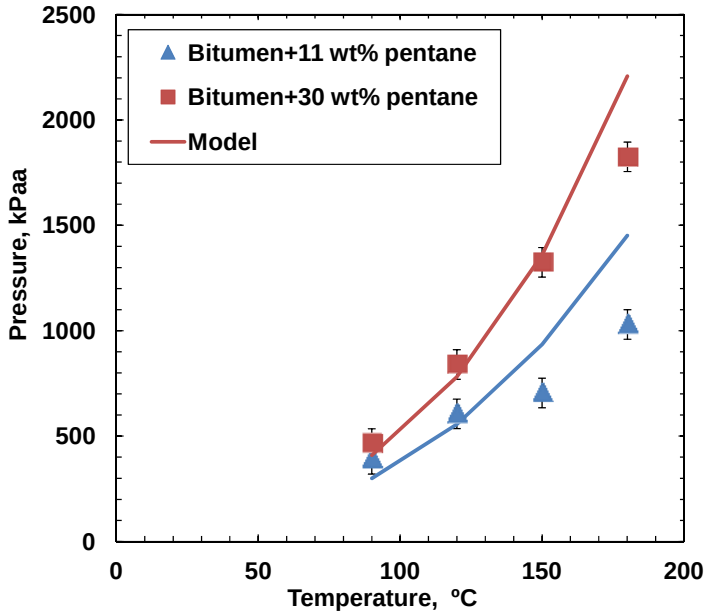

Figure 5.9: Saturation pressure of *n*-pentane/bitumen pseudo-binary. Symbols are experimental data and solid lines are model fit with temperature independent k_{ij}

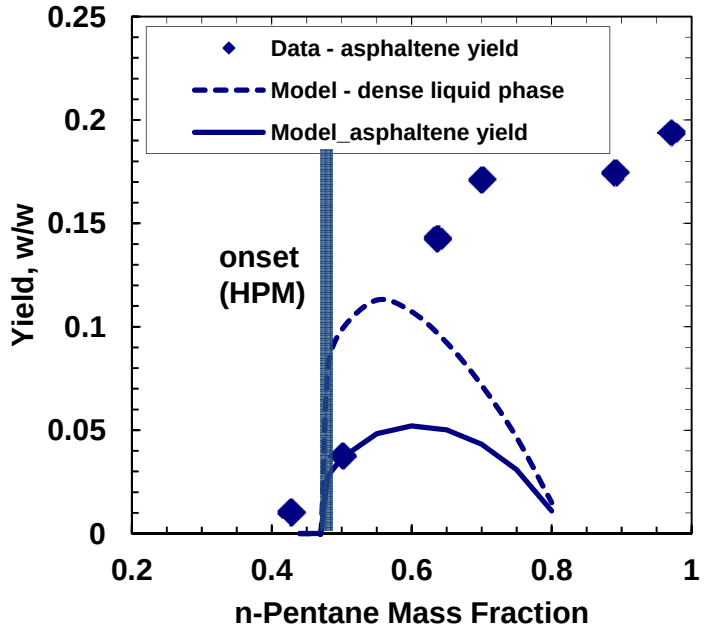

Figure 5.10: Measured and modeled asphaltene precipitation onset and yield at 23ºC. The dotted line is the predicted mass of asphaltene-rich liquid phase per unit mass of bitumen. The solid line is the predicted mass of precipitated asphaltenes per unit mass of bitumen

5.2.2 Temperature Dependent Interaction Parameters

In order to fit the saturation pressure data over a range of temperatures, the following temperature dependent binary interaction parameter correlation was used:

$$k_{ij} = k_{ij}^{0}\left(1+\frac{k_{ij}^{1}}{T}+k_{ij}^{2}\ln(T)\right) \qquad \textbf{5-2}$$

$$k_{ij}^{0} = 1-\left[\frac{2\sqrt{T_{Ci}T_{Cj}}}{T_{Ci}+T_{Cj}}\right]^{n} \qquad \textbf{5-3}$$

where k_{ij}^{1} and k_{ij}^{2} are constants.

To illustrate the effect of the parameters in Eq. 5-2, consider the P-T diagram of 0.5 wt% methane in bitumen, Figures 5.11 to 5.13. The general solution of the equation of state for this mixture includes a vapour-liquid region and a liquid-liquid region. The parameters shift the boundaries of the two-phase regions. In Figure 5.11, k_{ij}^{1} was changed while n and k_{ij}^{2} were held constant at 0.27 and -1.32, respectively. In Figure 5.12, k_{ij}^{2} was changed while n and k_{ij}^{1} were held constant at 0.27 and 1780, respectively. In Figure 5.13, n was changed while $k_{ij}^{1}$and k_{ij}^{2} were held constant at 1780 and -0.32, respectively.

First note that in all cases the phase diagram remains anchored at the critical point. Decreasing k_{ij}^{1} or increasing the magnitude of k_{ij}^{2} shifts the LL boundary to lower temperatures allowing saturation pressure to decrease before reaching the LLE point. k_{ij}^{2} decreases saturation pressure near critical point more than k_{ij}^{1} for the same shift in the minimum pressure. In particular, from 10 to 200ºC (shaded region), as k_{ij}^{1} increases the slope of the saturation pressure curve decreases while changing kij^{2} has little effect on the slope. Therefore, a combination of k_{ij}^{1} and k_{ij}^{2} can fit the desired shape of P-T envelope and LL boundary.

Now consider the effect of the exponent n, Figure 5.13. When n is decreased, the magnitudes of $k_{ij}^{0*}k_{ij}^{1}$ and $k_{ij}^{0*}k_{ij}^{2}$ are also decreased. Decreasing $k_{ij}^{0*}k_{ij}^{1}$ shifts the saturation pressure downward while $k_{ij}^{0*}k_{ij}^{2}$ shifts it upward. However, $k_{ij}^{0*}k_{ij}^{2}$ shifts the

saturation pressure more near critical point than $k_{ij}^{0*}k_{ij}^{1}$. The overall effect is to change the shape of the P-T envelope between the minimum saturation pressure and the critical point without significantly altering the minimum saturation pressure.

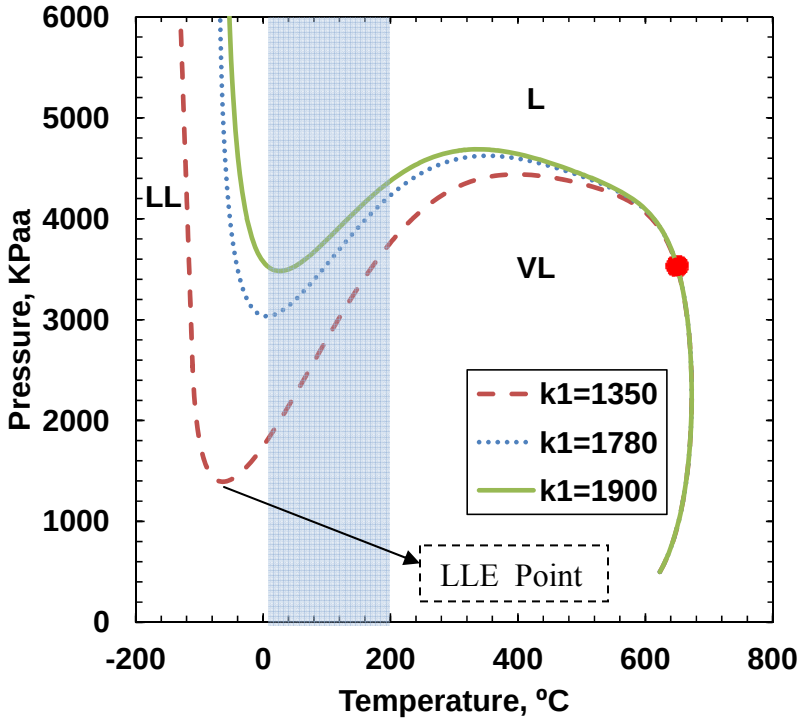

Figure 5.11: Effect of k_{ij}^{1} on saturation pressure prediction of 0.5 wt% methane in bitumen

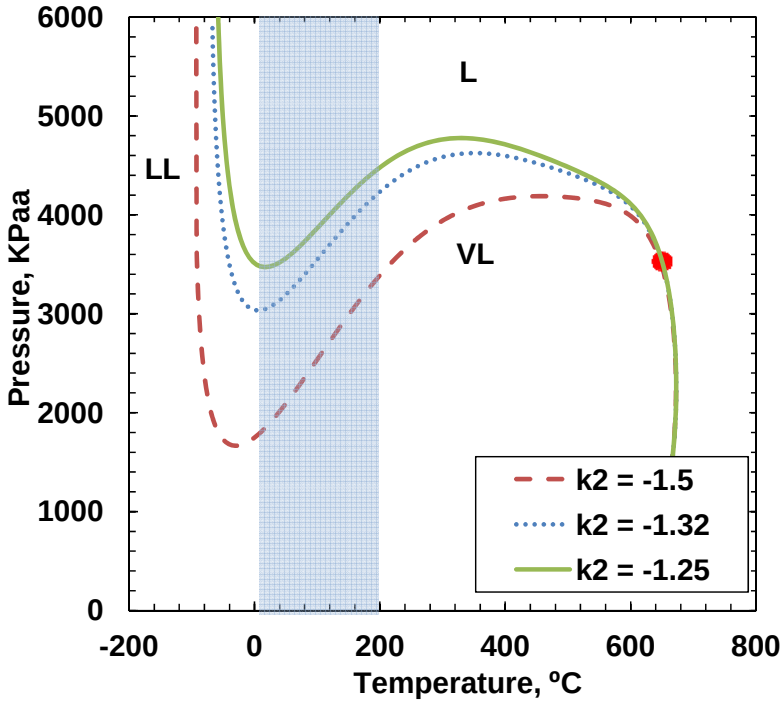

Figure 5.12: Effect of k_{ij}^2 on saturation pressure prediction of 0.5 wt% methane in bitumen

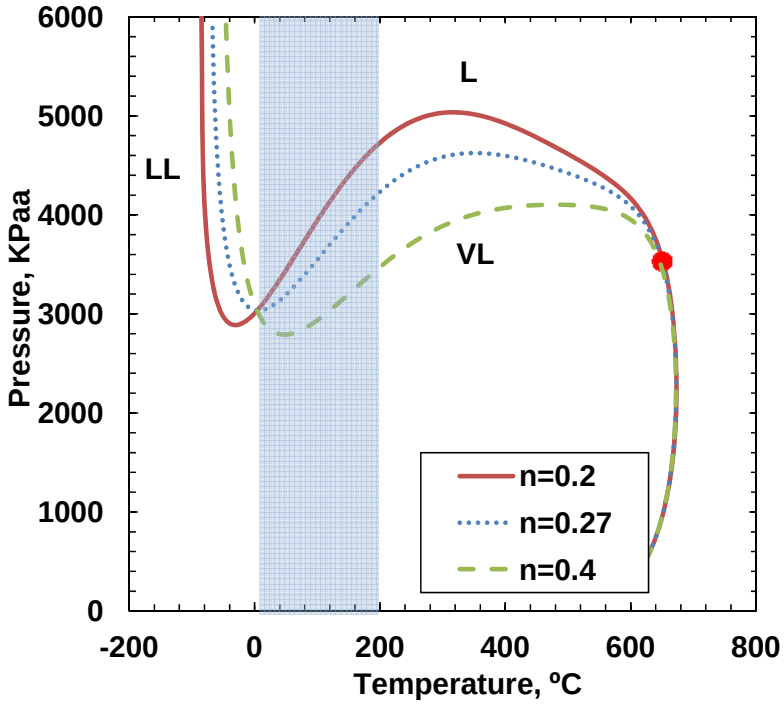

Figure 5.13: Effect of *n* on saturation pressure prediction of 0.5 wt% methane in bitumen

There is not a unique best fit solution to match the saturation pressure with three variable binary interaction parameters. Therefore, the exponent *n* was set to the default value of 0.27 and only k_{ij}^{1} and k_{ij}^{2} were adjusted. Note that, to be consistent, the temperature dependence was also applied to pseudo-component/pseudo-component interactions. The values of k_{ij}^{1}, k_{ij}^{2} which provided the best fit for the pseudo-binary mixtures are given in Table 5.9.

Table 5.9: Values of *n*, k_{ij}^{1}, k_{ij}^{2}, which provided the best fit for the binary mixtures. Here pseudo-components refer to bitumen pseudo-components.

Binary Pairs	***n***	k_{ij}^{1}	k_{ij}^{2}
CO2/pseudo-component	0.27	3060	-1.54
methane/pseudo-component	0.27	1780	-1.32
ethane/pseudo-component	0.27	2550	-1.50
n-pentane/pseudo-component	0.27	2550	-1.50
Pseudo-component/pseudo-component	0.27	2550	-1.50

Figures 5.14, 5.15, 5.16, and 5.17 show the measured (symbols) and fitted (lines) saturation pressures for the CO_2/bitumen, methane/bitumen, ethane/bitumen and *n*-pentane/bitumen pseudo-binaries, respectively. In all cases, the model with temperature dependent binary interaction parameters fit the saturation pressures to within the accuracy of the data. Note that for all hydrocarbon-hydrocarbon pairs excluding methane, the temperature dependent parameters are identical.

For the CO_2/bitumen pseudo-binary at 23°C, the model predicted the appearance of a light CO_2 rich phase at 10 wt% CO_2. For the ethane/bitumen pseudo-binary at 23°C, the model predicted the appearance of a light ethane-rich phase at 8 wt% of ethane. Both predictions are within 1 wt% of the measured liquid-liquid phase boundaries. As before, the model parameters for the *n*-pentane/bitumen pseudo-binary were tuned to fit the asphaltene onset at 22ºC. The model again failed to predict any asphaltene precipitation at 180ºC.

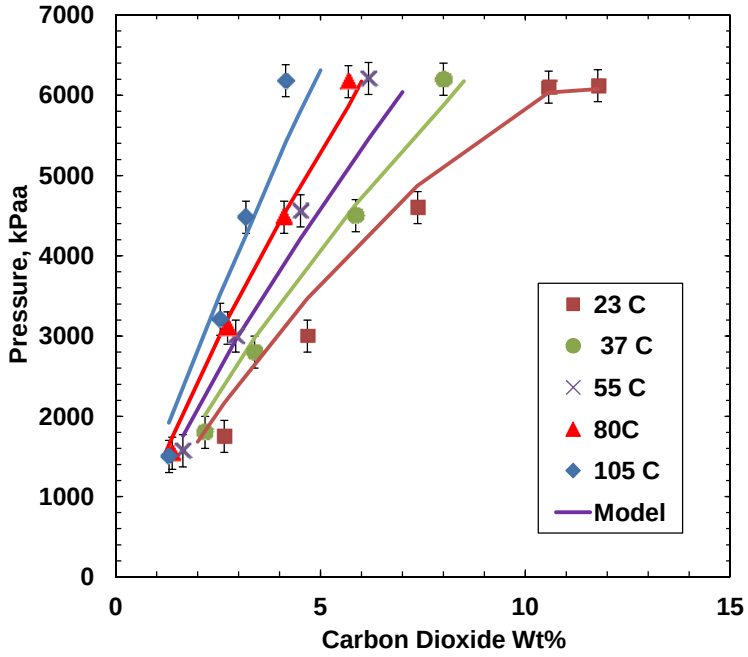

Figure 5.14: Saturation pressure of CO_2/Peace River bitumen pseudo-binary, Symbols are experimental data and solid lines are model fit with temperature dependent k_{ij}

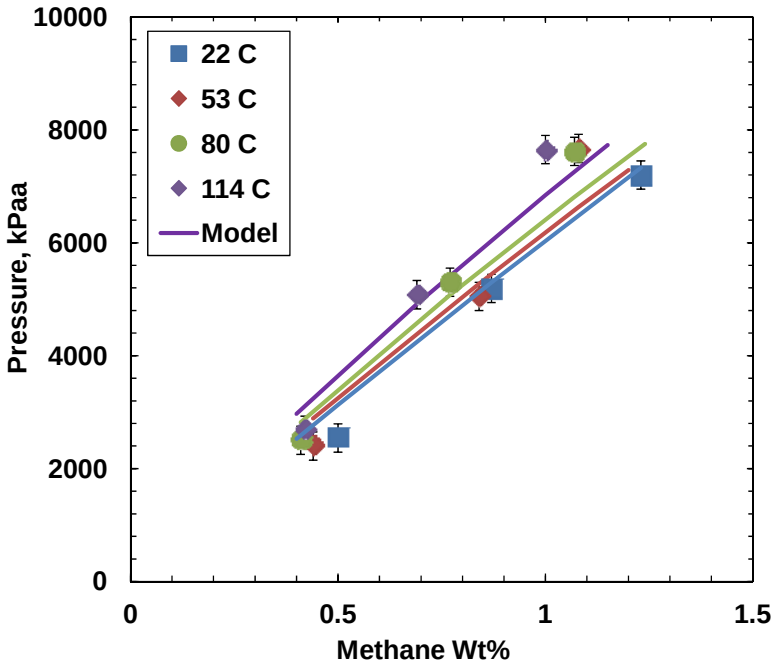

Figure 5.15: Saturation pressure of methane/Peace River bitumen pseudo-binary. Symbols are experimental data and solid lines are model fit with temperature dependent k_{ij}.

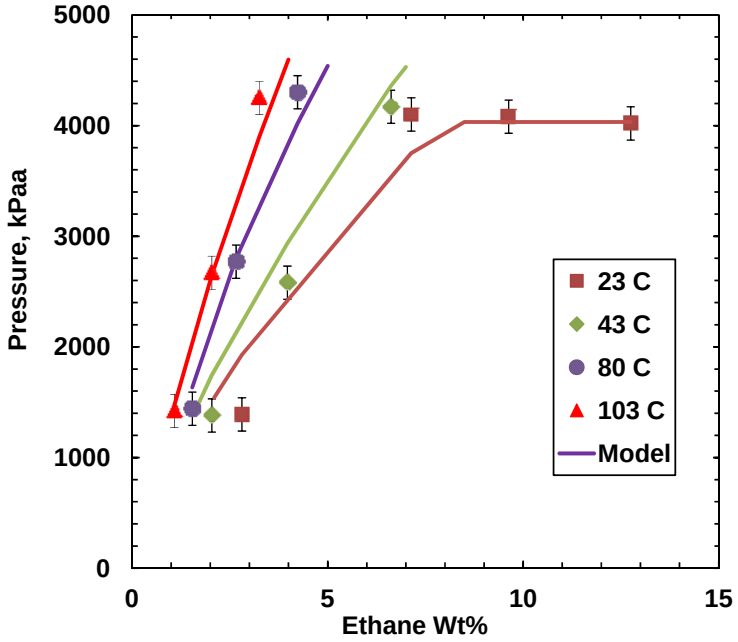

Figure 5.16: Saturation pressure of ethane/Peace River bitumen pseudo-binary. Symbols are experimental data and solid lines are model fit with temperature dependent k_{ij}.

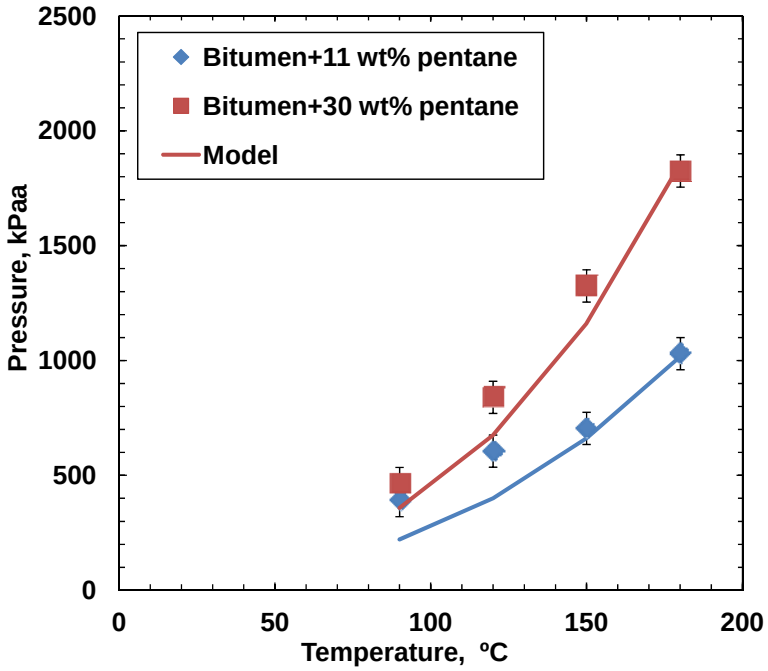

Figure 5.17: Saturation pressure of *n*-pentane/Bitumen A pseudo-binary. Symbols are experimental data and solid lines are model fit with temperature dependent k_{ij}.

5.2.2.1 Saturation Pressure Predictions

Bitumen/Propane Pseudo-Binary

One test of the model would be to predict saturation pressures for propane and *n*-butane diluted bitumen. If the model is consistent, the temperature dependent parameters for both solvents are expected to be the same as other hydrocarbons; that is, *n, kij*[1], and k_{ij}^{2} equal to 0.27, 2550 and -1.5 respectively. Unfortunately, there are no saturation pressure data available in the literature for propane/Peace River Bitumen or butane/Peace River bitumen pseudo-binaries. However, Badamchi-Zadeh *et al.* (2009) have collected saturation pressures for the propane/Athabasca bitumen pseudo-binary. Also, Castellanos Díaz *et al.* (2011) have characterized the same Athabasca bitumen using the methodology followed in the present study. Therefore, the Castellanos Díaz *et al.* (2011) characterization was used with the proposed temperature dependent interaction parameters to model the propane/Athabsaca bitumen saturation pressures, Figure 5.18. The model predicts the saturation pressures to within accuracy of the data at higher propane contents but there is a significant deviation at 5 wt% of propane content. As noted by Badamchizadeh *et al.* (2009), it is likely that the 5 wt% propane mixture did not reach equilibrium due to its very high viscosity. Also at 10°C, the model predicted the appearance of a light propane-rich phase at 18 wt% of propane. A second phase was not reported by the authors but may not have been detected since both phases may be opaque and the pressure-volume isotherm used to determine the saturation pressure is not significantly altered by the appearance of a second liquid phase.

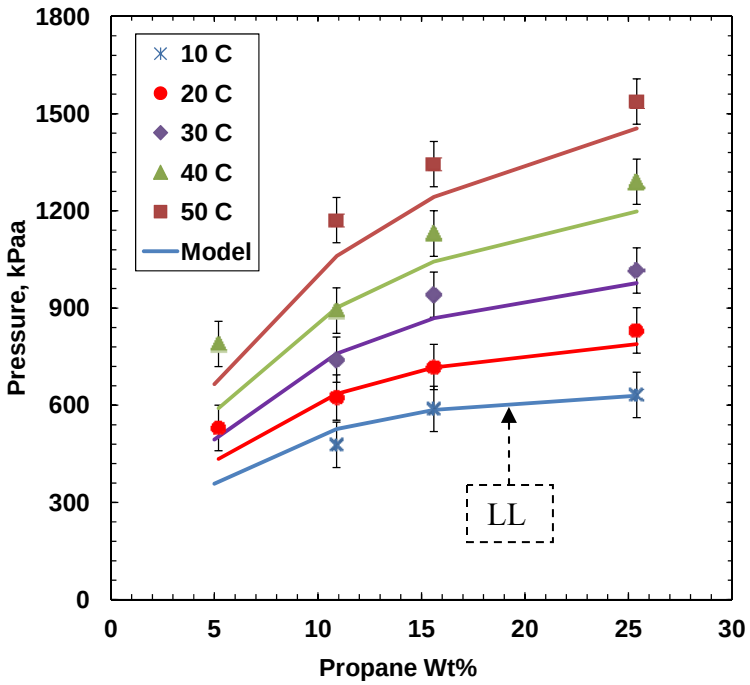

Figure 5.18: Saturation pressure of propane/Athabasca bitumen pseudo-binary. Symbols are experimental data and solid lines are model fit with temperature dependent k_{ij}.

Live Oil

Another test of the model is its ability to predict live oil saturation pressures from the live oil composition or, in this case, from the live oil preparation procedure. The preparation of Live Oil 1 and 2, described in Section 3.3, were simulated using VMGSim^{TM}. The binary interaction parameters between methane, CO_2, and bitumen pseudo-components were determined using Eqs. 5-2 and 5-3 and the n, k_{ij}^1, k_{ij}^2 from Table 5.9.

For the simulation of Live Oil 1 preparation, 430 g of dead bitumen and 40 g of synthetic gas (37.80 mol% methane, 61.11 mol% carbon dioxide, 1.09 mol% nitrogen) were mixed and then mixture was fed to a two phase separator set to 2140 kPaa and 17ºC, Figure 5.19. Live Oil 1 was taken out from the separator and its saturation pressure was determined at different temperatures. The predicted saturation pressures are within ±500 kPa of the measured saturation pressures, Figure 5.20. To determine the gas-oil ratio and composition of the dissolved gas, a small amount of live oil was injected into a second

two phase separator set to 82 kPaa and 17ºC. The gas-oil ratio was then converted to standard conditions. The model predictions for the gas-oil ratio and composition of the solution gas of Live Oil 1 are given in Table 5.10.

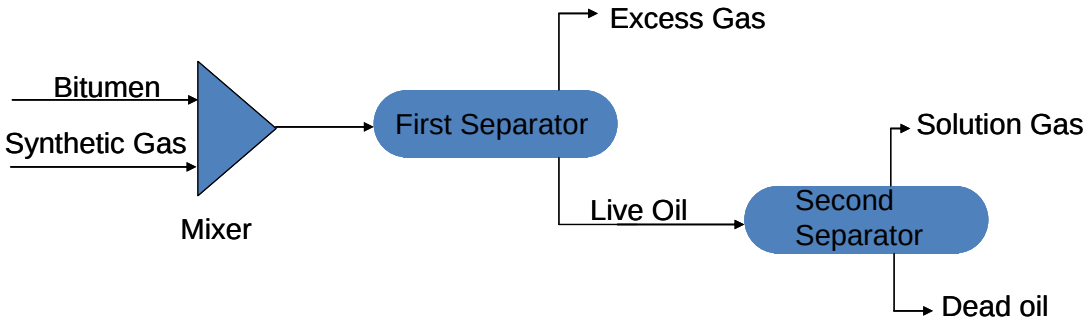

Figure 5.19: Simulation of the live oil preparation in VMGSim™

For the simulation of Live Oil 2 preparation, the same procedure was used as for Live Oil 1, except that pressure and temperature conditions for the first separator were 2650 kPaa and 18ºC. Model prediction for gas-oil ratio and composition of the solution gas of Live oil 2 are given in Table 5.10.

Table 5.10: Measured and modeled composition of solution gas and GOR for the Live Oils

Sample	Method	Mole Fraction			GOR* (m^3/m^3)
		Methane	Carbon dioxide	Nitrogen	
Live Oil 1	Measured	-	-	-	11±1
	Model	0.231	0.768	0.001	9.9
Live Oil 2	Measured	0.276	0.717	0.007	13±1
	Model	0.238	0.757	0.002	13.4

* at 15.6°C and 14.7 psia

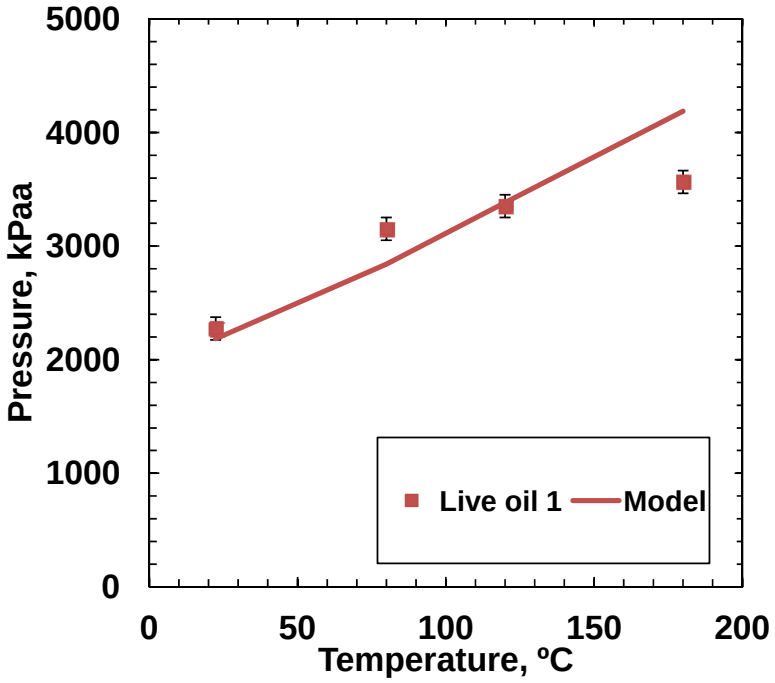

Figure 5.20: Experimental (symbols) and predicted (lines) saturation pressures for Live Oil 1

Live Oil and Condensate Mixtures

A final test is the prediction of the saturation pressure of a live oil diluted with a solvent, in this case, a multi-component condensate. The binary interaction parameters between the condensate pseudo-components and the bitumen pseudo-components were determined with Eqs. 5-2 and 5-3 and the same parameters that were fitted for the bitumen-bitumen pseudo-components: n, k_{ij}^{1} and k_{ij}^{2} equal to 0.27, 2550, and -1.5, respectively. The predicted saturation pressures of Live Oil 2 with 5.8 and 10 wt% condensate contents are compared with the measured pressures in Figure 5.21. The predictions are generally within ±400 kPa of the measured values with a deviation as high as 650 kPa at 180°C. The measured saturation pressures for both the live oil and the live oil/condensate mixtures appear to level off above 150°C. More data are required to confirm that this observation is not an experimental error. If the high temperature trend is verified, further refinement of the temperature dependent interaction parameters will be necessary.

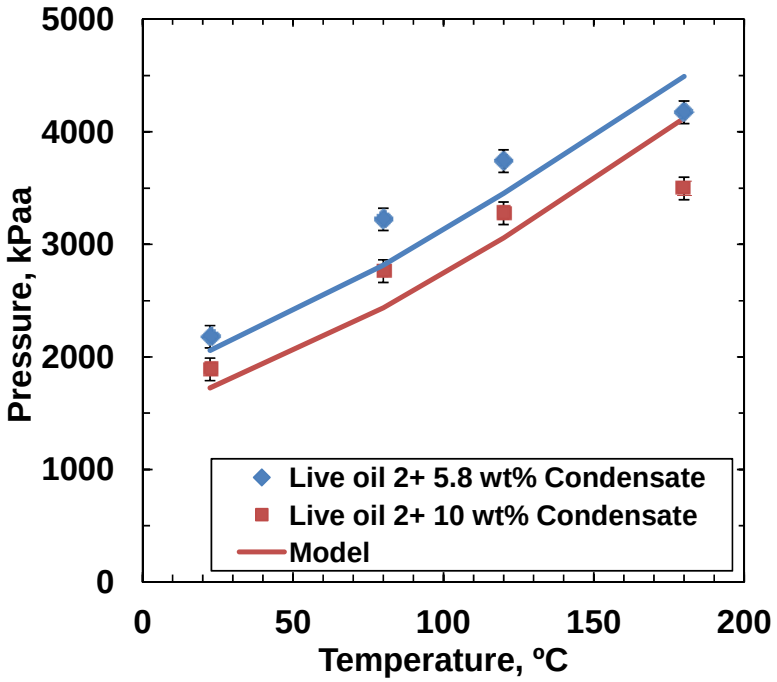

Figure 5.21: Experimental (symbols) and predicted (lines) saturation pressures for Live Oil 2 and condensate mixtures.

5.2.3 Tuning the Model for Asphaltene Precipitation

The model with temperature dependent binary interaction parameters fit the saturation pressures and liquid-liquid boundaries over a wide range of temperatures, generally within experimental error. The only exception was the onset of asphaltene precipitation at higher temperatures which the model failed to predict. Note, here "asphaltene precipitation" refers to the appearance of a dispersed asphaltene-rich liquid phase.

In order to fit both saturation pressure and asphaltene onset data over a wide range of temperatures, the temperature dependent binary interaction parameters ($k_{ij}^{1}$and k_{ij}^{2}) between the asphaltene pseudo-components and both the solvent and the maltene pseudo-components were modified to the values given in Table 5.11. Note, no precipitation of asphaltenes was observed for the CO_2/bitumen or methane/bitumen binaries because the solubility of these components is too low to cause precipitation. Therefore, the $k_{ij}^{1}$and k_{ij}^{2}

could not be tuned and were assumed to be the same as all the other asphaltene-pseudo-component parameters.

Table 5.11: Parameters for temperature dependent binary interaction parameters used to fit asphaltene onset and saturation pressure data over the range of the temperatures. Here maltenes refer to maltene pseudo-components and asphaltenes refer to asphaltene pseudo-components.

Binary Pairs	***n***	k_{ij}^{1}	k_{ij}^{2}
CO_2/maltenes	0.27	3170	-1.60
methane/maltenes	0.27	1920	-1.51
ethane/maltenes	0.27	2550	-1.50
Propane/maltenes	0.27	2550	-1.50
n-Pentane/maltenes	0.27	2550	-1.50
maltenes/maltenes	0.27	2550	-1.50
CO_2/asphaltenes	0.27	-811	0.69
methane/asphaltenes	0.27	-811	0.69
ethane/asphaltenes	0.27	-811	0.69
propane/asphaltenes	0.27	-811	0.69
n-pentane/asphaltenes	0.27	-811	0.69
maltenes/asphaltenes	0.27	-811	0.69
Asphaltenes/asphaltenes	0.27	-811	0.69

Figures 5.22, 5.23, 5.24, 5.25 show the measured (symbols) and fitted (lines) saturation pressures for mixtures of methane/bitumen, CO_2/bitumen, ethane/bitumen, *n*-pentane/bitumen respectively. Figure 5.27 shows the asphaltene onsets for *n*-pentane/bitumen mixtures at 22.4 and 180 ºC. The saturation pressures and liquid-liquid boundaries are fitted and predicted with the same accuracy as the previous model and now the asphaltene-onset at 180°C is also matched.

The predicted asphaltene yields from *n*-pentane diluted bitumen are also improved and the model predicts an *n*-pentane content in the asphaltene-rich between 5-6 wt% in better agreement with the 8 wt% maximum found by George *et al.* (2009). However, the model still under-predicts the yields at higher dilution suggesting the need for asymmetric mixing rules for modeling the asphaltene yield data.

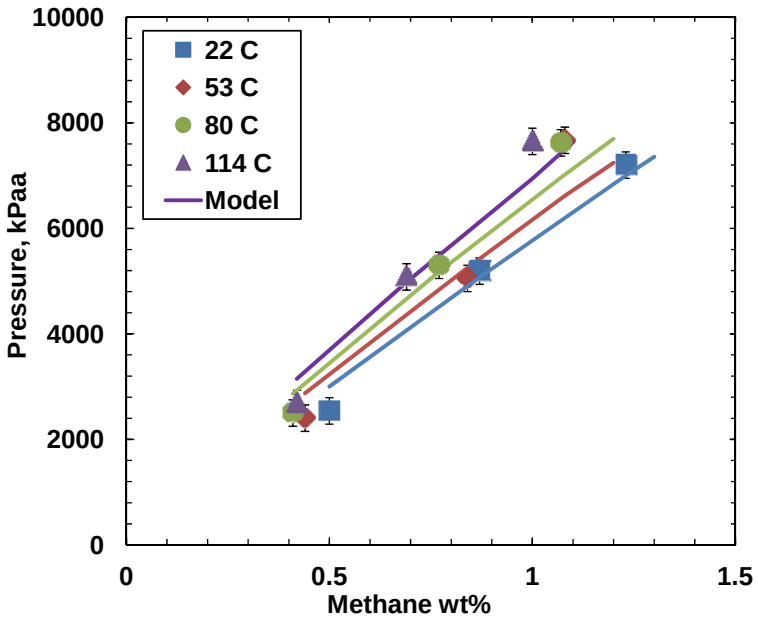

Figure 5.22: Saturation pressure of methane/Peace River bitumen pseudo-binary. Symbols are experimental data and solid lines are model with temperature dependent k_{ij} tuned to fit asphaltene onsets.

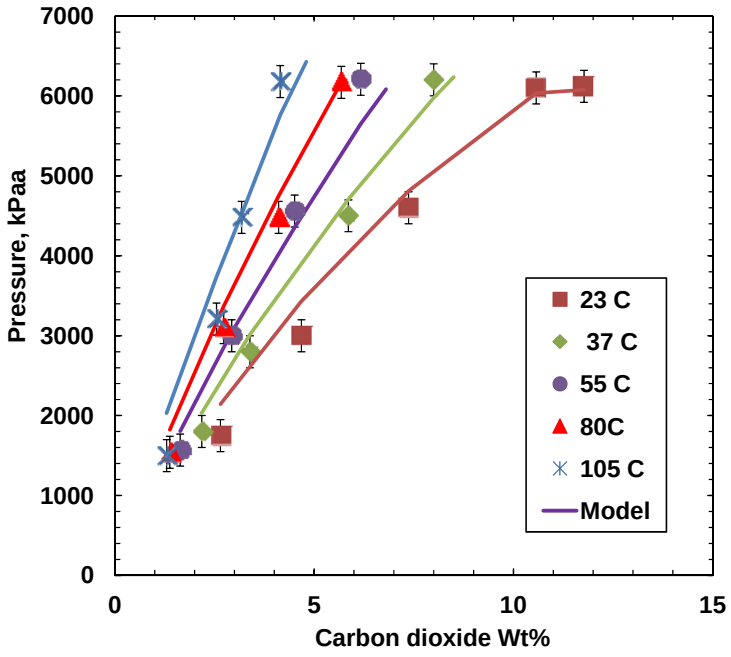

Figure 5.23: Saturation pressure of carbon dioxide/Peace River bitumen pseudo-binary. Symbols are experimental data and solid lines are model with temperature dependent k_{ij} tuned to fit asphaltene onsets.

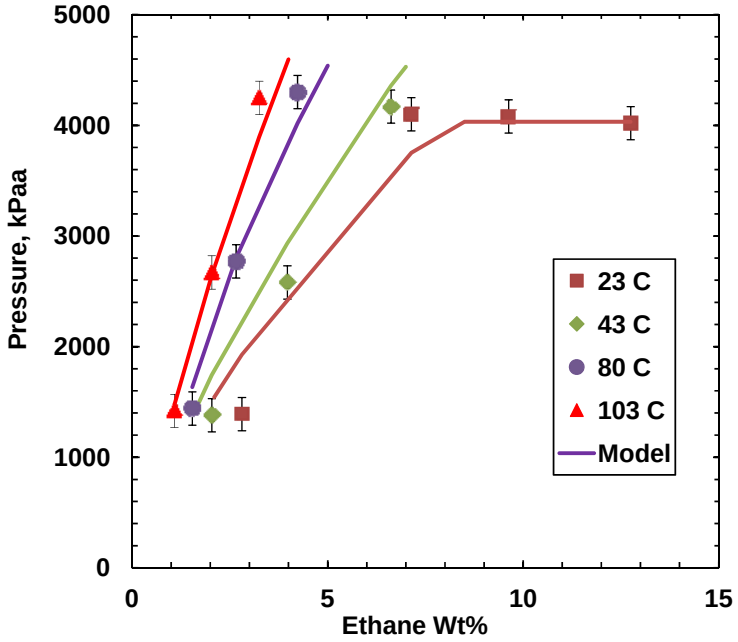

Figure 5.24: Saturation pressure of ethane/Peace River bitumen pseudo-binary. Symbols are experimental data and solid lines are model with temperature dependent k_{ij} tuned to fit asphaltene onsets.

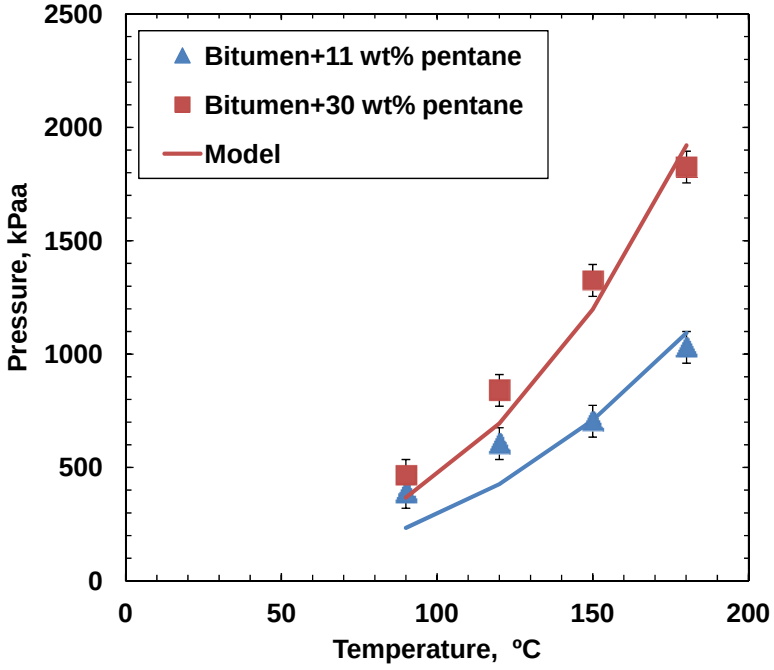

Figure 5.25: Saturation pressure of *n*-pentane/bitumen A pseudo-binary. Symbols are experimental data and solid lines are model with temperature dependent k_{ij} tuned to fit asphaltene onsets.

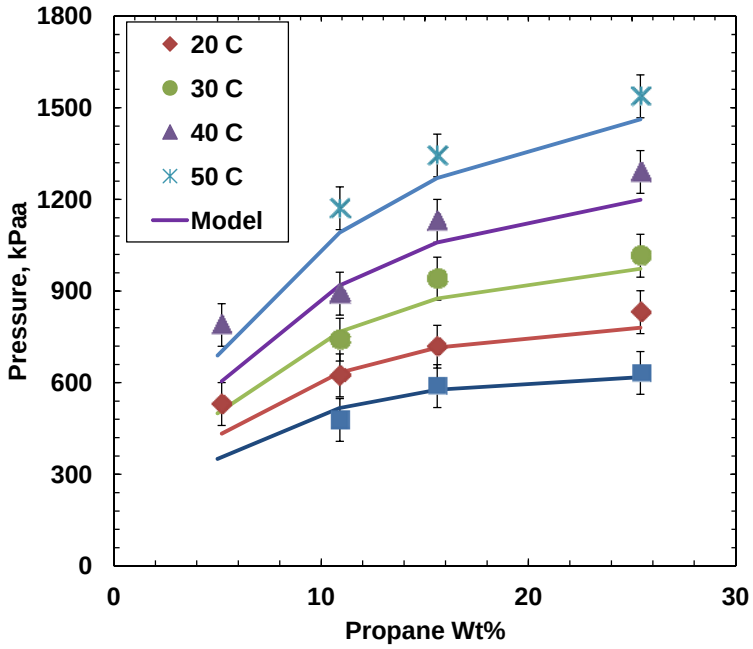

Figure 5.26 Saturation pressure of propane/bitumen B pseudo-binary. Symbols are experimental data and solid lines are model with temperature dependent k_{ij} tuned to fit asphaltene onsets.

Asphaltene onsets and yields were then *predicted* for the propane/bitumen pseudo-binary. Figure 5.28 shows that the model predicts onsets for asphaltene precipitation at 17 and 18 wt% propane at 22.4 and 180ºC, respectively. The predicted onsets are in excellent agreement with the measured onset of 17.5 wt% propane at 50°C, reported by Schlumberger-DBR (Section 5.1.4). The predicted propane content in the asphaltene rich phase asphaltene yield is from 3 to 4 wt%. Unlike the predictions for the *n*-pentane diluted bitumen; the predicted yields for the propane diluted bitumen do not disappear until very high dilution, Figure 5.28. Unfortunately, data are lacking to confirm the yield predictions.

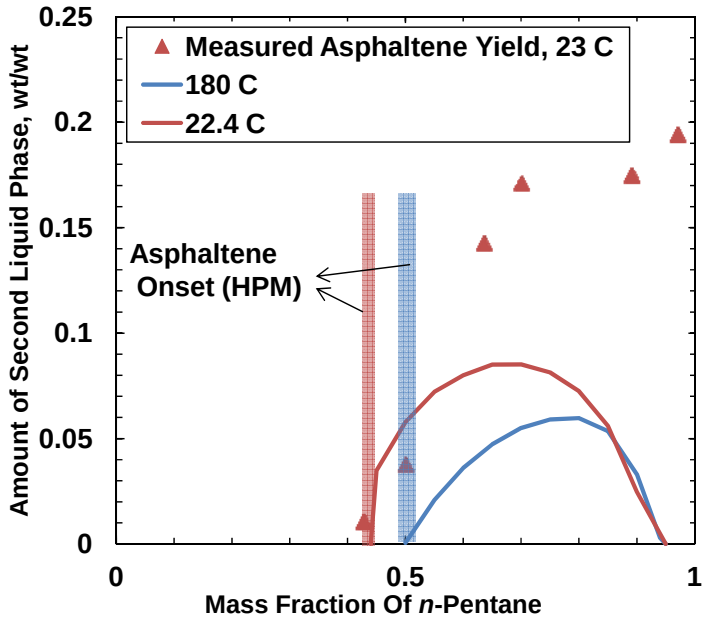

Figure 5.27: Measured and modeled asphaltene onset for *n*-pentane diluted bitumen at 23 and 180ºC. Symbols are measured asphaltene yield at 23ºC; solid lines are the predicted mass of asphaltene-rich liquid phase per unit mass of bitumen at 23 and 180ºC.

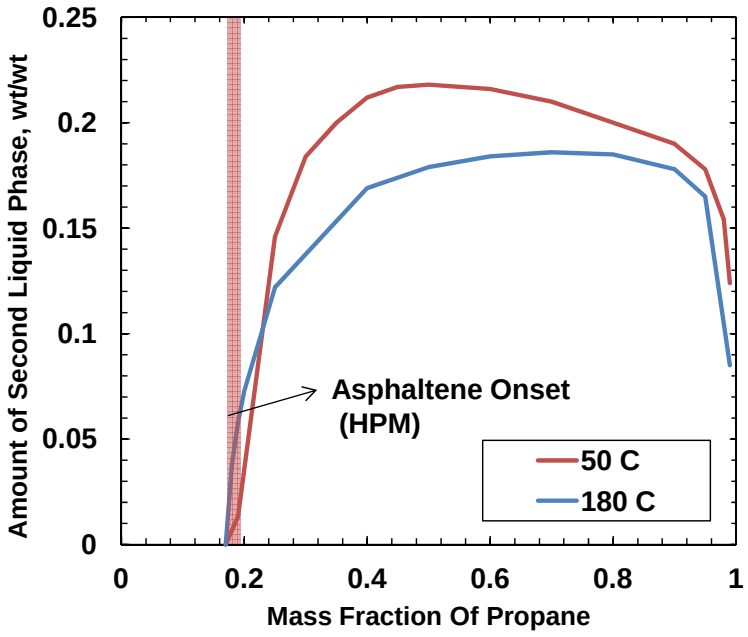

Figure 5.28: Measured and model predicted asphaltene onset for propane diluted bitumen. The solid lines are the predicted mass of asphaltene-rich liquid phase per unit mass of bitumen.

Finally, the saturation pressures for live oil and condensate mixtures were calculated as described in Section 5.2.2 but using the parameters from Table 5.11. Table 5.12 shows the gas-oil ratio and composition of solution gas predicted by the model. Figures 5.29 and 5.30 compare the predicted saturation pressures with the measured data. The predictions are not significantly altered from the previous case. Therefore, the model using the parameters in Table 5.11 fits all of the data in this study and is defined as the "base case" model.

Table 5.12: Measured and modeled composition of solution gas and GOR for the Live Oils

Sample	Method	Mole Fraction			GOR * (m^3/m^3)
		Methane	Carbon dioxide	Nitrogen	
Live Oil 1	Measured	-	-	-	11±1
	Model	0.235	0.763	0.001	9.9
Live Oil 2	Measured	0.276	0.717	0.007	13±1
	Model	0.239	0.758	0.002	13.3

* at 15.6°C and 14.7 psi

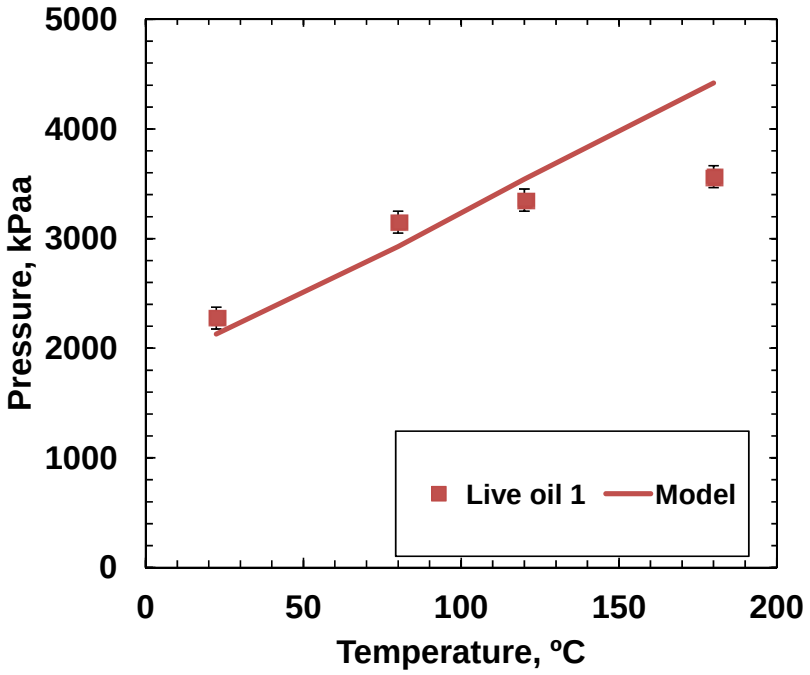

Figure 5.29: Experimental (symbols) and predicted (lines) saturation pressures for Live Oil 1.

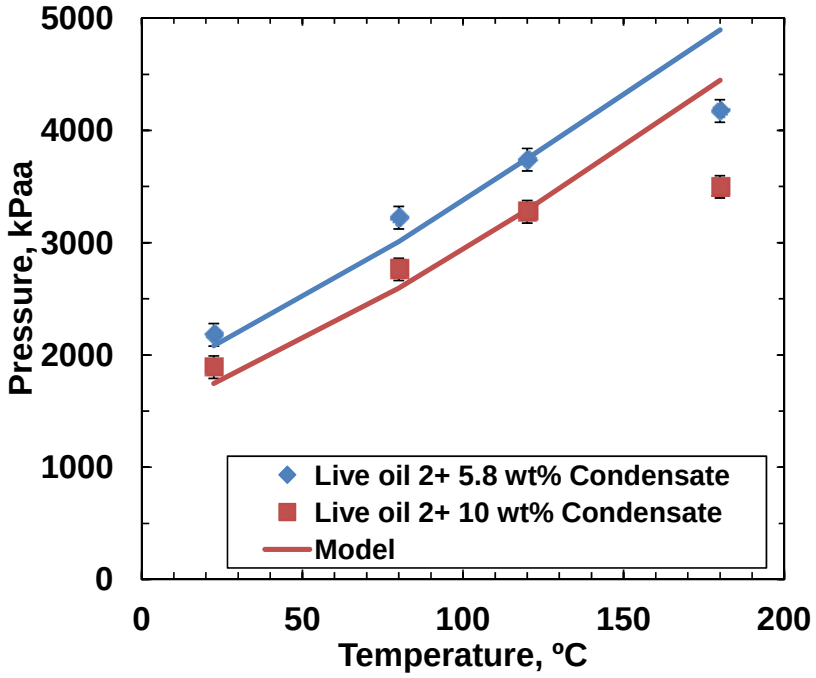

Figure 5.30: Experimental (symbols) and predicted (lines) saturation pressures for Live Oil 2 and condensate solvent mixture.

5.2.3.1 Effect of Pressure on Asphaltene Onset

The effect of pressure on the onset of asphaltene precipitation was not explicitly investigated in this study. However, it is well established that, in light oils, asphaltene precipitation can occur upon depressurization of the fluid (Tharanivasan *et al.* 2011). For an oil of a fixed composition, asphaltene precipitation is most likely to take place just above the saturation pressure, and increasing pressure above the bubble point will make the asphaltene phase dissolve. Below the saturation pressure, some gas will evaporate from the liquid and the gas concentration in the liquid phase will decrease which makes asphaltenes more soluble in the liquid and asphaltene phase will disappear (Pedersen *et al.*, 2007). The lowest pressure at which the last asphaltenes go into the solution is called the lower asphaltene onset pressure (lower AOP) and the highest pressure at which asphaltene go into the solution is called the upper asphaltene onset pressure (upper AOP).

The model predictions of the effect of pressure on asphaltene precipitation were tested for a mixture of 55 wt% *n*-pentane and Bitumen A. The predicted upper and lower asphaltene onset pressures at different temperatures are provided in Figure 5.31. The predicted yield at 150°C and different pressures is provided in Figure 5.32. The predictions are at least qualitatively correct with an asphaltene-rich phase appearing as pressure decreases, yields reaching a maximum at the saturation pressure, and then redissolving below the saturation pressure.

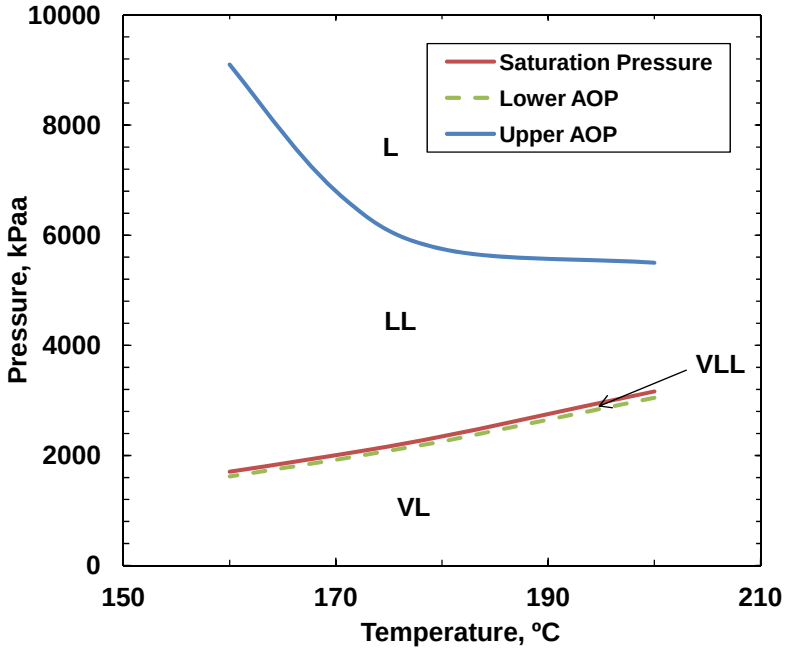

Figure 5.31: The effect of pressure on asphaltene onset for 55 wt% *n*-pentane in bitumen A.

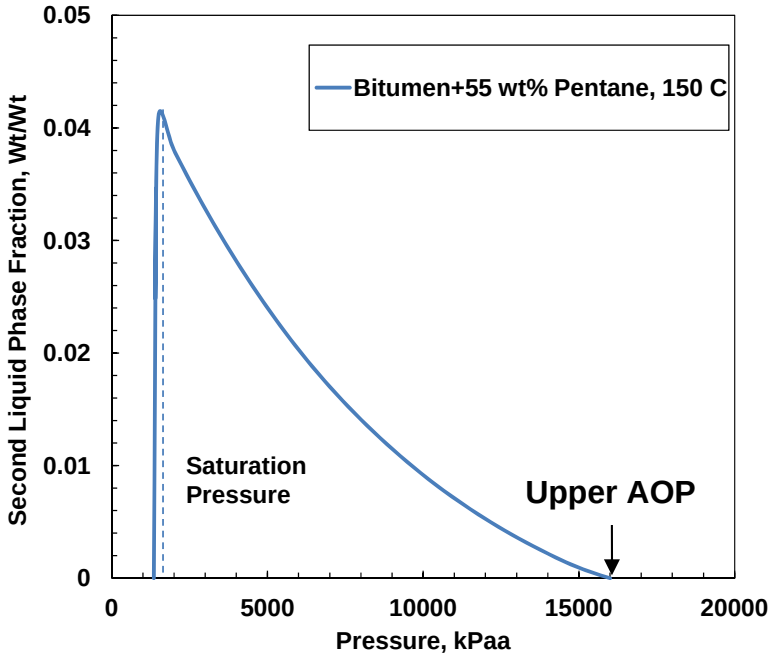

Figure 5.32: The effect of pressure on asphaltene yield for 55 wt% *n*-pentane in bitumen A at 150ºC

5.3 Sensitivity Studies

In this section effect of different NBP extrapolation, asphaltene average molecular weight and model sensitivity to a number of pseudo-components is examined.

5.3.1 NBP Extrapolation

Castellanos-Diaz *et al.* (2011) evaluated the effect of different NBP extrapolations on the prediction of phase equilibria for mixtures of bitumen, propane, and carbon dioxide. They found that the NBP extrapolation did not affect the prediction of saturation pressures since vapour-liquid equilibrium is mainly dominated by lighter components. The lightest 25 to 30 wt% of the normal boiling point distribution of the bitumen was measured and therefore was not altered in the different NBP extrapolations. However, liquid-liquid equilibrium predictions were found to be sensitive to the extrapolation.

Here, five cases are evaluated and compared to the base case to assess how NBP extrapolation affects the prediction of the asphaltene onset for *n*-pentane diluted bitumen mixtures. In all the cases, the critical properties and acentric factor were calculated using Lee-Kesler correlations. The average molecular weight and density of the bitumen were held at 580 g/mol and 1014.9 kg/m³, respectively. The binary interaction parameters were first determined using the values of *n,* k_{ij}^{1}, and k_{ij}^{2} from Table 5.11. Then, the $k_{ij}^{1}$and k_{ij}^{2} for the binary interaction parameters between the solvent and the asphaltene pseudo-components were adjusted to match the onset data. The average absolute relative deviation (AARD) between the predicted and measured saturation pressures was determined before and after tuning. The AARD is given by:

$$AARD = \sum_{i}^{N} \left| \frac{V_p^{\exp} - V_p^{calc}}{V_p^{\exp}} \right|$$

where N is the total number of the data points and $V_p^{\exp}$ and V_p^{calc} are the experimental and calculated saturation pressures, respectively. The five different NBP extrapolations are shown in Figure 5.33 and are discussed in detail below.

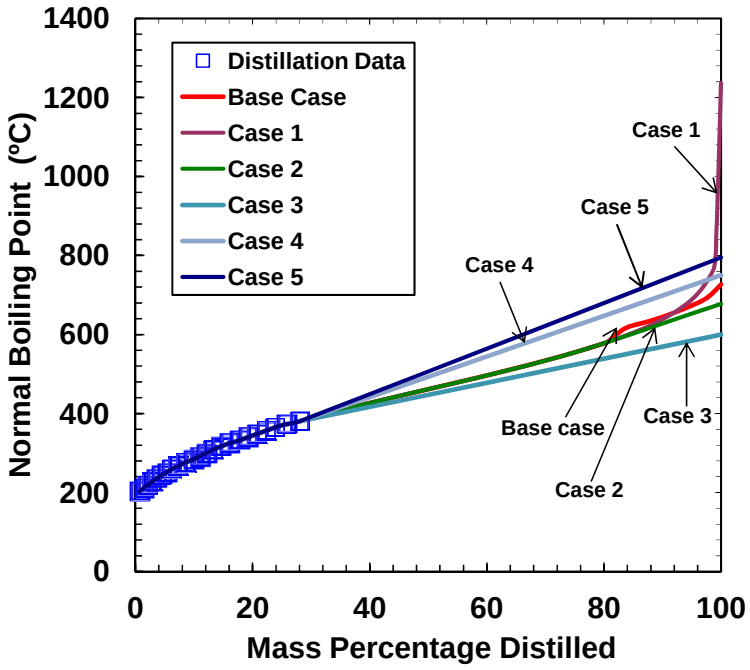

Figure 5.33: Extrapolations of bitumen distillation curve used in sensitivity study.

Case 1: It was assumed that asphaltenes followed the same Gaussian distribution as the maltenes which was extrapolated to a final boiling point (FBP) of 1237 ºC, Figure 5.33. This extrapolation created an unrealistic spike in the NBP of the asphaltenes which resulted in self incompatible bitumen. Therefore, this extrapolation was discarded.

Case 2: The distillation data were extrapolated over the maltenes using a Gaussian distribution (as with the base case) and using a linear extrapolation over the asphaltene fraction to an FBP of 727 ºC, Figure 5.33. With base case parameters, the model fit the saturation pressures as accurately as the base case, Table 5.14, but did not predict asphaltene precipitation at any temperature and solvent concentration. Therefore, *n* was adjusted to increase the binary interaction between solvent and asphaltene pseudo-components. Note that *n* value for solvent and maltenes pseudo-components was the same as the base case. The *n* values required to fit the asphaltene onset data are given in Table 5.13. After retuning, the AARD between predicted and measured saturation

pressures remain comparable to the base case, Table 5.14. The retuned model also predicted the liquid-liquid boundary with same accuracy as the base case for CO_2/bitumen mixture. For the ethane/bitumen and propane/bitumen mixtures, the liquid-liquid phase boundary prediction was within 0.5 wt% and 1 wt% of the base case, respectively.

Case 3, Case 4 and Case 5: In all these cases, an end point boiling temperature was assumed and distillation data was linearly extrapolated to the assumed end point. For Case 3, Case 4 and Case 5, the assumed end points were 600, 750 and 800 ºC respectively. Case 5 gives a self incompatible bitumen and was discarded. Cases 3 and 4 both still fitted the saturation pressure data without modification, Table 5.14. However, for Case 3 with base case parameters, the model did not predicted asphaltene precipitation at any temperature and solvent concentration. For Case 4, the model under-predicted the onsets for asphaltene precipitation (20 and 40 wt% *n*-pentane at 22 and 180ºC, respectively). The *n* values required to fit the asphaltene onset data are given in Table 5.13. In all the cases, *n* value was adjusted for solvent and asphaltene pseudo-components only. After retuning, the AARD between predicted and measured saturation pressures remain comparable to the base case, Table 5.14. For case 3 and 4, the retuned model also predicted liquid-liquid boundary with same accuracy as the base case for CO_2/bitumen mixture. For the ethane/bitumen and propane/bitumen mixtures, the liquid-liquid phase boundaries predictions were within 1.5 wt% of the base case.

Overall, as observed by Castellanos-Diaz *et al.* (2011), the FBP must be below 800°C to avoid a self-incompatible fluid. Changing the extrapolation of the NBP curve did not significantly affect saturation pressure prediction but did significantly affect asphaltene onset prediction. As the FBP increased, smaller binary interactions between solvent and asphaltene pseudo-components were required to fit the onsets.

Table 5.13: Values of n, k_{ij}^1, k_{ij}^2 used to match the onset of asphaltene precipitation in *n*-pentane diluted bitumen for different NBP extrapolations.

Case	n	k_{ij}^1	k_{ij}^2
Base Case	0.27	-811	0.69
Case 2	0.34	-811	0.69
Case 3	0.44	-811	0.69
Case 4	0.23	-811	0.69

Table 5.14: AARD of predicted saturation pressures of *n*-pentane diluted bitumen mixtures for different NBP extrapolations before and after tuning.

Cases	AARD (%) before tuning	AARD (%) after tuning
Base Case	-	1.30
Case 2	1.30	1.31
Case 3	1.31	1.32
Case 4	1.31	1.30

5.3.2 Asphaltene Average Molecular Weight

There is uncertainty in the measurement of asphaltene average molecular weight because asphaltenes self associate. Therefore, the sensitivity of the model predictions of the onset of asphaltene to the asphaltene average molecular weight was assessed. Again, initial predictions were made with the base case parameters and then the n for the binary interaction parameters between solvent and the asphaltene pseudo-components were adjusted to match the onset data. With base case parameters and an asphaltene average molecular weight of 3000 g/mol, the model predicted onsets for asphaltene precipitation at 33 and 48 wt% *n*-pentane at 22 and 180ºC, respectively. For 5000 g/mol, the model predicted onsets for asphaltene precipitation at 25 and 45 wt% *n*-pentane at 22 and 180ºC, respectively. The fitted n for asphaltene average molecular weights of 3000 and 5000 g/mol are given in Table 5.15. After tuning, the AARD of the predicted saturation pressures of the *n*-pentane/bitumen pseudo-ternary were 1.29 and 1.30 respectively, similar to the base case. The retuned model also predicted liquid-liquid boundary with

same accuracy as the base case for CO_2/bitumen mixture. For the ethane/bitumen and propane/bitumen mixtures, the liquid-liquid phase boundaries predictions were within 0.3 wt% of the base case. .

Table 5.15: Values of n, k_{ij}^1, k_{ij}^2 used for calculating binary interaction between solvent and asphaltene pseudo-components to fit the asphaltene onset

Asphaltene average molecular weight (g/mol)	n	k_{ij}^1	k_{ij}^2
2000 (Base Case)	0.27	-811	0.69
3000	0.25	-811	0.69
5000	0.23	-811	0.69

5.3.3 Number of Pseudo Components

In reservoir simulation, a larger number of pseudo components significantly increase the simulation time. Therefore, sensitivity to the number of pseudo-components was carried out to determine the minimum number of pseudo-components required to accurately predict phase behaviour of *n*-pentane/bitumen mixtures. In the base case, ten pseudo components were used for maltenes and six pseudo components were used for the asphaltenes. The number of pseudo-components could be reduced to two pseudo-components for maltenes and one pseudo-component for the asphaltenes without impacting the accuracy of the predictions; Table 5.16. Note the binary interactions were calculated using the base case parameters. The model also predicted asphaltene onsets with same accuracy as the base case. The three pseudo-components model also predicted the liquid-liquid boundaries with same accuracy as the base case in all cases. Table 5.17 provides the properties of the pseudo-components for the three pseudo-components case. With two components, the model predicts saturation pressure with same accuracy as base case; however the predicted onsets for asphaltene precipitation were incorrect (55 and 60 wt% *n*-pentane at 22 and 180ºC, respectively).

Table 5.16: AARD for cases with different number of pseudo-components

Number of Pseudo-components	16	11	5	3	2
n-pentane/bitumen	1.30	1.29	1.30	1.30	1.31

Table 5.17: Properties of three pseudo-components of bitumen

Components	Mass Fraction	MW (gm/mol)	NBP (°C)	Pc (kPa)	Tc (°C)	ω
PR_malt[282]C	0.583	448	377	1747	575	0.78
PR_malt[424]C	0.223	682	536	1084	709	1.16
Asph1*	0.194	2,000	714	945	899	1.28

5.4 Recommended Procedure for Characterization and Modeling

A procedure was developed to characterize heavy oils for phase behaviour modeling with the Advanced Peng-Robinson equation-of-state and is summarized below.

Extrapolate the distillation based NBP data for the bitumen over the maltene fraction using a Gaussian distribution. Divide the NBP curve into pseudo-components representing boiling fractions. Ten components are recommended to match the NBP data but as few as two can be used to model the phase behaviour. Calculate the molecular weight and specific gravity of each pseudo-component using the Lee-Kesler and Katz Firoozabadi correlations, respectively. Adjust the calculated molecular weight and specific gravity of each pseudo-component with a multiplier to fit the average values measured for the maltenes.

Represent the asphaltene fraction with a Gamma distribution of molecular weights (recommended inputs MWm= 840 g/mol, β = 2.5 and MW_{Avg} = 2000 g/mol). Divide the asphaltene fraction into pseudo-components. Six were used to represent the distribution but as few as two could fit the phase behaviour data. Calculate the specific gravity of

each pseudo-component based on an experimental derived density distribution. Calculate the NBP of the pseudo-components using the Søreide correlation.

Estimate the critical properties and acentric factor of the maltene and asphaltene pseudo-components with the Lee-Kesler correlations.

Tune the model to fit the available saturation pressure by adjusting binary interaction parameter between solvent and bitumen pseudo-components via the temperature dependent binary interaction parameter correlation, Equation 5-2. It is recommended to fix the exponent n at 0.27 and adjust k_{ij}^{1} and k_{ij}^{2} to fit saturation pressure data. Note, saturation pressures for heavy oils diluted with solvents are insensitive to the heavy end characterization used for asphaltene modeling. Therefore, the interaction parameters reported in this thesis (Table 5.11) can be used as a starting point for the model tuning.

Tune the model to fit the available asphaltene precipitation onset data by adjusting the temperature dependent binary interaction parameter between the asphaltene pseudo-components and solvent. When data at a variety of conditions are available, it is recommended to fix the exponent n at 0.27 and adjust k_{ij}^{1} and k_{ij}^{2}.

CHAPTER SIX: CONCLUSIONS AND RECOMMEDATIONS

6.1 Summary

Saturation pressures were measured for live oil and condensate solvent mixtures at condensate contents up to 10 wt% and temperatures from 22.4 to 180°C. Saturation pressures were also collected for *n*-pentane diluted bitumen mixtures at *n*-pentane contents up to 30 wt% and temperatures from 90 to 180°C. For *n*-pentane/bitumen mixtures, the onset of asphaltene precipitation (the minimum amount of solvent at which precipitation was observed at a given pressure and temperature) was measured at 22.4 and 180°C at low pressure. The amount of asphaltene precipitated from pentane diluted dead bitumen was also measured at different solvent contents at ambient conditions.

A bitumen characterization was developed for modeling the measured data, as well as literature data, with the Advanced Peng-Robinson equation-of-state (APR EoS). To characterize the bitumen, distillation data were extrapolated over maltenes fraction using Gaussian distribution. The boiling curve was divided into 10 pseudo-components representing boiling ranges. Asphaltenes were characterized based on a Gamma distribution of the molecular weights of self-associated asphaltenes. The molecular weight distribution was divided into 6 pseudo-components representing molecular weight ranges. Existing property correlations supplemented with molecular weight and density measurements were used to determine: first, the boiling point, specific gravity, and molecular weight; and then, the critical properties and acentric factor of all the pseudo-components.

The APR EoS model was tuned, in three steps, to fit saturation pressure and asphaltene onsets data of pseudo-binaries from the literature as well as data collected in this study. First, the binary interaction parameters were tuned to match ambient temperature data. Second, temperature dependent binary interaction parameters were introduced to match the data at higher temperatures. Third, the temperature dependent interaction parameters between asphaltene pseudo-components and other components were adjusted to fit onset

data. The tuned model was then tested on independent data for propane diluted bitumen and for live oils diluted with condensate. The model predictions for asphaltene yields were also evaluated. Finally, the effect of different NBP extrapolation, asphaltene average molecular weight and model sensitivity to a number of pseudo-components was also examined.

6.1 Conclusions

A significant conclusion from this study is that temperature dependent binary interaction parameters are required to fit the saturation pressures of dead bitumen mixed with solvent. For all hydrocarbon-hydrocarbon pairs excluding methane, the temperature dependent parameters were identical. Distinct interaction parameters were also required for carbon dioxide. The model using parameters obtained from matching the pseudo-binaries successfully predicted the saturation pressures of the live oils with and without added condensate. The tuned model also correctly predicted liquid-liquid boundaries where a second solvent-rich liquid phase formed.

A significant observation from this study is that asphaltenes precipitated from *n*-pentane diluted bitumen were glassy particles at ambient temperature but were a dispersed liquid phase at 180ºC. Despite the asphaltene-rich phase passing through an apparent glass transition, the onset of asphaltene precipitation changed very little with temperature. The asphaltene onset occurred between 46 to 48 wt% *n*-pentane at 22.4 ºC and between 48 to 52 wt% *n*-pentane at 180 ºC.

Distinct tuning of the interaction parameters between asphaltenes and other components was required to match the observed onset of asphaltene precipitation from *n*-pentane diluted bitumen at both ambient and higher temperatures. The tuned model, correctly predicted the onset of asphaltene precipitation in propane diluted bitumen.

Consistent with previous work, the experimental asphaltene yields in *n*-pentane diluted bitumen were observed to increase monotonically with *n*-pentane content. However, the model predicted that the asphaltenes become soluble at high dilution. For propane diluted bitumen, the predicted asphaltene yields remained nearly constant until very high dilution. However, there were no data available to test the prediction.

The model provided qualitatively correct predictions that an asphaltene-rich phase will form when single phase *n*-pentane diluted bitumen is depressurized. The yields were predicted to reach a maximum at the saturation pressure and then redissolving below the saturation pressure. This type of behaviour has been observed for depressurized live oils but no data were available for *n*-pentane diluted bitumen.

The following conclusions were drawn from the sensitivity study:

1. Extrapolation of NBP data using Gaussian distribution over maltenes and asphaltenes led to unrealistic spike in the NBP of the asphaltenes which results in self incompatible bitumen. Extrapolation of NBP with final boiling point above 800ºC also results in self-incompatible fluid.
2. Different extrapolations of the NBP curve did not affect saturation pressure prediction but did significantly affect the predicted asphaltene onsets. For lower final boiling points, higher binary interactions between solvent and asphaltene pseudo-components were required to fit the onset data.
3. Changing the asphaltene average molecular weight in the model did not affect saturation pressure prediction but did affect the predicted asphaltene onsets. For higher asphaltene average molecular weight, lower binary interactions between solvent and asphaltene pseudo-components were required to fit the onset data.
4. The number of pseudo-components had no effect on the prediction of saturation pressure and asphaltene onset as long as there were at least two pseudo-components used for maltenes and one pseudo-components used for the asphaltenes.

6.2 Recommendations

To improve the EoS model and to enhance its capability the following recommendation are made in terms of required experimental data and modeling methods:

1. The measured saturation pressures for both the live oil and the live oil/condensate mixtures appeared to level off above 150°C while the model predicted increasing saturation pressures. It is recommended to collect more data at high temperatures to confirm that the observed plateau in saturation pressure is not an experimental error. If the high temperature trend is verified, further refinement of the temperature dependent interaction parameters will be necessary.
2. The one significant failure of the model was the prediction of asphaltene precipitation at high dilution for the *n*-pentane/bitumen mixture. A CEoS with conventional mixing rules predicts that asphaltenes become soluble at high dilutions but the data prove otherwise. A possible remedy is an asymmetric mixing rule between the asphaltenes and the rest of the mixture. With asymmetric mixing rule, interaction between bitumen and solvent could be made composition dependent and a high interaction between asphaltene and solvent could be used at high dilution to match the observed yields and compositions.
3. Since the asphaltene-rich phase becomes liquid at higher temperatures, it is recommended to isolate a continuous asphaltene-rich phase which would allow accurate measurement of the phase composition. The compositional data are required to constrain any proposed asymmetric mixing rules.
4. It is recommended to collect asphaltene yield data for propane diluted bitumen to verify the model predictions. Although there is no standard procedure to collect asphaltene yield data for propane diluted bitumen, the following method can be used. Inject a known mass of propane and bitumen into the PVT cell at elevated temperature (approximately 150ºC) so that asphaltene-rich phase becomes a liquid. Mix propane and bitumen uniformly using the magnetic stirrer, giving sufficient time for the mixture to equilibrate. Pass the mixture slowly through the High Pressure Microscope cell to identify the boundary between the solvent-rich

phase and the asphaltene-rich phase. Transfer the asphaltene-rich phase to a pycnometer and measure its mass.

5. In order to verify the predicted effect of pressure, it is recommended to collect asphaltene onset data by depressurizing solvent diluted bitumen at different temperatures.

References

Ahmed, T., *Hydrocarbon Phase Behavior*, Gulf Publishing Company, Houston, **1989**

Agrawala,M., Yarranton, H.W., Asphaltene Association Model Analogous to Linear Polymerization, *Industrial and Engineering Chemistry Research*, 40 (21), 4464-4672, **2001**

Akbarzadeh, K., Alboudwarej, H., Svrcek, W.Y. and Yarranton, H.W., A Generalized Regular Solution Model for Asphaltene Precipitation from *n*-Alkane Diluted Heavy Oils and Bitumens; *Fluid Phase Equilibria, Vol. 232, Nos. 1-2, pp. 159-170,* **2005.**

Alboudwarej, H., *PhD. thesis*, University of Calgary, Calgary, AB, **2003.**

Alboudwarej, H., Beck, J., Svrcek, W.Y. and Yarranton, H.W., Sensitivity of Asphaltene Properties to Separation Techniques: *Energy and Fuels*, Vol. 16, pp. 462-469, **2002.**

Alboudwarej, H., Akbarzadeh, K., Beck, J., Svrcek, W.Y. and Yarranton, H.W., Regular Solution Model for Asphaltene Precipitation from Bitumens and Solvents: *AIChE Journal*, Vol. 49, No. 11, November **2003.**

Altgelt, K., Boduzinsky, M.M., Composition and Analysis of Heavy Petroleum Fractions, **1993.**

Andersen, S.I., Speight, J.G., Thermodynamics models for asphaltene solubility and precipitation: *Journal of Petroleum Science and Engineering* , Vol. 22, Issue 1-3, pp. 53-66*,* **1999.**

ASTM D2007 - 03e1 Standard Test Method for Characteristic Groups in Rubber Extender and Processing Oils and Other Petroleum-Derived Oils by the Clay-Gel Absorption Chromatographic Method; *ASTM International*, West Conshohocken, PA, May 10, **2003.**

Badamchi-Zadeh, A., Yarranton, H.W., Svrcek, W.Y. and Maini, B.B., Phase Behavior and Physical Property Measurements for VAPEX Solvents: Part I. Propane and Athabasca Bitumen: *Journal of Canadian Petroleum Technology*, Vol. 48, No. 1, pp. 54-61, January **2009**.

Badamchi-Zadeh, A., Yarranton, H.W., Satyro, M.A. and Maini, B.B., Phase Behavior and Physical Property Measurements for VAPEX Solvents: Part II. Propane, Carbon Dioxide and Athabasca Bitumen: *Journal of Canadian Petroleum Technology*, Vol. 48, No. 3, pp. 57-65, March **2009**.

Burke, N.E., Hobbs, R.E., and Kashou, S.F., Measurement and modeling of asphaltene precipitation: *JPT* 42 SPE-18273-PA, **1990.**

Canada's Oil Sands—Opportunities and Challenges to 2015: An Update.. http://www.neb.gc.ca/clf-nsi/rnrgynfmtn/nrgyrprt/lsnd/pprtntsndchllngs20152006/qapprtntsndchllngs20152006-eng.html, *National Energy Board of Canada,* 2007-06-30, **2007**

Castellanos Díaz, O., Modaresghazani, J., Satyro, M.A., and Yarranton, H.W., Modeling the Phase Behavior of Heavy Oil and Solvent Mixtures: *Fluid Phase Equilibria*, Vol. 304, Nos. 1-2, pp. 74-85, **2011.**

Chapman, W.G., Jackson, G., and Gubbins, K.E., Phase Equilibria of associating fluids, chain molecules with multiple bonding sites, *Mol. Phys*. 65, 1057-1079, **1988**

Chapman, W.G., Gubbins, K.E., Jackson, G., and Radosz, M., *Ind. Eng. Chem. Res.* 29**,** 1709-1721, **1990**

Chapman, W.G., Ting, P.D., Hirasaki, G.J., Modeling of Asphaltene Phase Behavior with the SAFT Equation of State, *Petroleum Science and Technology*, Vol. 21, Nos. 3&4, pp. 647-661, **2003.**

Chapman, W.G., Gonzalez, D.L., Hirasaki, G.J., Creek, J., Modeling of Asphaltene Preciptation Due to Changes in Composition Using the Perturbed Chain Statistical Associating Fluid Theory Equation of State, *Energy and Fuels*, 21, 1231-1242, **2007**

Chueh, P.L., Prausnitz, J.M., Calculation of High-Pressure Vapor-Liquid Equilibria, *Ind. Eng. Chem*., 60, No. 13, **1968**

Chung, K.E., Anderson, L.L., Wiser, W.H., New procedure for molecular weight determination by Vapor-Phase Osmometry, *Fuel*, 58, 847-852, **1979.**

Danesh A., PVT and Phase Behavior of Petroleum Reservoir fluids, *Elsevier Publications*, **2007**

Erwin, D.L., *Industrial Chemical Process Design*, McGraw-Hill Companies, **2002.**

Frauenfeld, T.W.J., Kissel, G. and Zhou, S.W., PVT and Viscosity Measurements for Lloydmister-Aberfeldy and Cold Lake Blended Oil Systems; paper SPE 79018 presented at the *SPE International Thermal Operations and Heavy Oil Symposium and International Horizontal Well Technology Conference*, Calgary, AB, 4-7 November **2002.**

Fu, C., Puttagunta, R., Pseudo-critical properties of heavy oils and bitumens, *Fluid Phase Equilibria*, vol. 30, 281-295, **1986.**

Freitag, N.P., Sayegh, S.G. and Exelby, R., A New Semiautomatic PVT Apparatus for Characterizing Vapex Systems; paper SPE 97783 presented at the *SPE/PS-CIM/CHOA International Thermal Operations and Heavy Oil Symposium*, Calgary, AB, 1-3 November **2005.**

Gao, G., Daridon, J.L., Saint-Guirons, H., Xans, P., A simple correlation to evaluate binary interaction parameters of the Peng-Robinson equation of state: binary light hydrocarbon systems: *Fluid Phase Equilibria*, Vol. 74, pp. 85-93, July **1992.**

George, S., Satyro, M.A., and Yarranton, H.W., Measurement and Modeling of Asphaltene-Rich Phase Composition, *World Congress of Chemical Engineering*, Montreal, August 23-17, **2009**.

Gross, J., and Sadowski, G., *Ind. Eng. Chem. Res.* 40**,** 1244-1260, **2001.**

Hirschberg, A., Dejong, N.J., Schipper, B.A., and Meijer, J.G., Influence of Temperature and Pressure on Asphaltene Flocculation, *Soc. Pet. Eng. J*., 24, 283-291, **1984.**

Jacoby, R.H., Phase Behavior of Light Hydrocarbon - Heavy Oil or Tar Systems, and Its Application to Recovery Processes; *In Situ*, Vol. 11, Nos. 2-3, pp. 145-167, **1987**.

Jia, N., Memon, A., Zuo, J., Zhao, H., Ng, H.-J., Huang, H., Three- Phase Equilibrium Study for Heavy-Oil/Solvent/Steam System at High Temperatures, *Journal of Canadian Petroleum Technology*, SPE 137453, **2011.**

Jiang,Q., Recovery of Heavy Oil Using Vapex Process in Homogeneous and Heterogeneous Reservoirs; *Ph.D. dissertation*. University of Calgary, Calgary, AB, **1997**

Jamaluddin, A.K.M, Joshi, N., Joseph, M.T., D'Cruz, D., Ross, B., Creek, J., Kabir, C.S., McFadden, J.D., Laboratory Techniques to define the asphaltene precipitation envelope, presented at the *Petroleum Society's Canadian International Conference* in Calgary, Canada, June **2000**

Jamaluddin, A.K.M, Joshi, N., Iwere, F., Gurpinar, F., An investigation of Asphaltene instability under nitrogen injection, SPE 74393 presented at *SPE International Petroleum Conference and Exhibition* in Villahermosa, Mexico, Feb **2002**

Jhaveri, B.S, and Youngren, G.K., Three parameter modification of the Peng Robinson equation of state to improve volume predictions, *SPE Res. Eng.,* 1033-1040, August **1988**

Jiang,Q., Recovery of Heavy Oil Using Vapex Process in Homogeneous and Heterogeneous Reservoirs; *Ph.D. dissertation* University of Calgary, Calgary, AB, **1997**

Jossy, C., Frauenfeld, T., Rajan, V., Partitioning of Bitumen-Solvent Systems into Multiple Liquid Phases, *Canadian International Petroleum Conference*, *SPE*, Jun 17-19, **2008**

Katz, D.L. and Firoozabadi, A., Predicting Phase Behavior of Condensate/Crude-Oil systems Using Methane Interaction Coefficients, *JPT*, November **1978**

Katz, D.L., *Handbook of Natural Gas Engineering*, McGraw-Hill Book Co. Inc., New York City, **1959**

Kontogeorgis, G., Voutsas, E., Yakoumis, I., Tassios, D., *Ind. Eng. Chem. Res.* 35, **1996**

Kokal, S.L. and Sayegh, S.G., Asphaltene: The cholesterol of petroleum: In: *SPE Middle East Oil Show*, Bahrain, Paper SPE 29787, March 11-14, **1995**.

Kokal, S., Sayegh, S.G., Phase Behavior and Physical Properties of the CO_2-Saturated Heavy oil and its constitutive fractions: Experimental Data and Correlation, *Journal of Petroleum Science and Engineering*, 9, 289-302, **1993**

Kordas. A., Tsoutsouras , K., Stamataki, S. and Tassios , D., A generalized correlation for the interaction coefficients of CO2-hydrocarbon binary mixtures, *Fluid Phase Equilibria* , 93, 141-166, **1994**

Kordas, A., Magoulas, K., Stamataki, S., Tassios, D., Methane-hydrocarbon interaction parameters correlation for the Peng-Robinson and the t-mPR equation of state: *Fluid Phase Equilibria*, Vol. 112, pp. 33-44, November **1995**.

Lastovka, V., Fulem, M., Becerra, M., Shaw, J.M., A similarity variable for estimating the heat capacity of solid organic compounds: Part II. Application: Heat capacity calculation calculation for ill-defined organic solids: *Fluid Phase Equilibria*, Vol. 268, pp. 134-141, June **2008.**

Lee, B.I. and Kesler, M.G., Improve Vapour Pressure Prediction, *Hydrocarbon Processing*, 163-167, July **1980**

Lee, B.I. and Kesler, M.G., Improve Predictions of Enthalpy of Fractions, *Hydrocarbon Processing*, 55, 153-158, March **1980**

Leontaritis, K.J., Mansoori, G.A., Asphaltene flocculation during oil recovery and processing: A Thermodynamics-Colloidal model, *SPE International Symposium on Oil Field Chemistry*, SPE-16258, San Antonio, **1987**.

Luo, P., Wang, X., GU, Y., Characterization of Asphaltenes Precipitated with Three Light Alkanes under Different Experimental Conditions: *Fluid Phase Equilibria*, Vol. 291, Issue 2, pp. 103-110, **2010.**

Maxwell and Bonnell, *Industrial Engineering Chemistry*, Vol 49, p. 1187, **1957**

Mehrotra, A.K. and Svrcek, W.Y., Measurement and Correlation of Viscosity, Density and Gas Solubility for Marguerite Lake Bitumen Saturated with Carbon Dioxide; *AOSTRA Journal of Research*, Vol. 1, No. 1, pp. 51-62, **1984**.

Mehrotra, A.K. and Svrcek, W.Y., Viscosity, Density and Gas Solubility Data for Oil Sand Bitumens. Part II: Peace River Bitumen Saturated with N2, CO, CH4, CO2 and C2H6; *AOSTRA Journal of Research,* Vol. 1, No. 4, pp. 269-279, **1985.**

Michelsen, M.L., the Isothermal Flash Problem. Part 1. Stability, *Fluid Phase Equilibria*, 9, 1, **1982**

Modaresghazani, J., *M.Sc. thesis*, University of Calgary, Calgary, AB, **2009**

Moschopedis, S.E., Fryer, J.F., Speight, J.G., Investigation of the Asphaltene Molecular Weights, *Fuel*, 55, 227-232, **1976**

Motahhari, H., Schoeggl, F. F., Satyro, M. A., Yarranton, H.W., Prediction of the Viscosity of Solvent Diluted Live Bitumen at Temperatures up to 175°C, *CURC 2011*, Calgary, **2011**

Nji, G.N., Svrcek, W.Y., Yarranton, H.W., Satyro, M.A., *Energy and Fuels*, 23, 366-373, **2008**

Nishiumi, H., Arai, T., Takeuchi, K., Generalization of the binary interaction of the Peng-Robinson equation of state by component family: *Fluid Phase Equilibria*, Vol 42, pp. 43-68, **1988**.

Pedersen, K.S., and Christensen, P. L., Phase Behavior of Petroleum Reservoir Fluids, *CRC Press, Taylor and Francis Group*, **2007**

Pedersen, K.S., Krejbjerg, K., Controlling VLLE Equilibrium with a Cubic EoS in Heavy Oil Modeling, presented at the *Petroleum Society's 7th Canadian International Petroleum Conference*, Calgary, Canada, June **2006**

Peneloux, A., Rauzy, E., Freze, R., A consistent correction for Redlich-Kwong-Soave Volumes, *Fluid Phase Equilibria*, 8, 7-23, **1982**

Peng, D.Y., Robinson, D.B., A New Two-Constant Equation of State, *Ind. Eng. Chem. Fundam*., 15, 59, **1976**

Peng, D.Y., Robinson, D.B., The Characterization of Heptanes and heavier Fractions for GPA Peng-Robinson Programs, *GPA Research Report* RR-28, **1978**

Perakis, C., Voutsas, E., Magoulas, K., Tassios, D., *Fluid Phase Equilib.,* 243, **2006**

Permanu, S., Singh, C., Agrawala, M., Yarranton, H.W., Investigation on the Reversibility of the Asphaltene Precipitation, *Energy and Fuels*, 15, 910-917, **2001**

Rachford, H.H., Rice, J.D., Procedure to Use Electrical Digital Computers in Calculating Flash Vaporizing, *JPT*, **1952**

Redlich, O., Kwong, J.N.S., On the Thermodynamics of Solutions. V: An Equation of State. Fugacities of Gaseous Solutions, *Chem. R.*, 44, 233*,* **1949**

Riazi, M.R., Daubert, T.E., Analytical Correlations Interconvert Distillation-Curve Types, *Oil and Gas J.,* 50, **1986**

Rogel, E. Studies on Asphaltene Aggregation via Computational Chemistry, Colloids and Surfaces A: *Physicochemical and Engineering Aspects*, 104, 85, **1995**

Satyro, M.A., Lee, J.V.D., The performance of state of the art industrial thermodynamic models for the correlation and prediction of acid gas solubility in water, *First International Acid Gas Injection Symposium*, Calgary, October **2009**

Shelton, J.L. and Yarborough, L., Multiple Phase Behavior in Porous Media During CO2 or Rich-Gas Flooding: *Journal of Petroleum Technology*, Vol. 29, No. 9, pp. 1171-1178, September **1976**

Soave, G., Application of a Cubic Equation of State to Vapor-Liquid Equilibria of Systems Containing Polar Compounds, *Inst. Chem. Eng. Symp*. Ser., 56, 1.2/1, **1979**

Soave, G., Equilibrium Constants from a Modified Redlich-Kwong Equation of State, *Chem. Eng. Sci*., 27, 1197, **1972**

Søreide, I., Improved Phase Behavior Predictions of Petroleum Reservoir Fluids From a Cubic Equation of State, "*Dr. Ing. Dissertation*, Norwegian Inst. Of Technology, **1989**

Speight, J.G., Long, R.B., Trowbridge, T.D., Factors Influencing the separation of Asphaltenes from Heavy Petroleum Feedstocks, *Fuel*, 63, 616-220, **1984**

Speight, J.G., *The Chemistry and Technology of Petroleum*, Second Edition, **1991**

Tharanivasan, A.K., Svrcek, W.Y. and Yarranton, H.W., Taylor, S.D., Merino-Gracia, D., Rahimi, P.M., Measurement and Modeling of Asphaltene Precipitation from Crude Oil Blends: *Energy and Fuels*, Vol. 23, No. 8, pp. 3971-3980, August **2009**

Tharanivasan, A.K., Yarranton, H.W., and Taylor, S.D., Application of a regular solution-based model to asphaltene precipitation from live oils: *Energy and Fuels*, Vol. 25, No. 8, pp. 528-538, February **2011**

Twu, C. H., *Fluid Phase Equilibria*, 16, 137-150, **1984**

Van Der Waals, On the Continuity of the gas and Liquid state, *PhD Thesis*, **1873**

Varotsis, N., Stewart, G., Todd, A.C., Clancy, M., Phase Behavior of Systems Comprising North Sea Reservoir Fluids and Injection Gases, *JPT*, November **1986**

Virtual Materials Group Inc VMG, VMGSim Version 6.0, *VMGSim user's manual*, Calgary, Canada, **2010**

Wang, J.X., Buckley, J.S., Burke, N.E., and Creek, J.L., A Practical Method for Anticipating Asphaltene Problems, *SPE Production Facilities*, 19, 152-160, **2004**

Wiehe, I.A., A Solvent-Resid Phase Diagram for Tracking Resid Conversion, *Industrial and Engineering Chemistry Research*, 31, 530-536, **1992**

Wertheim, M.S., *J. Stat. Phys.* 35, 19, **1984**

Wertheim, M.S., *J. Stat. Phys.* 42, 477, **1986**

Whitson, C. H., and Brulé, M. R., *Phase Behavior Monograph Volume 20*, Henry L. Doherty Series, Society of Petroleum Engineers Inc., USA, **2000**

Yarranton, H.W., Masliyah, J.H., Molar Mass Distribution and Solubility Modeling of Asphaltenes, *AIChE Journal*, 42(12), 3533, **1996**

Yarranton, H.W., Alboudwarej, H., Jakher, R., Investigation of Asphaltene Association with Vapor Pressure Osmometry and Interfacial Tension Measurements: *Ind. Eng. Chem. Res.*, Vol. 39, p 2916-2924, July **2000**

Yarranton, H.W., Fox, W.A., Svrcek, W.Y., Effect of resins on asphaltene self-association and solubility: *Canadian Journal of Chemical Engineering*, Vol. 85, No. 5, p 635-642, October **2007**

Yarranton, H.W., Asphaltene Self-Association, *Journal of Dispersion Science and Technology*, 29(2), 224-229, **2005**

Yazdani, A., Maini, B.B., Measurements and Modeling of Phase Behavior and Viscosity of as Heavy Oil/ Butane System, *JCPT*, Vol. 49, No. 2, Feb **2010**

Yen, T.F., Structure of Petroleum Asphaltene and Its Significance, *Energy Resources*, 1(4), 447, **1974**

Zou, X., Zhang, X., Shaw, J.M., Phase Behavior of Athabasca Vacuum Bottoms + n-Alkane Mixtures, *SPE Production and Operations*, May **2007**